Spring 2015

Natural polymer based gene activated matrices for bone regeneration

Sheetal Reginald D'mello
University of Iowa

NATURAL POLYMER BASED GENE ACTIVATED MATRICES FOR BONE REGENERATION

by

Sheetal Reginald D'mello

A thesis submitted in partial fulfillment
of the requirements for the Doctor of
Philosophy degree in Pharmacy
(Pharmaceutics)
in the Graduate College of
The University of Iowa

May 2015

Thesis Supervisor: Professor Aliasger Salem

Graduate College
The University of Iowa
Iowa City, Iowa

CERTIFICATE OF APPROVAL

PH.D. THESIS

This is to certify that the Ph.D. thesis of

Sheetal Reginald D'mello

has been approved by the Examining Committee
for the thesis requirement for the Doctor of Philosophy degree in Pharmacy (Pharmaceutics) at the May 2015 graduation.

Thesis Committee: _____
Aliasger Salem, Thesis Supervisor

_____
Satheesh Elangovan

_____
Maureen Donovan

_____
Daryl Murry

_____
Lewis Stevens

To my family

ACKNOWLEDGMENTS

When I came to the University of Iowa, I was quite apprehensive about the academic and cultural environment in a big school. And then gradually, I discovered the stimulating, supportive and friendly ambience that gave me the boost to enhance my scientific knowledge and skills in a high-quality way. I am very grateful to all people who, in a direct or indirect way, have helped me during the graduate program.

I am very grateful to my major advisor Dr. Aliasger Salem and my co-advisor Dr. Satheesh Elangovan for their constant guidance, cooperation and advice that were a vital part for the completion of my research. Their thoughtful feedback, data interpretation and implementation of new ideas and techniques were helpful in overcoming the problems encountered along the research path. Their constant efforts, patience and understanding have been very crucial while carrying out my research activities. They have been of immense help and an invaluable source of inspiration, experience and knowledge. I am very delighted to be a part of the tissue engineering projects. Their generous support and positive outlook has made this thesis possible.

I thank Drs. Maureen Donovan, Daryl Murry and Lewis Stevens for their time and effort while serving on my research and thesis committee.

I express my sincere thanks and gratitude to friends in Dr. Salem's lab: Sean Geary, Caitlin Lemke, Dahai Jiang, NaJung Kim, Yogita Krishnamachari, Vijaya Joshi, Kristan Sorenson, Amaraporn Wongrakpanich, Kawther Ahmed, Kareem Ebeid, Keerthi Atluri, Anh-Vu Do, Behnoush Khorsand, and Nattawut Leelakanok. Everyone has been very encouraging, supportive, and cheerful. Sharing of new ideas, knowledge and

experience has been very significant here. It has been a pleasure working with them. The Division of Pharmaceutics and Translational Therapeutics has been a fun place to learn and grow. I have always enjoyed the company of my friends and shall always remember the good times that we all have spent together.

The faculty and staff at the College of Pharmacy have been really cooperative and kind all the way along, and I thank them for everything. It has been a massive learning experience. I am also very grateful for the financial support from the division that has helped me pursue my degree smoothly.

I also thank Dr. Deborah Dawson in the Division of Biostatistics and Research Design, College of Dentistry for her help with statistical analysis of the data.

Lastly and most notably, I am highly indebted to my family for their unconditional love and support all throughout my study. My husband Denison deserves a special mention here for his patience. The long hours required in research and writing were always easy with his advice and cooperation. My parents and sisters have contributed greatly to my achievements so far. It would have not been possible without their invaluable support, understanding, encouragement and prayers at every moment of my life. Thank you for being with me through all the hard times, for listening to me patiently, for your understanding, for all the emotional and moral strength, and for making me a much stronger person each new day.

ABSTRACT

Gene therapy using non-viral vectors that are safe and efficient at transfecting target cells is an effective approach to overcome the shortcomings of delivery of growth factors in protein form. The objective of this study was to develop and test a non-viral gene delivery system for bone regeneration utilizing a collagen scaffold carrying polyethylenimine (PEI)-plasmid DNA (pDNA) complexes.

Two different pDNA were used: pDNA encoding platelet derived growth factor-B (PDGF-B) and pDNA encoding vascular endothelial growth factor (VEGF). The complexes were fabricated at an amine (N) to phosphate (P) ratio of 10 and then characterized for size, surface charge, as well as *in vitro* cytotoxicity and transfection efficacy in human bone marrow stromal cells (BMSCs). The influence of the PEI-pPDGF-B complex-loaded collagen scaffold on cellular attachment and recruitment was evaluated *in vitro* using microscopy techniques. The *in vivo* regenerative capacity of the gene delivery system, using PEI-pPDGF-B and PEI-pVEGF complexes, was assessed in 5 mm diameter critical-sized calvarial defects in Fisher 344 rats. A different biomaterial, chitosan, loaded with copper was also evaluated *in vivo*.

The complexes were ~100 nm in size with a positive surface charge. Complexes prepared at an N/P ratio of 10 displayed low cytotoxicity as assessed by a cell viability assay. High magnification scanning electron microscopy imaging demonstrated the recruitment and attachment of BMSCs into the collagen scaffold containing PEI-pPDGF-B complexes. Confocal microscopy revealed significant proliferation of BMSCs on PEI-pPDGF-B complex-loaded collagen scaffolds compared to empty scaffolds.
In vivo studies showed significantly higher new bone volume/total volume (BV/TV) % in

calvarial defects treated with the PEI-pPDGF-B complex-activated collagen scaffolds following 4 weeks of implantation when compared to the other treatment groups. Together these findings suggest that non-viral *PDGF-B* gene-activated collagen scaffolds effectively promote bone regeneration and are an attractive gene delivery system with significant potential for clinical translation.

PUBLIC ABSTRACT

Bone regeneration is critical in autogenous skeletal deficiencies, bone fractures and aging. Treatment with growth factors and recombinant human proteins is limited by a high degree of variability, limited bone formation, high cost and high physiological dosage needed. Lack of a continual supply of these proteins for a long time is also a limitation. Another alternative, viral gene therapy, is hindered due to safety concerns. One method to overcome these drawbacks is non-viral gene therapy.

Our aim was to develop an efficient non-viral gene delivery system using polyethylenimine (PEI) and plasmid DNA (pDNA) containing genes encoding for critical bone formation growth factors, platelet-derived growth factor (PDGF) and vascular endothelial growth factor (VEGF). I fabricated complexes of PEI and pDNA and loaded these particles, containing genes needed for producing bone, on a collagen platform. We inserted this bio-patch into a missing area of the bone in test animals. Cells located around the damaged area migrate into the scaffold, interact with the plasmid, the plasmid enters the cells, and the cells receive the genetic instructions to start producing proteins that enhance bone regeneration. In my experiments, the bio-patch successfully regrew bone fully enough to cover bone defects in test animals. It also stimulated new growth in human bone marrow stromal cells in culture.

Using this approach, I get local, sustained effect over a prolonged period of time without having to give continued doses of proteins. This bio-patch serves as an effective gene delivery and bone regeneration system with significant potential for clinical translation.

TABLE OF CONTENTS

LIST OF TABLES xii

LIST OF FIGURES xiii

CHAPTER I. BACKGROUND AND INTRODUCTION 1

Bone healing mechanism - understanding bone biology and biology underlying tissue formation 1
Tissue engineering strategies to regenerate bone 2
Growth Factor and Cytokine Based Approaches 4
Cell-Based Approaches 5
Gene therapy for bone regeneration 6
Viral vs Non-Viral Gene delivery 7
In Vivo vs *Ex Vivo* gene therapy 8
Role of GAMs in tissue engineering 11
Scaffold design criteria for gene delivery systems 11
Soft tissue healing 13
Hard tissue regeneration 15
Advantages and disadvantages of GAMs for bone regeneration: biocompatibility/safety of GAMs 17
Conclusions and future prospects for clinical applications 19

CHAPTER II. HYPOTHESES AND OBJECTIVES 26

Hypotheses 26
Rationale for proposed hypotheses 26
Specific aims 29

CHAPTER III. NON-VIRAL GENE DELIVERY SYSTEM IN HUMAN EMBRYONIC PALATAL MESENCHYMAL CELLS 31

Introduction 31
Materials and methods 32
Reagents and plasmids 32
Preparation of plasmid DNA (pDNA) encoding luciferase protein (LUC), enhanced green fluorescent protein (EGFP-N1) or platelet-derived growth factor B (PDGF-B) 34
Fabrication of calcium phosphate-pDNA complexes 34
Fabrication of PEI-pDNA complexes 35
In vitro characterization of pDNA (LUC) complexes 35
Size and polydispersity 35
Surface charge 36
Cell culture 36

In vitro evaluation of the transfection efficiency of pDNA (LUC) complexes 37
In vitro evaluation of cytotoxicity of PEI-pDNA (LUC) complexes 37
In vitro visualization of transfection with PEI-pDNA (EGFP-N1) complexes 38
In vitro evaluation of transfection with PEI-pDNA (PDGF-B) complexes 39
Agarose gel retardation assay for PEI-pDNA (LUC) complexes....40
Data presentation and statistical analysis....40
Results and discussion 41
Generation of pDNA encoding LUC, EGFP-N1 or PDGF-B proteins..... 42
Size and surface charge of calcium phosphate-pDNA (LUC) complexes 43
In vitro gene expression by calcium phosphate-pDNA (LUC) complexes 43
Size and surface charge of PEI-pDNA (LUC) complexes....45
In vitro gene expression by PEI-pDNA (LUC) complexes 45
In vitro cell viability assay for PEI-pDNA (LUC) complexes 48
In vitro gene expression by PEI-pDNA (EGFP-N1) complexes 50
In vitro gene expression by PEI-pDNA (PDGF-B) complexes....50
Gel retardation assay for PEI-pDNA (LUC) complexes 51
Conclusions....52

CHAPTER IV. GENE ACTIVATED MATRIX ENCODING FOR PLATELET DERIVED GROWTH FACTOR ENHANCES BONE REGENERATION 66

Introduction....66
Materials and methods....68
Materials 68
Preparation of pDNA encoding different proteins: pLUC, pEGFP-N1 or pPDGF-B....69
Fabrication of PEI-pDNA complexes....69
Size and surface charge of the PEI-pPDGF-B complexes....70
Cell culture....70
In vitro evaluation of the transfection efficiency of PEI-pLUC complexes in BMSCs....71
In vitro evaluation of toxicity of PEI-pLUC complexes in BMSCs....71
In vitro visualization of transfection of BMSCs with PEI-pEGFP-N1 complexes 72
In vitro evaluation of transfection of BMSCs with PEI-pPDGF-B complexes 73
Fabrication and characterization of PEI-pPDGF-B complex-loaded scaffolds 73
Attachment and proliferation of BMSCs on collagen scaffolds 74
SEM sample preparations 74
Immunocytochemical staining....75

In vivo implantation of complex-loaded collagen scaffolds 76
micro-CT measurement 77
Histological observation of rat bone samples 77
Data presentation and statistical analysis.....78
Results and discussion 79
Generation of pDNA encoding LUC, EGFP-N1 or PDGF-B proteins..... 79
Size and surface charge of PEI-pPDGF-B complexes.....80
In vitro gene expression by PEI-pLUC complexes.....80
In vitro cell viability assay for PEI-pLUC complexes.....82
In vitro gene expression by PEI-pEGFP-N1 complexes.....83
In vitro investigation of gene expression by PEI-pPDGF-B complexes 84
SEM analysis of collagen scaffolds 85
SEM and confocal analysis of attachment and proliferation of BMSCs on collagen scaffolds.....86
In vivo bone regeneration.....88
Conclusions.....90

CHAPTER V. COMBINATORIAL NON-VIRAL GENE DELIVERY FOR BONE REGENERATION.....101

Introduction.....101
Materials and methods.....104
Results and discussion 106
Conclusions.....109

CHAPTER VI. COPPER-LOADED CHITOSAN SCAFFOLDS FOR BONE REGENERATION 114

Introduction.....114
Materials and methods.....116
Materials 116
Scaffold fabrication.....116
Morphological characterization of the scaffolds.....116
Surgical procedure: *In vivo* implantation of scaffolds 117
Micro-CT analysis 118
Histological analysis of rat bone defects 118
Data presentation 119
Results and discussion 119
SEM analysis of chitosan scaffolds and chitosan-copper scaffolds.....119
In vivo bone regeneration: Micro-CT scans.....120
In vivo bone regeneration: new bone volume fraction.....121
In vivo bone regeneration: H & E staining.....122
Conclusions.....124

CHAPTER VII. CONCLUSIONS AND FUTURE WORK 129

REFERENCES 132

LIST OF TABLES

Table 1.1. A list of growth factors and their role in bone regeneration.....21

Table 1.2. A list of different polymeric scaffolds implicated in tissue engineering applications with their respective modifications.....22

Table 1.3. A list of different types of GAMs investigated for induction of bone formation.....24

Table 3.1. Ca/P ratios with corresponding phosphate concentrations (in mM phosphate) used in preparing calcium phosphate-pDNA (LUC) complexes 53

Table 3.2. N/P ratios with corresponding PEI amounts used in preparing PEI-pDNA (LUC/EGFP-N1/PDGF-B) complexes 54

Table 4.1. PEI amount in different N/P ratios used for formulating PEI-pDNA complexes (using 1 µg pDNA) 92

LIST OF FIGURES

Figure 1.1. Schematic of the gene delivery system (GAMs) demonstrating the proposed mechanism of action for bone regeneration 25

Figure 3.1. Effect of different Ca/P ratios on size of calcium phosphate-pDNA (LUC) complexes; Inset: Table displaying average size of the complexes (with standard deviation) corresponding to different Ca/P ratios (a) and transfection efficiency of calcium phosphate-pDNA (LUC) complexes in HEPM cells at 4 h of incubation time (b) (*p < 0.05; **p < 0.01; ***p < 0.001).....55

Figure 3.2. Characterization of PEI-based gene delivery system. Schematic showing the formation of PEI-pDNA complexes (a); effect of the various N/P ratios on size of PEI-pDNA (LUC) complexes; Inset: Table displaying average size of the complexes (with standard deviation) corresponding to different N/P ratios (b); surface charge of PEI-pDNA (LUC) complexes; Inset: Table displaying average surface charge of the complexes (with standard deviation) corresponding to different N/P ratios (c); and TEM images of PEI-pDNA (LUC) complexes prepared at a N/P ratio of 10 (d). Scale bar, 100 nm (*p < 0.05; ***p < 0.001).....57

Figure 3.3. Transfection efficiency (a) and biocompatibility (PEI toxicity) (b) of PEI-pDNA (LUC) complexes fabricated at different N/P ratios in HEPM cells at 4 h or 24 h (*p < 0.05; **p < 0.01; ***p < 0.001) 61

Figure 3.4. Confocal laser scanning microscopic images (Z-series, 63 X) demonstrating EGFP-N1 protein expression in HEPM cells at 4 h or 24 h after transfection with plasmids alone (a) and PEI-pDNA (EGFP-N1) complexes prepared at a N/P ratio of 10 after 4 h (b) or 24 h (c) of transfection: nuclei (blue, DAPI-stained); cytoplasm and cell membrane (red, phalloidin-stained); and EGFP-N1 (green). Scale bar, 20μm 63

Figure 3.5. Expression of PDGF-BB protein in HEPM cells at 4 h after transfection of the cells with PEI-pDNA (PDGF-B) complexes prepared at a N/P ratio of 10 (**p < 0.01).....64

Figure 3.6. Agarose gel electrophoresis images of pDNA and PEI-pDNA (LUC) complexes prepared at a N/P ratio of 10.....65

Figure 4.1. Luciferase assay assessing the effect of N/P ratio on the transfection capability of PEI-pLUC complexes in BMSCs at 4 h or 24 h (n = 3) 93

Figure 4.2. MTS assay assessing the effect of N/P ratio on the biocompatibility of PEI-pLUC complexes in BMSCs at 4 h or 24 h (n = 3) 94

Figure 4.3. Confocal microscopy demonstrating transfection in BMSCs after 4 h or 24 h of treatment with PEI-pEGFP complexes fabricated at a N/P ratio of 10. Scale bar, 20 µm 95

Figure 4.4. ELISA assay demonstrating the expression of PDGF-BB protein as a result of transfection of BMSCs with PEI-pPDGF-B complexes for 4 h (n = 3) 96

Figure 4.5. SEM images of empty collagen scaffolds (a) and collagen scaffolds embedded with PEI-pPDGF-B complexes (b); SEM images showing complex-loaded scaffolds seeded with BMSCs, low magnification (200X) (c) and adhesion of BMSCs to the complex-loaded scaffolds, high magnification (3500X) (d) at day 6 of incubation 97

Figure 4.6. Influence of the complex-loaded scaffolds on proliferation of BMSCs: confocal image demonstrating proliferating cells [DAPI (blue)- and PCNA (green)-positive cells] on empty scaffolds (20X) (a) and on PEI-pPDGF-B complex-loaded scaffolds (20X) (b); measurement of proliferation of BMSCs seeded on empty scaffolds compared to complex-loaded scaffolds (c) at day 3 of culture (n = 6). Scale bar, 20 µm 98

Figure 4.7. Evaluation of *in vivo* bone formation: representative micro-CT scans showing the level of regenerated bone tissue after 4 weeks in empty defects (a, d, n = 3); empty scaffolds (b, e, n = 5); and PEI-pPDGF-B complex-loaded scaffolds (c, f, n = 5); assessment of regenerated bone volume fraction (g) and bone connectivity density (h) in different groups. Scale bar, 1 mm 99

Figure 4.8. Representative histology sections demonstrating the extent of new bone formation in the defects at 4 weeks due to various treatments: empty defects (a); empty scaffolds (b); and PEI-pPDGF-B complex-loaded scaffolds (c). OB = old bone and NB = new bone. Note the complete bridging of new bone in the PEI-pPDGF-B complex-loaded test group indicated by the arrows. Scale bar, 50 µm 100

Figure 5.1. Detection of PDGF-BB and VEGF proteins in cell supernatants by ELISA after BMSC transfection with PEI-pPDGF-B and PEI-pVEGF complexes, respectively (n = 3, ***$p < 0.001$). The data were compared by ANOVA, followed by a Tukey post-test analysis (Prism 5.0, GraphPad Software Inc., San Diego, CA). The differences between the groups were considered to be statistically significant at $p < 0.05$ 110

Figure 5.2. Schematic of the gene delivery system along with TEM of the

complexes prepared at N/P ratio of 10 along with the proposed mechanism of action for bone defect repair.....111

Figure 5.3. Representative micro-CT images of bone specimens demonstrating the extent of regenerated bone in the calvarial defects at four weeks in untreated, open defects (a); defects filled with empty collagen scaffolds (b); defects filled with PEI-pPDGF-B complex-loaded scaffolds (c); defects filled with PEI-pVEGF complex-loaded scaffolds (d); defects filled with PEI-(pPDGF-B + pVEGF) complex-loaded scaffolds (e); regenerated bone volume fraction (f); and connectivity density across different groups (g). Each defect within an animal was considered as being independent (n = 3, *p < 0.05; **p < 0.01; ***p < 0.001). The data were compared by ANOVA, followed by a Tukey post-test analysis (Prism 5.0, GraphPad Software Inc., San Diego, CA). The differences between the groups were considered to be statistically significant at p < 0.05. Scale bar, 1 mm.....112

Figure 5.4. Representative histology sections of bone specimens showing the extent of regenerated bone in the calvarial defects at four weeks in untreated, open defects (a); defects filled with empty collagen scaffolds (b); defects filled with PEI-pPDGF-B complex-loaded scaffolds (c); defects filled with PEI-pVEGF complex-loaded scaffolds (d); defects filled with PEI-(pPDGF-B + pVEGF) complex-loaded scaffolds (e). OB = old bone and NB = new bone. Note the complete bridging of the bone defects by the regenerated tissue in the group treated with the PEI-pPDGF-B complex-loaded scaffolds as indicated by the arrows. Scale bar, 50 μm 113

Figure 6.1. Diagrammatic showing the formulation approach of copper-chitosan scaffolds 125

Figure 6.2. SEM images of chitosan scaffolds (a) and chitosan scaffolds embedded with copper (b) 126

Figure 6.3. Evaluation of *in vivo* bone formation: representative micro-CT scans showing the level of regenerated bone tissue after 4 weeks in empty defects (a, n = 3); chitosan scaffolds (b, n = 2); and copper-loaded chitosan scaffolds (c, n = 2); assessment of regenerated bone volume fraction in defects treated with different groups (d). Scale bar, 1 mm 127

Figure 6.4. Representative histology sections demonstrating the extent of new bone formation in the defects at 4 weeks due to various treatments: empty defects (a); chitosan scaffolds (b); and copper-loaded chitosan scaffolds (c). OB = old bone and NB = new bone. Note the partial bridging of new bone in the copper-loaded chitosan test group indicated by the arrows. Scale bar, 50 μm 128

CHAPTER I
BACKGROUND AND INTRODUCTION

Bone healing mechanism-understanding bone biology and biology underlying tissue formation

Bone is a dynamic, highly vascularized tissue whose main function is to provide mechanical and structural support to the body [1]. It has good capacity to heal as it has high amount of vasculature that supply osteoprogenitor cells and can mobilize minerals especially calcium, when needed. Bone healing involves a complex set of events encompassing large number of genetic and molecular triggers, morphogens, signaling molecules and transcriptional regulators that act in concert during specific stages of the healing process [2, 3]. The steps involved are: blood clotting, inflammation, granular tissue formation, macrophage and osteoclast activity, bone resorption and finally followed by bone deposition. Repair process starts with the formation of a blood clot, followed by an inflammatory phase to remove the potential antigens or foreign material from the wound bed. Any impairment in the clotting process due to local or systemic factors or due to the use of anticoagulation drugs may lead to impaired healing. The blood clot is then gradually replaced by the granulation tissue and mediators such as vascular endothelial growth factor (VEGF) and angiopoietins play crucial role in this phase. The granulation tissue is highly vascularized which is replaced by callus of cartilage and primary bone by intramembranous and endochondral ossification. Macrophage colony stimulating factor (M-CSF) and receptor activator of nuclear factor kappa-B ligand (RANKL) mediates the activity of macrophages and osteoclasts in the resorption of hard tissue debris [2]. In the reparative phase, growth factors such as

transforming growth factor-β (TGF-β), basic fibroblast growth factor (bFGF), platelet-derived growth factor-BB (PDGF-BB), and insulin-like growth factor-I (IGF-I) help in the induction of callus formation within the granulation tissue. Endothelial cells proliferate and chondroblasts differentiate in the clot area due to lack of oxygen, ultimately resulting in the formation of hyaline cartilage. Chondroblasts after synthesizing the cartilaginous matrix become hypertrophic and produce VEGF and bFGF. New blood vessels are formed in this region which results in the transport of osteoprogenitor and haematopoeitic cells, resulting in the formation and replacement of cartilage with bone and bone marrow.

Tissue engineering strategies to regenerate bone

The healing capacity of bone in some situations might be limited or insufficient to heal the damage caused to large bone defects. Major progression was done in the bone tissue engineering like bone grafting but it has several limitations. Bone substitutions were produced in the area of material sciences but no adequate bone substitute is made. Thus most of the injuries caused to bone still remain untreated. Each year there are around a million cases of skeletal defects that need bone grafting to achieve union. Current treatments are based on autologous or autogenous bone grafting which is considered as the gold standard approach for bone healing and regeneration [4]. Autografts are bones transferred from a different part of patient's own body and provides excellent osteoconductive, osteoinductive, and osteogenic properties. However, due to second surgical site morbidity, associated pain, and limitation in the amount of autograft that can be obtained from the patient, this strategy is currently utilized only in minimal

cases. Allograft is the technique in which bone is taken from a different individual. But again, there are several limitations such as possibilities of immune rejection, pathogen transmission from donor to host, and infrequent infections after transplantation. The graft incorporation rate is also lower than the autograft. Other alternatives are usage of metals and ceramics. They too, possess some disadvantages such as poor integration with the tissue at the site of defect and may fail due to fatigue or infection caused due to their loading. Ceramics, in contrast, are very brittle and cannot be used in the locations of high stress or mechanical load. Over the last few decades, identification of key molecules involved in bone development and fracture healing has led to the introduction and rapid expansion of biomimetic materials [5, 6]. One such advancement is the introduction of growth factors, cytokines, and morphogens for clinical use. Tissue engineering is an emerging field of science that has been gaining importance from the last 15 years. Langer and Vacanti, defined tissue engineering as ‘‘an interdisciplinary field of research that applies the principles of engineering and the life sciences towards the development of biological substitutes that restore, maintain, or improve tissue function’’[7]. For successful tissue engineering, cells, extracellular matrix, intercellular communications, cell-matrix interactions and growth factors are essential. Healing of the fracture requires integration of engineered tissues with surrounding host tissues. The tissue engineered bone should be similar to the normal natural bone both structurally and functionally. As the bone has three-dimensional structure and the cells when used alone cannot grow in a three-dimensional manner, supportive substances that can mimic bone substances like scaffolds are also required for the success of bone tissue remodeling. Tissue-engineering strategies for bone regeneration have included protein therapy to deliver osteogenic

cytokines and growth factors in the form of recombinant proteins [8], delivery of genes encoding growth factors for mesenchymal stem cell gene transfer that promotes bone growth [9], and transplantation of osteogenic cells at sites of bone defects [10]. The cells can be utilized as such or can be either transduced with viruses or transfected with non-viral vectors. These approaches for tissue engineering applications may be modified by combining with biomimetic biomaterial scaffolds to boost the therapeutic response and bone repair process [11]. The 3-dimensional macroporous scaffolds fabricated from biodegradable polymers act as osteoconductive substrates for direct implantation *in vivo*, recruiting progenitor cells to the wound site. The biomaterial scaffold-based delivery systems are to be designed such that they can control and maintain the activity of the incorporated therapeutics and serve to prolong their residence time. Osteoconductivity can be achieved using an ideal scaffold that allows for blood vessel network formation by bFGF, VEGF, PDGF-BB, TGF-β and angiopoietins-1 and 2 (that play a key role in angiogenesis), and cells to attach and migrate [12].

Growth factor and cytokine based approaches

Growth factors control cell migration, differentiation and proliferation by binding to the receptors on cell surface (Table 1.1). Thus, growth factors which act in a concentration and time dependent manner, can be used in the engineering of damaged tissues [13]. Osteoinductivity is achieved by the action of bone morphogenetic proteins (BMPs, BMP-2 to BMP-8), TGF-β and other growth factors that directly stimulate osteogenesis [14]. Delivery of multiple growth factors has been shown to synergistically promote enhanced angiogenesis and bone regeneration than delivery of the individual

growth factors alone [15, 16]. For regenerating bone, therapeutic protein treatment with osteoinductive factors (such as BMPs) possesses the capability of inducing bone formation. However, one significant drawback of the current protein-based therapies is their lack of specificity for osteoblasts or bone-forming cells. Even though very small quantities of proteins are required for osteoinduction, high doses are necessary for direct clinical application, taking into account their short half-lives and rapid degradation. Additionally, the functional heterogeneity and large dose administration (in milligrams) of proteins may form unwanted bone in undesired parts of the body, along with other unpredictable adverse events, and together with cost considerations, may therefore limit their usage [17].

Cell-based approaches

Cell therapy is another approach that is based on transplantation of key cells which can synthesize the desired therapeutic growth factors. Isolated autologous cells that are expanded by *ex vivo* cell culture can be genetically modified to produce growth factors and they can be transplanted into the defect. Cell based bone tissue engineering includes both the somatic and the undifferentiated stem cells. Somatic cells have limited potency, lack self-renewal ability and are committed to the production of only a single cell type in contrast to the stem cells. Hence, they have very limited use in the complex tissue engineering processes. As a result, most of the research is concentrated on stem cells. Genetic engineering of human mesenchymal stem cells (MSCs) can also result in multiple growth factor delivery. Combinations of growth factors like bFGF and VEGF, BMP-2 and BMP-7 proteins, and VEGF and BMP-4 can be produced by changing the

culture conditions of the genetically-modified MSCs. Mesenchymal stem cells have been mainly isolated from the adipose tissue, bone marrow, umbilical cord, and teeth (dental pulp and periodontal ligament) in addition to other sources [18]. Before implantation at the defect site, gene transfer to these cells can be performed *ex vivo* using viral vectors and mixing with polymers such as collagen type I to create cell/polymer constructs [19]. Various studies have also reported the use of *ex vivo* expanded autologous bone marrow-derived osteoprogenitor cells grow on macroporous hydroxyapatite scaffolds for implantation at the lesion sites. This treatment, devoid of any cellular genetic modifications, was intended for the repair of large bone defects in long bones and demonstrated repair and functional recovery of segmental bone defects [20, 21].

Gene therapy for bone regeneration

Proteins have short half-lives, so supra-physiological doses of proteins are required to be delivered to achieve therapeutic efficacy of inducing bone formation [22]. These large doses can lead to systemic toxicities and adverse effects. For example, high doses of BMP-2 has been reported to result in soft tissue swelling, radiculitis and ectopic bone formation [23, 24]. In order to overcome the limitations of using high protein doses, gene therapy can be considered as a means of delivering growth factors to provide sustained protein delivery. Gene therapy is the introduction of genetic material into cells to enhance their expression and protein production that has autocrine and/or paracrine effects on cells at the implanted site. Apart from sustained delivery/release of growth factors at the intended site of bone formation, gene therapy has several other advantages over protein therapy. Gene delivery is more cost-effective than the protein delivery and it

can be well-controlled. Moreover, delivery of multiple genes is possible and customization is relatively less complicated Thus, gene therapy is considered to be an effective alternative to protein therapy [25]. The three essential components of gene therapy include target protein coding plasmid DNA, vector to carry and transfer genetic material that encodes protein, and target tissue or cells that produce the desired protein. Most of the gene therapy models use vectors to carry and transport genes to the cells being transduced or transfected by viral or non-viral vectors, respectively.

Viral vs non-viral gene delivery

An ideal vector for successful gene therapy must possess a number of crucial attributes that allow for therapeutic levels of transgene expression for adequate duration of time. The transgenes must be delivered to the target cell nuclei in a selective manner that ensures efficient transfection associated with minimal cytotoxicity and safety concerns. In addition, it should ideally be target cell-specific and have a controllable timeframe of protein expression [26-29]. Non-viral gene delivery systems are an attractive alternative to viral vectors because of their long safety record but they suffer from lower transfection efficiency, significantly hampering their potential in the past. Tremendous growth in the field of nanotechnology in the last decade has led to the production of safer non-viral vectors with improved transfection efficiency. Recently, studies have explored the *in vivo* and *ex vivo* delivery of genes (encoding growth factors or transcriptional factors) using non-viral vectors for bone regeneration. The non-viral gene delivery agents are advantageous over viral vectors in that the responses to the treatment are less immunogenic, less toxic, and there are no pathogenic, carcinogenic or

other mutagenic concerns, thus making them safer for clinical applications. Moreover, the gene expression induced is transient and the gene expression levels can be tightly regulated as needed depending on the acute or chronic nature of the disease condition. It is also relatively easy to alter and optimize the properties of these gene carriers for cell gene transfer so as to result in a balance between the transfection and cytotoxicity attributes [30]. The plasmid DNA can be condensed via electrostatic interactions with liposomes, polymers or other polycations to form either lipoplexes or polyplexes. Among the numerous non-viral gene vectors studied, polyethyleneimine (PEI), especially the branched 25 kDa PEI polymer is the most successful gene transfer agent to-date, both *in vitro* and *in vivo* [29, 31-33]. PEI exhibits higher transfection efficiencies due to a phenomenon known as the 'proton sponge effect'[34-37] and the level of transfer efficiency attained with PEI is considered as comparable with that of viral vectors [38].

In vivo vs ex vivo gene therapy

The gene is incorporated into an expression vector, usually a plasmid or virus construct designed to introduce a specific gene into a target cell for protein expression. There are two main methods of gene transfer for tissue regeneration: 1) transfection of MSCs *in vitro* and subsequent transplantation into the site of the defect [10], and 2) direct application of osteogenic genes to the defect site. The plasmid or viral vector containing the cDNA equivalents of the therapeutic genes can be present by itself or the plasmid can be complexed with polycations to form nanoparticulates. These methods could be used in conjunction with scaffolds, while being embedded in a scaffold matrix for enhanced bone regeneration [9, 39]. Mesenchymal stem cells are the non-haematopoeitic stromal cells

that are the part of the cell-based bone defect repair strategies. These cells are inherently able to differentiate into bone tissue cells under the appropriate environment favorable for bone tissue engineering [40, 41]. For treating bone loss, these cells can either be used alone or in combination with scaffolds [42].

Gene transfer can be classified as *in vivo* and *ex vivo* delivery. *In vivo* gene transfer is the direct injection of vector-gene complex (genes encoded by virus or plasmid DNA which may be condensed further by non-viral vectors) into the defect site. With this approach, it is difficult to obtain targeted gene delivery to specific cells, as the cells surrounding the target tissue of interest may also be transfected. Considerable amount of transfection of host cells and the resulting protein production is required for the *in vivo* gene delivery approach to be effective. Moreover, when using viral vectors, viruses are directly administered to the body, thereby limiting safety testing of the treatment. In *ex vivo* gene transfer the isolated, culture-expanded cells are either transduced (with viral vectors) or transfected (with non-viral vectors) *in vitro* and are then implanted into the defect. *Ex vivo* gene therapy can target specific cell population of interest and permits selection, control, and scrutiny of the genetically-altered cells prior to re-implantation. However, compared with *in vivo* gene therapy, the *ex vivo* approaches are generally more surgically invasive, technically complex and tedious, and expensive, thus reducing its scope for clinical translation [43]. Therefore, there is growing interest in the development of non-viral vectors with higher transfection efficiencies that can deliver multiple gene-encoding plasmid DNA *in vivo*.

Gene-activated matrices (GAMS) are inert scaffold systems containing viral or non-viral gene delivery vectors that have been widely investigated and have found

extensive use in wound healing and tissue engineering approaches. In the gene therapy applications with this technology, cytokines and growth factors are delivered in the form of genes, not recombinant proteins. The vectors can commandeer the host cell's machinery and mechanism for protein synthesis to produce the protein encoded by the gene. Following gene delivery, the recombinant protein could be expressed *in situ* by endogenous would repair cells. Although secreted in small amounts, protein expression for prolonged period of time leads to bone regeneration [44]. Scaffolds are biomaterial substitutes that have been modified to contain genes encoding growth factors to facilitate healing of defects. They temporarily serve as three-dimensional templates for tissue formation and guide the growth of new functional tissue. The GAMs are an approach to encapsulate and retain the gene within the sponge matrices for longer duration of efficient gene transfer and cell expression during bone formation [45]. This has been known to enhance matrix deposition and blood vessel formation in the developing bone tissue. On the other hand, direct injection of the gene mediates shorter cellular expression and does not significantly affect tissue formation [46]. Our recent work has demonstrated the ability of a GAM design comprising a collagen scaffold injected with non-viral PEI condensed and complexed plasmid DNA encoding PDGF-B (Figure 1.1) [47]. On implantation into an osseous defect, the complexes are released into the surrounding tissues and the plasmid DNA is delivered to the infiltrating reparative cells. When transfected, these cells express the transgene/protein and an autocrine and paracrine osteogenic environment is thus created. Very promising results were obtained in critical-sized cranial defect model in rats.

Although viral gene therapy is proven to be efficacious in several animal studies, its reputation for being unsafe presents challenges in conducting human clinical trials and ultimately its clinical application, especially for non-lethal diseases is believed to be risky [48]. In spite of lower transfection efficiency compared to that of the viral vectors, non-viral vectors are safer to use and can be clinically translated for potential bone regeneration. Hence the main focus of this review is on the utilization of non-viral vectors, mainly polymers as gene delivery vectors. The non-viral delivery of genes *in vivo* can significantly enhance bone regeneration and can potentially address the drawbacks of protein therapy. Since this system employs non-viral vectors, we also overcome the safety concerns associated with viral vectors. The long-term goal of utilizing bone tissue engineering is to develop a safe and efficient non-viral gene delivery system to deliver multiple genes *in vivo* for periodontal and bone regeneration and other orthopedic applications.

Role of GAMs in tissue engineering

Scaffold design criteria for gene delivery systems

Gene-activated matrices are scaffolds containing gene delivery vectors and/or mesenchymal stem cells (MSCs) that act as a gene depot for local tissue regeneration. Additionally, they may also incorporate ligands that enhance adhesion of cells to the matrix and cell-cell communication. Together with the gene-expressed soluble growth factors, signaling cell populations can initiate and promote cellular recruitment, proliferation, and cell differentiation [13]. The scaffolds are essentially composed of biodegradable and biocompatible polymeric materials that are bioresorbable upon *in vivo*

implantation into osseous defects. The scaffold matrix provides structural support for osteogenesis or bone remodeling by the infiltrating reparative cells expressing the transgene. The three-dimensional GAMs are typically highly porous in nature and can be fabricated with different desired geometries that can regenerate the functional bone tissue while maintaining its original size and shape. A biologically active scaffold specifically engineered for bone tissue regeneration must possess a number of key qualities necessary for enabling new tissue deposition [49]. Ideally, biomaterials need to be osteoconductive and mechanically compatible with and integrate with the surrounding native bone in the repair process. The matrix must be suitable for creating and maintaining appropriate space and favorable environment *in vivo* to support tissue development and control the size and shape of the space-filling regenerating tissue. It must also be structurally and mechanically stable, and homogenously porous suitable for promoting cell adhesion and growth. For bone healing involving the guided bone regeneration strategy, it is critical that the scaffold matrices possess suitable physical and mechanical properties for supporting cell survival and proliferation. The ability of the scaffolds to engineer the bone tissue and control its structure is defined by the mechanical properties and degradation rate of the scaffolds. For this reason, the scaffold must maintain architectural integrity after placement *in vivo*, essential for the gradual filling-in of critical-sized defects during the process of bone formation. The biological scaffold must degrade at a rate such that it is insoluble and remains intact especially during cellular activities critical for bone repair. Eventually, new bone tissue is formed, gradually replacing the sponge-like scaffold. The scaffold itself must be biocompatible with non-toxic degradation products. It is desirable that the chemical composition of the scaffold contains binding

sites (ligands) appropriate for specific cell populations. In addition, the optimal pore size must allow maximal cell entry and migration through the pores (large enough), yet retain a high specific surface area for cell attachment and matrix deposition (small enough) [50-52]. The scaffold should allow for migration and attachment of progenitor cells from the surrounding tissue into the scaffold. With cell sizes smaller than the pore sizes, the macroporous scaffolds provide space within the scaffolds for the cells to anchor themselves and subsequently proliferate, differentiate and ultimately form the mineralized tissues [53]. It is also necessary for the cell growth and efficient transport of cells, metabolites, and nutrients, that the scaffolds possess large pore volume fraction (high porosity, usually > 90 %) together with an interconnected pore network [54]. The pore size, pore shape, and the porosity of the scaffold are critical parameters governing the availability of total specific surface area as well as ligand distribution to the cells. The regenerative process involves an interplay between the scaffolds, infiltrating cells and the right structural, mechanical, and biological cues necessary for the cells to start the remodeling process. For bone regeneration applications, a series of scaffolds with tailored structural, and mechanical and biological properties can be fabricated that facilitate cellular adhesion, migration, and tissue development (Table 1.2). This may significantly enable engineering of the bone tissue with pre-defined structures.

Soft tissue healing

In addition to the bone defect repair, some bone defects such as those resulting from trauma need treatment for reconstructing other soft tissue injuries as well. These include repair of blood vessels, cartilage, muscles, ligaments and tendons, neural tissue, and skin. Even the process of bone formation alone requires integration among a number

of physiological events, angiogenesis being one of them [55, 56]. New blood vessels are essential for supplying oxygen and providing nutrients necessary to sustain cell metabolism of the highly metabolically active repair cells. They also serve to carry inflammatory and mesenchymal tissue progenitor cells to, and waste, breakdown products from the wound site. By modifying vascularization through exogenous delivery of various growth factors including VEGF, PDGF, BMPs and FGF, bone regeneration and healing can be accelerated/improved. This could be a viable therapeutic approach for healing of soft tissues too. The well-vascularized soft tissue envelopes, periosteum and endosteum, restores normal blood supply at the fracture site. By combining the osteogenic and angiogenic inductive growth factors, complete wound healing can be potentially achieved. Work by Shea et al. showed that polymeric PLGA scaffolds incorporating gene encoding VEGF resulted in local and sustained delivery of the growth factor at the site of implantation [57]. The system led to increased blood vessel density at the local tissue site. In a separate animal study, Mooney at al showed that when plasmid DNA encoding gene for a human recombinant PDGF-B was encapsulated into PLGA matrices, an increase in granulation tissue and vascularization was observed [46]. There was a statistically significant increase in the granulation tissue thickness, and number and area of blood vessels from two weeks to four weeks, thus demonstrating continuous expression of the delivered gene and its sustained, increasing effect on tissue formation over time. Enhancement of skeletal muscle repair was reported by Pierce's group using collagen-gelatin matrix-immobilized gene vectors encoding either FGF-2 or FGF-6 transgenes [58]. When delivered to excisional muscle defects, these biomatrices were responsible for producing angiogenesis that later remodeled to form arteries. Along with

enhancing the density of endothelial cells and muscular arterioles at the treatment sites, myotube regeneration and muscle repair was also facilitated. For cartilage engineering purposes, Zhang and colleagues carried out a study employing porous chitosan-gelatin scaffolds containing the TGF-β1 gene for sustained release [59]. This GAM proved effective for the proliferation of chrondrocytes and also increased the synthesis of major ECM components, thereby promoting cartilage regeneration. The GAM approach can be similarly utilized for gene delivery in the regeneration of other soft tissues [60-62].

Hard tissue regeneration

By immobilizing and localizing the gene-vector constructs within the scaffolds, the duration and location of DNA delivery and gene expression can be controlled. These localized depots create a platform for bone development at the region of defect [63]. For engineering the bone tissue, only transient transfection is typically needed with growth factor production and signaling for time period of weeks. This application is now enhanced when the GAMs are implanted at the desired site of bone formation. Furthermore, the localized gene expression evades the unwanted adverse effects associated with systemic exposure to other parts of the body. A variety of natural, synthetic, and semi-synthetic polymers can be used as substrates for gene delivery. An advantage of employing synthetic polymers as depot systems is that they can be tailored specifically with properties favorable for bone tissue regeneration. These modifications provide control over the amount embedded, presentation and availability to the cells, and the release kinetics. Thus, the time frame of gene expression and cell or spatial specificity can be modulated. The GAMs may also contain the therapeutic gene of interest

encapsulated or entrapped into polymeric nanospheres or microspheres for prolonging the release even further. When formulating plasmid DNA into these spherical particles, either the uncondensed (naked) or condensed form (with polycations) can be incorporated. Alternatively, the lyophilized plasmid DNA can either be mixed with the polymer particles or pre-encapsulated into polymer microspheres before processing the polymer particles or microspheres into porous scaffolds. The latter approach may result in a more even distribution of plasmid DNA throughout the matrix, with release being regulated by the degrading microspheres. These two approaches may be combined to provide delivery of multiple genes (encoding different growth factors), each with a distinct release rate and delivery kinetics from the same structural scaffold unit. The different phases of bone healing rely on the action of multiple growth factor signaling typically presented to MSCs at distinct stages for regulating differentiation, mitosis, and chemotaxis [64, 65]. Using the aforementioned combinatorial approach for tissue-specific controlled dose and rate of delivery, these signals can be then temporally and spatially manipulated so as to enhance the cellular events necessary for bone regeneration. Again, the formulation properties such as polymer concentration, polymer molecular weight, and the method of preparation can influence the loading efficiency, rate of release to the exterior environment, and the bioactivity of the released plasmid DNA. The kinetics of gene construct release can also be varied by altering the polymer degradation rate using various polymer formulations. The polymer constructs can be fabricated from synthetic polyesters such as PLGA, PGA, and polycaprolactone, and natural polymers such as chitosan, alginate, hydroxyapatite, calcium phosphate, collagen, and hyaluronan (Table 1.3).

Advantages and disadvantages of GAMs for bone regeneration:

biocompatibility/safety of GAMs

Major barriers exist with protein therapies involving growth factors, transcriptional factors and morphogenetic proteins, either administered as such or merged with the scaffolds [9, 66, 67]. Being recombinant proteins, the therapy is accompanied by their high costs. In order to compensate for the shorter duration of action of the protein drugs *in vivo*, they are utilized in supra-physiological dosage to obtain therapeutic efficacy. This, along with adding further to the expense, is associated with the risk of inducing toxicity and presents serious health concerns [17, 68]. Side effects have been increasingly reported with high-dose protein delivery. Moreover, the exogenously supplied proteins are more prone to instability, rapid clearance from the body due to short half-lives, poor tissue distribution, thus leading to low bioavailability, loss of functional bioactivity, and the need for frequent dosing [29]. When entrapped into polymeric nanospheres and microspheres for protection against degradation and controlled release, they may in fact be denatured by the harsh processing conditions itself. An additional concern is protein aggregation prior to release, leading to its inactivation [69]. Also, when compared to the endogenously occurring proteins, the recombinant proteins may not offer the same degree of therapeutic benefit owing to the absence of inherent typical post-translational modifications [70, 71]. One approach to overcome these shortcomings of protein-based strategies is gene therapy with GAMs [72, 73]. As discussed above, gene therapy using viral vectors is perceived as unsafe and more risky than the non-genetic modes of treatment. However, for bone healing applications, it is important to take into consideration the relatively small doses that will be delivered locally, and if *ex vivo*

methods are employed, the safety issues can be addressed. Utilizing non-viral GAMs for tissue engineering has been shown to be more advantageous in generating a sustained expression of the recombinant growth factors by the transfected infiltrating wound repair cells, more cost-effective, and may be safer for use clinically as compared to the large amounts of recombinant protein and viral therapy [9, 26, 74, 75]. The implanted GAMs provide for gene expression and protein production for an extended period of time that stimulates an enhanced therapeutic response to osteogenesis and bone repair. Localized gene therapy also has been reported to eliminate or reduce systemic toxicity resulting from dose dumping occurring during bolus parenteral protein presently administered in the clinic [76, 77]. Alternatively, gene delivery system using GAMs is less expensive than the recombinant protein delivery system. The *in vitro* production of plasmid DNA is relatively simple and economical as compared to the commercial protein production which is quite expensive [78]. In addition, it has been shown that localized gene delivery via GAM approach directs the production of endogenous proteins which are less altered and thereby less immunogenic, in a targeted, controlled manner at the site of implantation [79]. The *in situ* production of proteins by the transfected bone repair cells ensures efficient cell surface receptor targeting. Consequently, significantly lower doses of proteins are required to attain similar or even higher levels of therapeutic effect for enhanced bone regeneration, when compared to protein delivery [26]. Also, with the GAMs, a long term healing effect due to induced continuous, sustained transgene expression can be achieved and maintained *in vivo* [80]. The gene transfer from GAMs causes specific cells to be differentiated into desired, selected cell types over time. This abolishes the need for repeated administration [81]. Moreover, rather than direct

introduction, incorporation of the gene vectors into the porous scaffold affords protection from physiological degradation and delays clearance from the wound site. Hence, this design of distribution throughout the matrices renders them more available to the cells for transfection and subsequently, effective transgene concentrations are maintained long term. This is critically important for enhanced efficacy of gene therapy to the defect [82] Also, formulation-wise, the GAM constructs are designed to be stable. However, in the field of regenerative medicine, the GAM material system for new tissue deposition is a recent development. There is incomplete knowledge on the amount of proteins actually produced by transfected cells and the amount needed for therapeutic effect in a given clinical situation. We need to seek answers to questions such as how much protein is required to be synthesized for bone healing applications, and at what phases, time frames and duration of the healing process. Regarding clinical applications, the lack of preclinical data in large animal models due to the highly expensive and time consuming nature of the studies is a major hindrance. Even if the encouraging data is obtained readily by simple, available technologies, still the funding and the regulatory environment raises issues and pose additional impediments to progress [83].

Conclusions and future prospects for clinical applications

Severe bone damage occurring due to genetic disorders and trauma may not be capable of self-healing and regeneration without intervention. This necessitates treatments for repairing skeletal defects that facilitate rapid new bone development and reduce the healing times. Gene therapy is being investigated in pre-clinical models as a way to treat tissue loss and enhance the regenerative process. Gene transfer can be

performed using a variety of viral and non-viral vector as gene carriers. Depending on the biology of the indication (bodily location and treatment time), either *in vivo* or *ex vivo* methods can be implemented. To address the safety aspects of clinical translation, non-viral vectors may be preferred. In engineering bone tissue, the GAM technology for sustained gene delivery and localized gene transfer, and extended expression of tissue inductive growth factors is a highly versatile approach. Enhanced and prolonged high gene transfection levels can be obtained locally without being distributed to distant tissues, thereby reducing any possible immune responses to the system. The polymeric scaffold design can control tissue development by controlling the release and maintaining sufficient availability of growth factors to the site of injury. The combination of tissue engineering scaffolds with gene therapy has immense capability of targeting any cellular processes and promoting bone regeneration. The GAM design provides a powerful and useful tool to study, regulate and manipulate cell functions in the bone developmental processes important in our understanding of the biology beneath tissue formation and regeneration. The GAM delivery system can be readily fabricated in a variety of structures with different geometries for engineering numerous types of tissues. This system might be of potential use in different therapies and biological processes as well and therefore holds a great promise in the areas of tissue engineering and regenerative medicine.

Table 1.1. A list of growth factors and their role in bone regeneration.

Growth factor/Protein	**Known activities**
EGF [84]	Growth and proliferation of mesenchymal and fibroblast cells, induction of granulation tissue formation and angiogenesis
PDGF-BB [85, 86]	Acts as a chemo-attractant, induces mitogenesis, promotes angiogenesis, and extracellular matrix synthesis and deposition
TGF-β [87, 88]	Regulation of cell proliferation, differentiation, and matrix synthesis
rhBMP [89, 90]	Stimulation of angiogenesis and migration, induces proliferation and differentiation of mesenchymal stem cells into cartilage and bone-forming cells
VEGF [91, 92]	Promotes chemotaxis of MSCs, indirectly induces proliferation and differentiation of osteoblast precursor cells
bFGF [93, 94]	Stimulates migration and proliferation of endothelial cells, hypertrophic chondrocyte differentiation, and osteoblast/osteoclast recruitment to the growth plate
Activin [95-97]	Induction of osteoblastic cell proliferation and collagen synthesis
IGF-I [98, 99]	Induces cellular proliferation and matrix synthesis

EGF: Epidermal Growth Factor

Table 1.2. A list of different polymeric scaffolds implicated in tissue engineering applications with their respective modifications.

Scaffold material	Variation Examined	Outcome
Collagen-GAG [100, 101]	Addition of GAG to collagen scaffolds, constant cooling rate during the freezing process prior to lyophilization	GAG effectively improves attachment, migration, and infiltration of cells throughout the porous scaffold; uniform porous structure and less variation in mean pore size
Collagen-GAG [102]	Collagen concentration (0.25 %, 0.5 %, and 1 %) and crosslink density (dehydrothermal crosslinking processes at 105 ^{o}C for 24 h and 150 ^{o}C for 48 h)	Significant improvement in the biological and mechanical properties of the scaffold with increased collagen amount (1 %) and crosslinking (at 150 ^{o}C for 48 h); enhanced pore size, permeability, compressive strength, cell number, and cell metabolic activity
Hyaluronic acid-based polymer scaffold [103-105]	Chemical modification through total esterification of carboxylic groups	Insoluble polymer with good stability against acidic hydrolysis; covalent binding of hydroxyl functional moieties; promote cell adhesion, proliferation, ECM production, osteogenic differentiation, and mineralization
Hydroxyapatite/β-tricalcium phosphate ceramic implants [106]	MSCs loaded onto the porous carrier	Stronger bone formation superior to the carrier alone
Collagen-PGA [107, 108]	Collagen sponge mechanically reinforced by incorporation of PGA fiber **(**dehydrothermal cross-linking)	Enhancement in compression strength; sustained release of plasmid DNA complex; significant attachment of fibroblasts, greater and deeper cell proliferation and infiltration; reduction in sponge shrinkage
Gelatin-PLGA [109]	PLGA microspheres loaded into gelatin scaffold	Increased mechanical strength and flexibility; delivery of multiple genes with distinct release kinetics
PLA, PGA, PLGA [110]	Type of polymer, molecular weight, intrinsic viscosity	High porosity with low molecular weight, low intrinsic viscosity PLGA; superior mechanical properties with higher lactic acid content

Table 1.2. Continued

PLGA [111]	Partial fusion of NaCl porogen in the solvent casting-particulate leaching process	Scaffolds with enhanced pore interconnectivity and compressive modulus
PLLA [112]	Scaffold surface modification using gelatin spheres as porogen	Higher compressive modulus; significant improvement in initial cell adhesion and proliferation, cell spreading and matrix secretion
Hyaluronan [113]	Modification with gelatin using disulfide crosslinking	Hyaluronan-gelatin sponge promoted cell attachment, growth, and spreading
PLGA [114]	Coating PLGA microspheres with polydopamine	Increased incorporation and slowed release of plasmid DNA from the scaffold
Collagen [115]	Calcium-phosphate coating for collagen scaffolds	Improved mechanical properties (higher compressive modulus/stiffness)
Collagen [116, 117]	Nano-hydroxyapatite inclusion in the scaffold	Enhanced cell function and osteointegration; significantly increased scaffold stiffness and pore interconnectivity
PCL [118]	Coupling resveratrol through a hydrolysable covalent bond with the carboxylic acid groups in PCL surface grafted with acrylic acid	Significant increase in osteogenesis
Alginate [119]	Mixing octacalcium phosphate (OCP) with alginate solution	Increased elastic modulus and pore size with increasing the OCP amount
Collagen [80]	Specific binding of biotinylated PEI-plasmid DNA complexes to avidin-modified collagen	Enhanced transfection efficiency by immobilizing complexes in the matrix through biotin/avidin bond; inhibits aggregation of complexes; higher loading efficiency and bioavailability of complexes

PGA: poly(glycolic acid), PLLA: poly(L-lactic acid), GAG: glycosaminoglycan, PCL: poly-ε-caprolactone, PLGA: poly(lactide-co-glycolide)

Table 1.3. A list of different types of GAMs investigated for induction of bone formation.

Scaffold material	Vector	Transgene	Model
Collagen [120]	Plasmid DNA	PTH 1-34 or/and BMP-4	Rat femoral defect
Collagen [121]	Plasmid DNA	PTH 1-34	Dog tibial defect
PLGA [122]	PEI-plasmid DNA complexes	BMP-4	Rat cranial defect
Poly(propylene fumarate) [123]	Triacrylate/amine polycationic polymer (TAPP)-plasmid DNA polyplexes complexed with gelatin microparticles	BMP-2	Rat cranial defect
Collagen [47]	PEI-plasmid DNA complexes	PDGF-B	Rat cranial defect
Collagen or autologous bone graft [124]	BMP-2 condensed with liposomal vector	BMP-2	Pig cranial defect
Collagen [66]	CaP-plasmid DNA precipitates	BMP-2	Rat tibial defect
Collagen [125]	Plasmid DNA	PTH 1-34	Lumbar interbody fusions in sheep
Collagen [126]	Plasmid DNA	$VEGF_{165}$	Rabbit radial defect
Calcium phosphate cement [127]	Plasmid DNA complexed with poly(ethyleneglycol) (PEG)-block-polycation	caALK6 and Runx2	Mouse cranial defect
Collagen [128]	Plasmid DNA	Osteogenic protein-1 (OP-1 or BMP-7)	Rat lumbar interbody arthrodesis
Collagen/calcium phosphate [129]	Plasmid DNA complexed with PAMAM dendrimer	$VEGF_{165}$	Mouse intra-femoral defect
Hydroxyapatite [130]	Plasmid DNA condensed with cationic liposome	BMP-2	Rabbit cranial defect

(PEG-b-P[Asp-(DET)]): PEG-b-polyasparagine carrying the *N*-(2-aminoethyl)aminoethyl group $(CH_2)_2NH(CH_2)_2NH_2$ as the side chain)

caALK6: constitutively active form of activin receptor-like kinase 6
Runx2: runt-related transcription factor 2

Figure 1.1. Schematic of the gene delivery system (GAMs) demonstrating the proposed mechanism of action for bone regeneration.

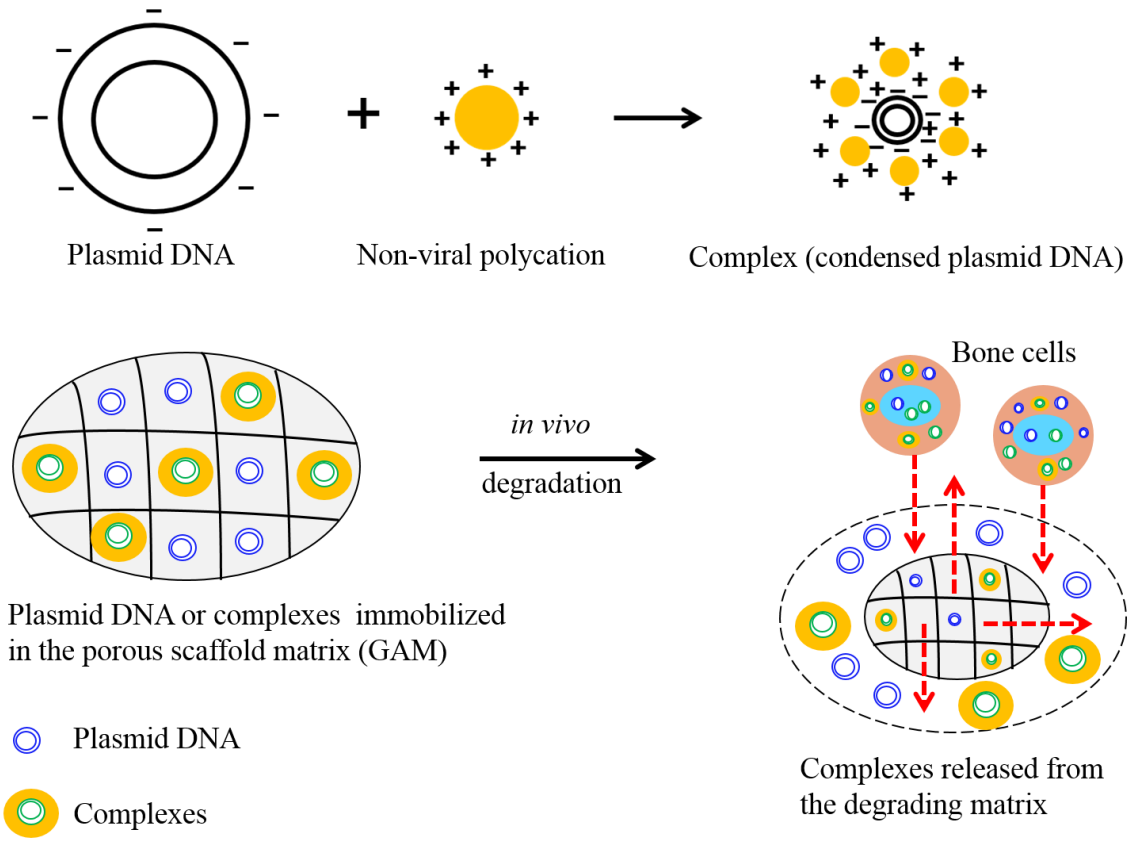

CHAPTER II

HYPOTHESIS AND OBJECTIVES

Hypotheses

We have proposed two major hypotheses:

1. Non-viral gene delivery systems, vector-plasmid DNA (pDNA) complexes, utilizing PEI and calcium phosphate as vectors, can effectively transfect pre-osteoblasts *in vitro*.
2. Non-viral delivery of pDNA (encoding PDGF-B/VEGF) can significantly enhance bone regeneration *in vivo*.

Rationale for proposed hypotheses

Tissue engineering approaches for bone regeneration have included protein therapy to deliver osteogenic cytokines and growth factors such as bone morphogenetic proteins (BMPs), delivery of genes encoding protein factors that promote bone growth, and implantation of osteogenic cells at sites of bone defects. These approaches may be combined with biomimetic scaffolds to enhance the regeneration process. The major drawback of protein therapy is that it requires supra-physiological doses of growth factors which is expensive and runs the risk of inducing toxicity. In addition, exogenously supplied proteins are susceptible to instability, rapid clearance due to short half-lives, and loss of bioactivity. The alternative use of gene therapy is less expensive because the *in vitro* production of pDNA is relatively simple and economical as compared to commercial protein production. In addition, local cell-mediated production of growth factors *in situ* would promote efficient cell surface receptor targeting and require less

protein to achieve similar levels of therapeutic effect when compared to protein therapy. Using implanted gene-activated matrices, prolonged plasmid gene expression and continuous protein production is achieved that stimulates osteogenesis and bone repair *in vivo*. Localized gene therapy also averts systemic toxicity that can occur as a result of dose dumping during protein therapy.

There are two primary methods of gene therapy for bone regeneration: 1) transfection of cells *in vitro* and subsequent transplantation into the site of the bone defect, and 2) direct delivery of osteogenic plasmid genes immobilized in a scaffold matrix. The latter approach has been shown to be more advantageous in generating a persistent expression of the growth factors by the transfected wound repair cells, more cost-effective, and may be more clinically safe for use. Plasmid DNA is non-toxic and relatively high doses can be administered to achieve sustained gene expression and therapeutic quantities of protein production. The main concern with the use of pDNA is the safety and efficacy of the gene delivery vehicles. Both, viral and non-viral vectors systems can be used for gene transfer. Viral vectors such as adenoviruses and retroviruses are usually capable of high transfection efficiencies. However, viral vectors have the potential to stimulate host immune responses, inflammatory and toxic reactions, and random insertion of the viral genome and mutagenesis that hinders the clinical translatability of this approach. Non-viral vectors lack such drawbacks and are easy to synthesize. Although non-viral gene delivery systems generally display lower transfection efficiencies when compared to viruses, they nevertheless have the potential to be applied to a wide array of applications in dental and craniofacial fields. The long

term goal is to develop a safe and efficient non-viral gene delivery system that can deliver multiple genes *in vivo* for periodontal, bone and other orthopedic applications.

Platelet derived growth factor (PDGF) is a potent mitogen and chemoattractant for mesenchymal and osteogenic cells and a stimulant for the expression of angiogenic molecules that play a pivotal role in bone healing. There are several preclinical and clinical reports that have shown the safety and efficacy of PDGF in achieving bone regeneration. Past studies on the use of PDGF have been through viral vector delivery or as a recombinant protein. Following tissue injury, platelets release PDGF at the site of the injury that act on specific cell surface receptors enhancing cell migration (chemotaxis) and proliferation (mitogenesis). The chemotactic ability of PDGF has been demonstrated on several cell types including osteoblasts. Vascular endothelial growth factor (VEGF), a growth factor known for its role in angiogenesis, is also involved in both intra-membranous and endochondral ossification. This property has led to the development of delivery systems that releases these factors for bone tissue engineering applications. Combining PDGF with VEGF was shown to significantly enhance angiogenesis, maturation of the blood vessels, and to dramatically reverse experimentally induced ischemia in animals. Furthermore, there is growing evidence that delivery of PDGF along with VEGF has a synergistic effect on bone regeneration that is greater than either factor alone. Hence, in in one of our study, we propose to develop a non-viral gene delivery system that can simultaneously deliver both *PDGF* and *VEGF* genes *in vivo* for bone regeneration.

Human embryonic palatal mesenchymal (HEPM) cells and bone marrow stromal cells (BMSCs) are osteogenic progenitors and therefore clinically relevant in bone tissue

regeneration. These cell types have been widely used as *in vitro* model cells to study osteogenesis. Type I collagen constitutes the main protein component of natural extracellular matrices and plays an important role in the process of repair of damaged tissue. Type I collagen matrices serve as a platform for cell adhesion and migration, and direct the growth of cells. Chitosan is another biomaterial that aids in hemostasis and plays a role in activation of macrophages and cytokine stimulation. Chitosan has also been reported to induce collagen synthesis and angiogenesis in the early wound healing and tissue remodeling phases of wound repair. Owing to these attributes, chitosan has generated significant interest for a broad range of wound healing applications. It has been shown that chitosan forms a chelate complex with metal ions and that copper ions strongly interact with chitosan, leading to the formation of tightly packed chitosan gel. Copper has been reported to act as an endogenous stimulator of angiogenesis by inducing the migration and proliferation of endothelial cells. Copper has also been demonstrated to induce VEGF expression *in vitro* and *in vivo*. The quality of regenerating tissue was also shown to be distinctly improved with a high density of cells in the granulation layer of copper-treated wounds. Copper-sensitive pathways are implicated to be involved in the regulation of key mediators of wound healing such as angiogenesis and tissue extracellular matrix remodeling.

Specific aims

1. Demonstrate transfection with vector-pDNA (encoding LUC) complexes in HEPM cells and BMSCs *in vitro*.

2. Fabricate complexes with varying PEI-pDNA (N/P) and calcium phosphate-pDNA (Ca/P) ratios and evaluate the influence of ratio stoichiometry on the size, surface charge, and stability of the complexes, and transfection efficiency and toxicity in HEPM cells and BMSCs.

3. Evaluate transfection efficiency of calcium phosphate versus PEI as gene delivery vectors for pDNA (encoding LUC/GFP/PDGF-B) *in vitro*.

4. Use of vector-pDNA (encoding PDGF-B) complex-loaded scaffold in gene therapy for bone regeneration *in vivo* using three-dimensional collagen scaffolds.

5. Explore the feasibility and efficacy of combinatorial non-viral gene delivery of PDGF-B and VEGF plasmids simultaneously from the same carrier system to evaluate the potential synergistic effects on the bone repair process *in vivo*.

6. Develop and investigate the effect of copper crosslinked chitosan scaffolds on bone tissue engineering in critical-sized calvarial defects *in vivo*. This proof of concept study will be followed by another study loading the PDGF-B plasmid as complexes into these scaffolds for enhanced bone regeneration.

CHAPTER III

NON-VIRAL GENE DELIVERY SYSTEM IN HUMAN EMBRYONIC PALATAL MESENCHYMAL CELLS

Introduction

Gene therapy involves treatment of diseases by the delivery of foreign genetic material into specific cells of the host [131]. The genetic material in the form of plasmid DNA encoding a functional gene for a therapeutic protein can be used to supplement or alter the expression of existing genes or replace a mutated gene within the affected host cells. Depending on the nature of the disease, either short term or long term gene expression may be needed. The main prerequisites of a successful gene therapy is that it should be safe, highly efficient, controllable and selective to the target cells [132].

Tissue engineering approaches for bone regeneration have included protein therapy to deliver osteogenic cytokines and growth factors such as bone morphogenetic proteins (BMPs) [133], delivery of genes encoding protein factors that promote bone growth [120], and implantation of osteogenic cells at sites of bone defects [134]. These approaches may be combined with biomimetic scaffolds to enhance the regeneration process [11]. The major drawback of protein therapy is that it requires supra-physiological doses of growth factors which is expensive and runs the risk of inducing toxicity [120, 135]. In addition, exogenously supplied proteins are susceptible to instability, rapid clearance due to short half-lives, and loss of bioactivity. The alternative use of gene therapy is less expensive because the *in vitro* production of plasmid DNA is relatively simple and economical as compared to commercial protein production [78]. In

addition, local cell-mediated production of growth factors *in situ* would promote efficient cell surface receptor targeting and require less protein to achieve similar levels of therapeutic effect when compared to protein therapy. Using implanted gene-activated matrices, prolonged plasmid gene expression and continuous protein production is achieved that stimulates osteogenesis and bone repair in vivo [121]. Localized gene therapy also averts systemic toxicity that can occur as a result of dose dumping during protein therapy [76, 77].

Human embryonic palatal mesenchymal (HEPM) cells are osteogenic progenitors and are clinically relevant models for bone tissue regeneration. HEPM cells have been widely used as an *in vitro* model to study osteogenesis. The HEPM cells are also a good cell type to study palatal growth and closure [136]. In this study, as a proof of concept, HEPM cells were evaluated for their ability to internalize cationic complexes of plasmid DNA, undergo transfection and produce proteins of interest. The long term goal of this study is to develop a safe and efficient non-viral gene delivery system that can deliver multiple genes *in vivo* for periodontal, bone and other orthopedic applications. In this study, we show for the first time that HEPM cells can be genetically manipulated using cationic complexes of plasmid DNA to produce functional proteins.

Materials and methods

Reagents and plasmids

Branched polyethylenimine (PEI, mol. wt. 25 kDa) was purchased from Sigma-Aldrich® (St. Louis, MO). Analytical grade calcium chloride dihydrate and dextrose monohydrate were from Sigma-Aldrich®, sodium chloride and HEPES free acid from

RPI Corp. (Mt. Prospect, IL), and potassium chloride and sodium phosphate tribasic dodecahydrate were from Fischer Scientific (Fair Lawn, NJ). Plasmid DNA (6.4 Kb) encoding the firefly luciferase reporter protein (pLUC) driven by a cytomegalovirus (CMV) promoter/enhancer (VR1255 plasmid DNA), plasmid DNA (4.7 Kb) encoding the enhanced green fluorescent protein (pEGFP-N1) driven by a CMV promoter/enhancer, and plasmid DNA (4.9 Kb) encoding the platelet derived growth factor B (pPDGF-B) were used in this study. The GenElute™ HP endotoxin-free plasmid maxiprep kit was obtained from Sigma-Aldrich® (St. Louis, MO). A luciferase assay system was purchased from Promega (Madison, WI). The microBCA™ protein assay kit was purchased from Pierce (Rockford, IL). The PDGF-BB ELISA kit was purchased from Quantikine® (R & D Systems®, Minneapolis, MN). All the reagents used for transmission election microscopy (TEM) were from Electron Microscopy Services (Ft. Washington, PA). Agarose was obtained from Bio-Rad Laboratories (Hercules, CA). All other chemicals and solvents used were of reagent grade. Human palatal mesenchyme stem cells (HEPM) were purchased from American Type Culture Collection (ATCC®, Manassas, VA). Eagle's Minimum Essential Medium (EMEM) was obtained from ATCC® (Manassas, VA). Trypsin-EDTA (0.25%, 1X solution) and Dulbecco's phosphate buffered saline (PBS) was purchased from Gibco® (Invitrogen™, Grand Island, NY). Fetal bovine serum (FBS) was obtained from Atlanta Biologicals® (Lawrenceville, GA). Gentamycin sulfate (50 mg/ml) was purchased from Mediatech Inc. (Manassas, VA). MTS cell growth assay reagent (Cell Titer 96® AQueous One Solution cell proliferation assay) was purchased from Promega Corporation (Madison, WI). Alexa Fluor® 568 phalloidin was purchased from Invitrogen, NY. Triton X-100 was obtained

from Sigma-Aldrich®. Vectashield®, Hardset™ mounting medium with 4',6-diamidino-2-phenylindole (DAPI) was obtained from Vector Labs Inc., Burlingame, CA.

Preparation of plasmid DNA (pDNA) encoding luciferase protein (LUC), enhanced green fluorescent protein (EGFP-N1) or platelet-derived growth factor B (PDGF-B)

The chemically competent DH5α™ bacterial strain (*Escherichia coli* species, Carlsbad, CA) was transformed with the necessary pDNA to amplify the plasmid. The pDNA in the transformed cultures was then expanded by amplification of the *E. coli* cells in Lennox L Broth (LB Broth, RPI Corp.) overnight at 37^{o}C in an incubator shaking at 300 rpm (New Brunswick Scientific, NJ). The pDNA was extracted using the GenElute™ HP endotoxin-free plasmid maxiprep kit. The extracted pDNA was analyzed using a NanoDrop 2000 UV-Vis Spectrophotometer (Thernoscientific**,** Wilmington, DE) for purity by measuring the ratio of absorbance (A260 nm/A280 nm). The concentration of pDNA solution was determined by UV absorbance at 260 nm. The size and quality of the extracted pDNA was determined by agarose gel electrophoresis.

Fabrication of calcium phosphate-pDNA complexes

Calcium phosphate-pDNA (LUC) complexes were prepared by a standard method as described previously [137, 138]. Briefly, 500 µl of a calcium precursor solution in water comprised of 62 µl 2 M $CaCl_2.2H_2O$ and 50 µg pDNA (LUC) was added dropwise, while slowly vortexing, to an equal volume of a phosphate precursor solution in water, pH 7.5, containing varying amounts of $Na_3PO_4.12H_2O$ ranging from 0.83 mM to 2.48 mM of phosphate to formulate complexes with different Ca/P ratios (Table 3.1). The

calcium concentration in the calcium precursor solution was fixed at 248 mM. The mixture was incubated at room temperature for 20 min. The final volume of the complexes used in the transfection experiments was 20 µl containing 1 µg of pDNA.

Fabrication of PEI-pDNA complexes

Complexes were prepared by adding 500 µl PEI solution in water dropwise to 500 µl pDNA (LUC/EGFP-N1/PDGF-B) solution in water containing 50 µg pDNA and mixed by vortexing for 20 s. The mixture was incubated at room temperature for 30 min to allow complex formation between the positively charged PEI (amine groups) and the negatively charged pDNA (phosphate groups). Complexes were fabricated using different N (nitrogen) to P (phosphate) ratios (molar ratio of amine groups of PEI to phosphate groups in pDNA backbone) by varying the PEI amounts while keeping the amount of pDNA constant (Table 3.2). The final volume of the complexes utilized in the transfection and biocompatibility experiments was 20 µl containing 1 µg of pDNA.

In vitro characterization of pDNA (LUC) complexes

Size and polydispersity

Size measurements of the complexes in water were carried out using a Zetasizer Nano-ZS (Malvern Instruments, Westborough, MA), and the mean hydrodynamic diameter of the samples was determined by cumulative analysis. The particle size and particle size distribution by intensity were measured by photon correlation spectroscopy (PCS) using dynamic laser light scattering (4 mW He-Ne laser with a fixed wavelength of 633 nm, 173 ° backscatter at 25 °C) in 10 mm diameter cells. All measurements were

done in triplicate. Complexes with a N/P ratio of 10 were placed on carbon-coated grids for 1 min and negatively stained with 1 % uranyl acetate for 20 s. After drying, the samples were imaged with a JEOL JEM-1230 TEM.

Surface charge

Zeta potential (surface charge) determinations of the complexes in water were based on the electrophoretic mobility of the complexes using folded capillary cells in automatic mode of measurement duration using the Zetasizer Nano-ZS. Surface charge measurements were performed by the laser scattering method using the Smoluchowski model (Laser Doppler Micro-electrophoresis, He-Ne laser 633 nm at 25 °C). The mean value was recorded as the average of three measurements.

Cell culture

The HEPM cells were maintained in EMEM supplemented with 10 % FBS and 50 μg/ml gentamycin in a humidified incubator (Sanyo Scientific Autoflow, IR Direct Heat CO_2 Incubator) at 37 ^oC containing 95% air and 5 % CO_2. The cells were plated and grown as a monolayer in 75 cm^2 polystyrene cell culture flasks (Corning Incorporated, Corning, NY) and subcultured (subcultivation ratio of 1:6) after 80-90 % confluence was achieved. Cell lines were started from frozen stocks and the medium was changed every 2-3 days. The passage number at which the cells were used in experiments ranged between 4 and 8.

In vitro evaluation of the transfection efficiency of pDNA (LUC) complexes

PEI-pDNA (LUC) complexes were prepared using N/P ratios of 1, 5, 10, 15 and 20. Calcium phosphate-pDNA (LUC) complexes were prepared using Ca/P ratios of 100, 150, 200 and 300. Cells were seeded at a density of 80,000 cells/well in 24-well plates. The following day, at ~ 70 % cell confluency, the cell culture media was changed to serum-free media and the plasmid-containing treatments were gently vortexed and added dropwise into the wells. Each well was treated with 20 µl complexes containing 1 µg pDNA. The complexes were incubated with the cells for 4 h or 24 h. At the end of each treatment period, the cells were washed with 1X phosphate buffered saline (PBS, pH 7.4) and fresh complete media was added to the cells until analysis. After a total incubation time of 48 h, the cells were washed with 1X PBS and treated with 1X lysis buffer (Promega) and subjected to 2 freeze-thaw cycles. The cells were scraped from the wells, collected in 1.5 ml microcentrifuge tubes, and centrifuged at 14,000 rpm (Eppendorf centrifuge 5415 D) for 5 min. Luciferase expression was detected by a standard luciferase assay system using a Lumat LB 9507 luminometer (EG&G Berthold, Bad Wildbad, Germany). The relative light unit (RLU) values per mg of the total cell protein, indicative of the transfection efficiency, were normalized against the protein concentration in the lysed cell extracts using a microBCA protein assay kit.

In vitro evaluation of cytotoxicity of PEI- pDNA (LUC) complexes

Cell survival assays were conducted to demonstrate the effect of N/P ratio of the PEI-pDNA (LUC) complexes on the biocompatibility of complexes in HEPM cells over a period of time. Cells were seeded in clear polystyrene, flat bottom, 96-well plates

(Costar®, Corning Inc, NY) at a density of 10,000 cells/well and allowed to attach overnight. The following day, the complete medium was replaced with serum-free media and the cells were treated with complexes containing 1 µg pDNA in a volume of 20 µl. Untreated cells were used as controls. Cells treated with PEI alone or uncomplexed pDNA alone served as additional controls. The complexes were incubated with the cells for 4 h or 24 h to mimic the conditions used in the transfection experiments. At the end of the treatment period, the cells were washed with 1X PBS and fresh complete media was added to the cells followed by addition of 20 µL of MTS (3-(4,5-dimethylthiazol-2-yl)-5-(3-carboxymethoxyphenyl)-2-(4-sulfophenyl)-2H-tetrazolium) cell growth assay reagent. The plates were incubated at 37 ^{o}C in a humidified 5 % CO_2 atmosphere for 4 h. The amount of soluble formazan produced by reduction of the MTS reagent by viable cells was measured spectrophotometrically using a SpectraMax® Plus^{384} plate reader (Molecular Devices, Sunnyvale, CA) at 490 nm. The cell viability was expressed by the following equation: Cell viability (%) = (Absorbance intensity of treated cells / Absorbance intensity of untreated cells (control)) x 100.

In vitro visualization of transfection with PEI-pDNA (EGFP-N1) complexes

To determine the qualitative fluorescence expressed by EGFP-N1, HEPM cells were plated at a density of 50,000 cells/well in clear, flat-bottom, 8-chambered glass slides with covers (Lab-Tek, Nunc™, NY) that were previously coated with 0.1 % poly-L-lysine. The cells were allowed to attach overnight and the following day, the cell culture medium was removed. The cells were treated with complexes containing 1 µg pDNA (N/P 10) in serum-free media. Untreated cells, cells treated with uncomplexed

pDNA and cells treated with PEI alone (PEI amount of 1.30 µg corresponding to a N/P ratio of 10) were used as controls. The complexes were incubated with the cells for 4 h or 24 h. At the end of each treatment period, the cells were washed with 1X PBS and fresh complete media was added to the cells until analysis. After a total incubation time of 48 h, the cells were washed with 1X PBS. The cells were then fixed with 4 % paraformaldehyde (Hatfield, PA), followed by permeabilization of the cells with 0.2 % Triton® X-100 in PBS. The cells were later treated with phalloidin (diluted 1/200 in PBS) to fluorescently tag the cellular actin with Alexa Fluor® 568 phalloidin. The specimen was finally mounted with Vectashield® Hardset™ mounting medium containing DAPI. The cells were washed with PBS following each step in this process. The cellular fluorescence was observed using confocal laser scanning microscopy (60X, Carl Zeiss 710, Germany) equipped with Zen 2009 imaging software. The images were processed using ImageJ® software (National Institutes of Health, MD).

In vitro evaluation of transfection with PEI-pDNA (PDGF-B) complexes

The transfection in HEPM cells was further evaluated by using pDNA encoding for the PDGF-B protein. PEI-pDNA complexes were prepared using a N/P ratio of 10. The cells were plated at a seeding density of 80,000 cells/well in 24-well plates. The following day, at ~ 70 % cell confluency, the cell culture media was changed to serum-free media and the plasmid-containing treatments were gently vortexed and added dropwise into the wells. Each well was treated with complexes containing 1 µg pDNA. The complexes were incubated with the cells for 4 h. At the end of the treatment period, cells were washed with 1X PBS and fresh complete media was added to the cells until

analysis. After a total incubation time of 48 h, the cell culture supernatants were collected by centrifugation and analyzed for PDGF-BB using a PDGF-BB ELISA kit. Untreated cells and cells treated with naked, uncomplexed plasmids were employed as controls.

Agarose gel retardation assay for PEI-pDNA (LUC) complexes

The condensation of pDNA by polycationic PEI polymer and the subsequent retention and stability of pDNA within the complexes (N/P ratio of 10) was assessed using gel electrophoresis. Samples were loaded into the wells of a 1 % agarose gel (prepared in TAE buffer (1X) containing 0.5 μg/ml ethidium bromide) with BlueJuice gel loading buffer (2X final concentration). Electrophoresis was carried out at 80 mA in 1X TAE running buffer. The pDNA bands were visualized using a UV transilluminator (Spectroline, Westbury, NY).

Data presentation and statistical analysis

Numerical data was reported as mean ± standard deviation (S.D.) from at least three replicate samples. The graphs were generated using Prism 5.0 (GraphPad Software Inc., San Diego, CA). The data were compared by ANOVA followed by a Tukey post-test analysis. The differences between the groups were considered to be statistically significant when the p value was < 0.05. Statistical analyses were performed using Prism 5.0 software.

Results and discussion

Plasmid DNA is non-toxic, and relatively high doses can be administered to achieve sustained gene expression and therapeutic quantities of protein production [139]. The main concern with the use of pDNA is the safety and efficacy of the plasmid delivery vehicles. Both, viral and non-viral vectors systems can be used for gene transfer. Viral vectors such as adenoviruses and retroviruses are usually capable of high transfection efficiencies [140]. However, viral vectors have the potential to stimulate host immune responses, inflammatory and toxic reactions, random insertion of the viral genome and mutagenesis that hinders the clinical translatability of this approach [135]. On the other hand, non-viral vectors lack such drawbacks and are easy to synthesize. Although non-viral gene delivery systems generally display lower transfection efficiencies when compared to viruses, they nevertheless have the potential to be applied to a wide array of applications in dental and craniofacial fields. In this study, we explored the non-viral delivery of different genes to HEPM cells using PEI-pDNA complexes. Polyethylenimine has proven to be an effective vehicle for pDNA in many applications [141-143]. Branched PEI has yielded significantly higher transfection efficiencies than linear PEI, and is therefore commonly used for polymer-mediated pDNA delivery. Attributes of branched PEI such as effective protonability and buffering capacity, high cationic charge density potential and tight condensation of pDNA, contribute to its high transfection efficiency [141, 144]. The transfection efficiencies of three different molecular weights of PEI (25, 50, and 800 kDa) were examined *in vivo* and it was found that 25 kDa PEI resulted in the highest transfection efficiency. PEI-pDNA complexes made using low molecular weight PEIs (10 kDa and lower) readily dissociated and resulted in lower

transfection efficiencies [145, 146]. We used a systematic approach to identify the optimal amine to phosphate (N/P) ratio at which PEI-pDNA complexes could generate maximum transfection in HEPM cells whilst maintaining low cytotoxicity. The transfection efficiency of the PEI vector was also compared to an alternative calcium phosphate vector that is widely used for pDNA delivery due to its biocompatibility and biodegradability [138, 147, 148]. The calcium/phosphate (Ca/P) ratio of the calcium phosphate-pDNA complexes is a measure of the amount of calcium to phosphate used in preparing a particular precipitate. In order to optimize the stoichiometry of these complexes, formulations with varying N/P and Ca/P ratios were fabricated and the influence of ratio stoichiometry on complex size, charge and stability, transfection efficiency and toxicity in HEPM cells was evaluated. The zeta potential and size of the pDNA complexes are very critical parameters governing the interaction of the complexes with the cells and their uptake into the cells via endocytosis. This ultimately affects the maximum transfection efficiency attained and cell viability [149, 150]. The optimized complex ratio can improve the transfection efficiencies by overcoming the formulation and various other barriers in the intracellular and intra-nuclear transport of pDNA. Transfection efficiencies of these complexes are reported to vary significantly in different cell types and hence it was necessary that the transfection method be optimized for each cell line used.

Generation of pDNA encoding LUC, EGFP-N1 or PDGF-B proteins

The recovery and purity of the isolated pDNA was determined by spectrophotometric analysis. The ratio of absorbance at A260 nm/A280 nm (optical

density of pDNA solution) was within the range of 1.8 to 2.0, as recommended by the protocol from Sigma-Aldrich®.

Size and surface charge of calcium phosphate-pDNA (LUC) complexes

In preparing these complexes, the amount of calcium precursor (248 mM) and pDNA (1 μg) was maintained at a constant level, while the amount of phosphate precursor was varied so as to generate different Ca/P ratios: 100, 150, 200 and 300 (Table 3.1). This was done to assess the effect of Ca/P stoichiometry on the particle size of the resulting complexes. The size of the complexes was found to directly correlate with the Ca/P ratio (Figure 3.1a). The size decreased from 2317 ± 163 nm to 538 ± 6 nm with an increase in the Ca/P ratios from 100 (2.48 mM phosphate) to 300 (0.83 mM phosphate). With a decline in the phosphate concentration in the phosphate precursor solution from 2.48 mM to 0.83 mM (increasing Ca/P ratios), the pDNA bound and condensed more efficiently forming smaller, more stable complexes. The surface charge of the complexes prepared at Ca/P ratio of 200 was found to be - 11 ± 0.9 mV. This negative surface charge on the complexes may lead to decreased pDNA binding and condensation, and decreased cellular interactions, thus rendering instability to the complexes and hindering their uptake by the cells.

In vitro gene expression by calcium phosphate-pDNA (LUC) complexes

Plasmid DNA was complexed with various Ca to P ratios (Table 3.1) to determine the influence of the Ca/P stoichiometry in achieving the optimum transfection efficiency in HEPM cells. Cells were treated with complexes containing 1 μg of pDNA for 4 h or 24

h and processed as described in the Methods section. Untreated cells and cells treated with uncomplexed pDNA served as controls. The values are expressed as mean ± SD for each treatment (n = 3). The results demonstrated that the Ca/P ratio of the complexes significantly affected the expression of *luc* gene in HEPM cells ($p < 0.05$). The amount of transfection obtained was higher for complexes with Ca/P ratios of 200 (1.24 mM phosphate) than with Ca/P ratios of 100 (2.48 mM phosphate), 150 (1.65 mM phosphate) or 300 (0.83 mM phosphate) (Figure 3.1b). The different transfection efficiencies obtained with different Ca/P ratios may partly be attributed to the sizes of these complexes. It has been reported that the particle size of calcium phosphate-pDNA complexes significantly affects the extent of transfection obtained. Calcium phosphate complexes tend to aggregate with time, resulting in a reduction in the level of transfection attained [151, 152]. As the Ca/P ratios increased from 100 to 200, the sizes of complexes obtained decreased almost 4-fold from an average size of 2317 nm to 605 nm. A Ca/P ratio of 200 consequently showed the highest transfection efficiency and a Ca/P ratio of 100 exhibited the lowest transfection efficiency among the various ratios tested. A Ca/P ratio of 300 had the smallest average particle size of 538 nm and we would expect its transfection capacity to be at least comparable or better than that of Ca/P 200. However, low pDNA binding capacity and/or low pDNA condensation capacity of Ca/P 300 may have contributed to the drop in the transfection [138]. It is also possible that Ca/P 300 contained lower amount of complexes than Ca/P 200, and hence failed to achieve efficient transfection. Nevertheless, this reduction in transfection was found to be statistically insignificant when compared to transfection with Ca/P 200. The lower transfection capabilities of Ca/P 100 and in particular, Ca/P 150 (average size of 823 nm)

could also be due to the reduced binding and condensation of pDNA within the complexes. The gene expression attained at the second treatment time point of 24 h was much lower than that attained at 4 h of treatment (data not shown).

Size and surface charge of PEI-pDNA (LUC) complexes

The PEI-pDNA (LUC) complexes were fabricated using a constant amount (1 μg) of pDNA and varying amounts of PEI in order to generate N/P ratios of 1, 5, 10, 15 and 20 (Table 3.2, Figure 3.2a). With increasing N/P ratios, the sizes of the complexes progressively decreased from 157 ± 1 nm for N/P 1 to 82 ± 2 nm for N/P 20 (Figure 3.2b) whilst the surface charge of these complexes increased from - 22 ± 2 mV for N/P 1 to + 45 ± 0.3 mV for N/P 20 (Figure 3.2c). These findings were the results of complexation, coating and condensation of the entire length of the pDNA by PEI [153-156]. Complexes prepared at a N/P ratio of 10 were typically in the 100 nm size range with a net surface charge of ~ + 35 mV. The particle size distribution is described by the polydispersity index (PDI). Lower values of PDI indicate narrow size distributions and homogeneity of the sample. In our study, the PDI was < 0.3, confirming the relative uniformity of the particle size distribution. Transmission electron microscopy images of complexes prepared at a N/P ratio of 10 showed the formation of discrete, spherical particles of ~ 30-80 nm in size (Figure 3.2d).

In vitro gene expression by PEI-pDNA (LUC) complexes

Plasmid DNA was complexed with various amounts of PEI (Table 3.2) to determine the N/P ratio that would yield maximum transfection efficiency and optimum

levels of gene expression in HEPM cells. Cells were treated with the complexes containing 1 μg of pDNA for 4 h or 24 h and processed as described before. Untreated cells were the controls while cells treated with PEI alone were the negative controls. Cells treated with uncomplexed pDNA served as a control comparison with complex-treated cells. The values are expressed as mean ± SD for each treatment (n = 3). The *luc* gene expression levels were dependent on the transfection efficiencies of the N/P ratios used in this experiment (Figure 3.3a). The transfection efficiency increased as the N/P ratio increased from 1 (0.13 μg PEI) to 10 (1.30 μg PEI). Transfection efficiencies then dropped when the N/P ratios increased to ≥ 15. The different transfection efficiencies obtained with different N/P ratios could be attributed to the size and surface charge of the complexes, extent of pDNA binding and condensation, and toxicity of the complexes. Complexes prepared with a N/P ratio of 1 had a size of 157 nm and a surface charge of -22 mV. The pDNA binding and condensation capacity of complexes with a N/P ratio of 1 is also lower than complexes prepared at higher N/P ratios, thus contributing to the instability of the complex [153, 155]. These factors resulted in low transfection efficiencies. Although complexes prepared at a N/P ratio of 5 had a net positive surface charge, the size of the complexes remained larger than complexes prepared at a N/P ratio of 10. Incubation of the complexes prepared at a N/P ratio of 5 with the cells for 24 h showed an increase in the level of transgene expression obtained relative to that obtained at 4 h of incubation. This may be attributed to higher uptake and entry of the complexes into the cells over time. After 4 h of treatment, complexes prepared at a N/P ratio of 10 were able to transfect HEPM cells more efficiently than complexes prepared at other N/P ratios. This may be a result of their small size (100 nm) and high positive surface charge

(+ 35 mV) compared to complexes with N/P ratios < 10, and the negative impact on cell viability due to PEI (see below) for N/P ratios > 10. However, the transgene expression decreased in cells treated with complexes prepared at a N/P ratio of 10 at 24 h due to induction of cytotoxicity by PEI (see below). For the same reason, even though complexes prepared at N/P ratios of 15 and 20 had small sizes and highly positive surface charges, the amount of transgene expression in the cells declined with these treatments. For complexes prepared at a N/P ratio of 15, the gene expression generated was found to be lower than gene expression generated by complexes prepared at a N/P ratio of 10 at both 4 h or 24 h of treatment. The transfection resulting at 4 h of treatment from complexes prepared at a N/P ratio of 20 was lower than the transfection generated from complexes prepared at a N/P ratio of 15, which decreased further at 24 h of incubation time. The optimal transfection efficiency obtained at 4 h of treatment with PEI-pDNA complexes at a N/P ratio of 10 was nearly 12-fold higher than that obtained with calcium phosphate-pDNA complexes (Ca/P ratio of 200). Possible reasons for this observation are the high positive surface charge and smaller sizes of the PEI-pDNA complexes, accompanied by strong pDNA binding and condensation capacity of PEI, which are factors that favor high transfection efficiency of gene delivery vectors.

Polyethylenimine is able to condense pDNA efficiently, deliver pDNA into the cells by ionic interactions with the cell membrane and releases pDNA into the cytoplasm from endocytic vesicles. Within the acidic endo-lysosomal compartments, protonation of PEI causes it to act as a ‘proton sponge’, thus triggering osmotic swelling and vesicle disruption [141]. In contrast, calcium phosphate-pDNA complexes are reported to enter the cells through the cell membrane calcium ion channel-mediated endocytosis [157].

When the complexes are prepared by calcium phosphate co-precipitation reaction technique, they aggregate rapidly with time and increase in particle size, and consequently the transfection reproducibility and efficiency is decreased [151]. Transfection efficiencies of the calcium phosphate-pDNA complexes strongly depend on the formulation parameters including pH, temperature, and standing time between preparation and application, therefore resulting in inherently poor method reproducibility compared with PEI-based transfection methods [151, 158-160]. In addition, inefficient pDNA binding and condensing capacities, reduced cellular and nuclear uptake, limited endosomal escape, and very little protection of pDNA from nuclease degradation can all lead to lower levels of gene expression while using calcium phosphate as vector, when compared to PEI [161]. Polyethylenimine-pDNA complexes were therefore more effective for delivering genes of interest to HEPM cells than the calcium phosphate-pDNA complexes.

In vitro cell viability assay for PEI-pDNA (LUC) complexes

Cell viability assays were performed to assess the effect of co-culture of PEI-pDNA (LUC) complexes with HEPM cells on cell survival at 4 h or 24 h incubation times. Plasmid DNA (1 μg) was complexed with different amounts of PEI (Table 3.2) to generate complexes with varying N/P ratios. The cells were treated with complexes for 4 h or 24 h and processed as described in the Methods section. Untreated cells, cells treated with uncomplexed pDNA and PEI-treated cells served as controls. Values are expressed as mean ± SD for each treatment performed in triplicate. The percent cell viability was quantified at both the treatment time points, and we observed a PEI dose- and time-

dependent cytotoxicity (Figure 3.3b). The fact that complexes prepared at a N/P ratio of 10 were able to transfect HEPM cells more efficiently than complexes prepared at N/P ratios ≥ 15 at 4 h is consistent with the cell viability data (Figures 3.3a-b). The cell viability results at 4 h showed relatively low cellular toxicity (13 %) for complexes prepared at a N/P ratio of 10 when compared to the cytotoxicity induced by complexes prepared at N/P ratios ≥ 15. Approximately 87 % of the cells were viable at 4 h when incubated with complexes prepared at a N/P ratio of 10. However, the cell viability decreased to 20 % at 24 h for cells incubated with N/P 10 complexes. This effect on cell viability explains the corresponding decrease in transfection efficiency observed for N/P 10 complexes at 24 h. Similarly, the amount of PEI used in complexes prepared at N/P ratios of 15 and 20 caused a dramatic decrease in cell survival at both 4 h or 24 h and consequently had a significant negative impact on their transfection efficiencies ($p < 0.05$) (described above). These data clearly indicate that the amount of PEI used for transfecting the HEPM cells and the incubation time are critical factors determining the degree of transfection efficiency and toxicity. Complexes prepared at N/P ratios of 1 and 5 were relatively non-toxic to the cells, but they displayed low transfection efficiencies. Of all the complexes prepared, only the PEI-pDNA complexes prepared at a N/P ratio of 10 demonstrated high transfection efficiencies at 4 h of treatment time with minimum cytotoxicity. Hence, only the complexes prepared at a N/P ratio of 10 were used for cell transfections in the subsequent *in vitro* experiments.

In vitro gene expression by PEI-pDNA (EGFP-N1) complexes

Transfection in HEPM cells was further investigated by confocal microscopy. Plasmid DNA encoding for the EGFP-N1 protein (1 μg) was complexed with 1.3 μg PEI to form complexes at a N/P ratio of 10. Cells were exposed to the complexes for 4 h or 24 h and further processed as described above. Using fluorescent markers, successful transfection occurring in cells at both the treatment time points of 4 h or 24 h was investigated (Figure 3.4). The confocal images (Z-series, 63 X) revealed the transfected cells appearing green as a whole as evidenced by expression of the EGFP-N1 fluorescent protein throughout their cytoplasm. In these fixed cells, phalloidin permeated the plasma membrane to stain the cytoplasmic F-actin red. The cell nuclei were stained blue using DAPI. The control cells (untreated, or incubated with naked pDNA or PEI alone) did not show any green fluorescence, thus ruling out transfection with naked pDNA or autofluorescence from the cells, pDNA or PEI. Confocal microscopy imaging, along with the quantitative results obtained earlier, confirms the ability of PEI-pDNA complexes to transfect HEPM cells efficiently.

In vitro gene expression by PEI-pDNA (PDGF-B) complexes

Since our future goals are ultimately targeted towards stimulation of new bone tissue formation, we investigated the transgene nuclear delivery and expression of growth factor protein, PDGF-B. Platelet-derived growth factor plays an important role in angiogenesis, is chemotactic and mitogenic for osteoblast and vascular endothelial cells, and stimulates osteoblast type-1 collagen synthesis and extracellular matrix formation [162, 163]. Based on the prior N/P ratio optimization experiments, we evaluated the

efficiency of PEI-pDNA complexes prepared at a N/P ratio of 10. One microgram of pDNA was complexed with 1.3 μg PEI to form complexes at a N/P ratio of 10. Cells were exposed to the complexes for 4 h and processed as described for other transfection experiments. The data is represented as mean ± SD for each treatment carried out in triplicate. The PDGF-BB ELISA test demonstrated that the produced PDGF-BB levels (PDGF-BB concentration of 56 pg/ml) were 3.5-fold higher in cells treated with complexes prepared at a N/P ratio of 10 compared to uncomplexed, naked pDNA (PDGF-BB concentration of 16 pg/ml) (Figure 3.5). These results confirmed the ability of PEI-pDNA complexes to transfect HEPM cells with genes that are therapeutically relevant to bone regeneration.

Gel retardation assay for PEI-pDNA (LUC) complexes

We evaluated the structural integrity of the complexes prepared at a N/P ratio of 10 by determining the electrophoretic mobility of the complexes on a 1 % agarose gel. To establish conditions similar to those used in the transfection experiments, complexes with N/P 10 were incubated with cell culture growth medium (containing 10 % fetal bovine serum) for 1 h at 37 ^{o}C. This was performed to assess the effect of degradative enzymes such as DNases and proteins present in the growth medium on complex dissociation and pDNA degradation. Uncomplexed pDNA was used as the control. The gel retardation assay demonstrated the stability of pDNA within the complexes (Figure 3.6). The uncomplexed pDNA moved freely in the gel (towards the positive terminal) as discrete bands, whereas the complexed pDNA was retarded in the loading well of the gel. This result suggests that PEI entraps pDNA and restricts its mobility in the gel. Upon

treatment with the cell culture growth medium, the free plasmid appeared to undergo enzymatic digestion as visualized by fragmentation, smear and band dislocation. By contrast, the complex structure and the incorporated pDNA were completely unaffected. The complexes containing pDNA remained in the wells with no sign of decomplexation. The presence of serum DNases and proteins in the growth medium had no adverse effect on the complex conformation or the entrapped pDNA. Thus, PEI was able to effectively bind, package and condense the pDNA, consequently forming strong and stable complexes with pDNA. The condensation of DNA by PEI enables the formation of compact particles for endocytosis and also protects the entrapped pDNA from intracellular nuclease digestion [164].

Conclusions

Cationic complexes incorporating pDNAs encoding the LUC, EGFP-N1 or PDGF-B proteins were successfully prepared. Two different non-viral vectors, PEI and calcium phosphate, were empirically assessed as gene delivery vectors. It was found that PEI is a more effective vector for delivering genes of interest to pre-osteoblastic HEPM cells than calcium phosphate. The cell-complex incubation time, amount of PEI in complexes, size and surface charge of the complexes were critical parameters for achieving efficient transfections. *In vitro* experiments demonstrated that PEI-pDNA complexes prepared at a N/P ratio of 10 were able to transfect *LUC*, *EGFP-N1* and *PDGF-B* genes efficiently into HEPM cells with relatively lower cytotoxicity than complexes prepared at other N/P ratios.

Table 3.1. Ca/P ratios with corresponding phosphate concentrations (in mM phosphate) used in preparing calcium phosphate-pDNA (LUC) complexes (using 248 mM $CaCl_2.2H_2O$).

Ca/P ratio	Phosphate precursor (mM phosphate)
100	2.48
150	1.65
200	1.24
300	0.83

Table 3.2. N/P ratios with corresponding PEI amounts used in preparing PEI-pDNA (LUC/EGFP-N1/PDGF-B) complexes (using 1µg pDNA).

N/P ratio	PEI amount (µg)
1	0.13
5	0.65
10	1.30
15	1.95
20	2.6

Figure 3.1. Effect of different Ca/P ratios on the size of calcium phosphate-pDNA (LUC) complexes; Inset: Table displaying average size (diameter, d in nm) of the complexes (with standard deviation) corresponding to different Ca/P ratios (a) and transfection efficiency of calcium phosphate-pDNA (LUC) complexes in HEPM cells following 4 h of incubation time (b) (*p < 0.05; **p < 0.01; ***p < 0.001).

(a)

Ca/P ratio	Size (d. nm) ± S.D.
100	2317 ± 163
150	823 ± 3
200	605 ± 16
300	538 ± 5

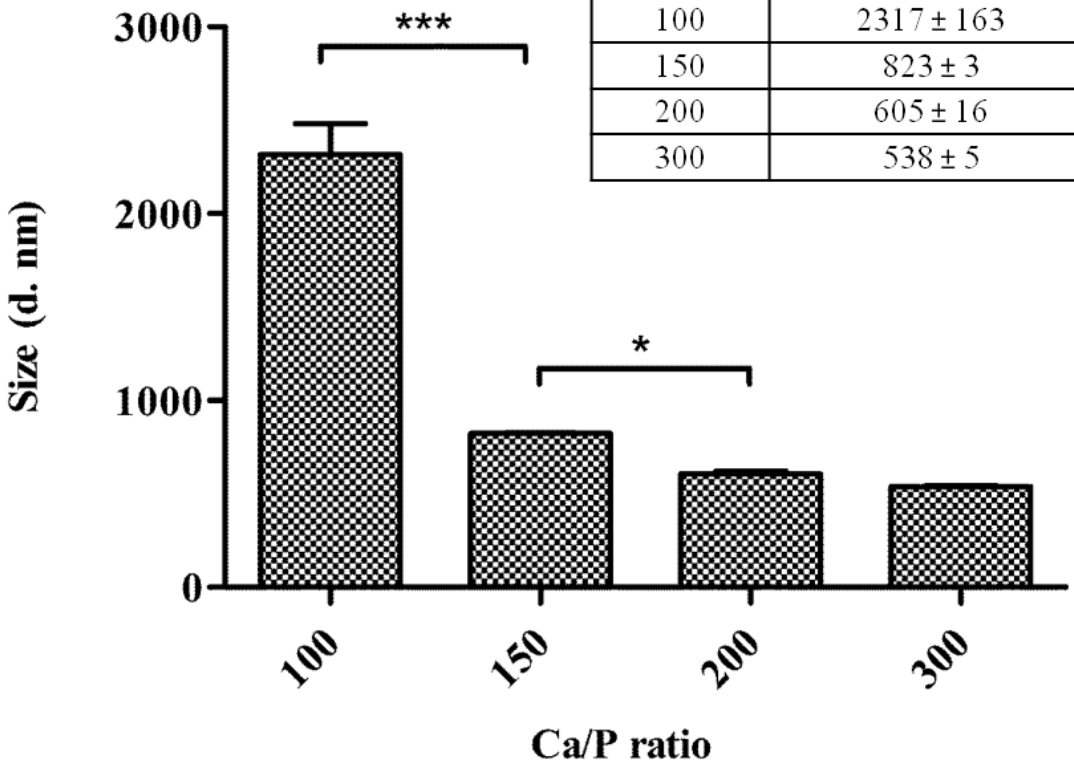

Figure 3.1. Continued

(b)

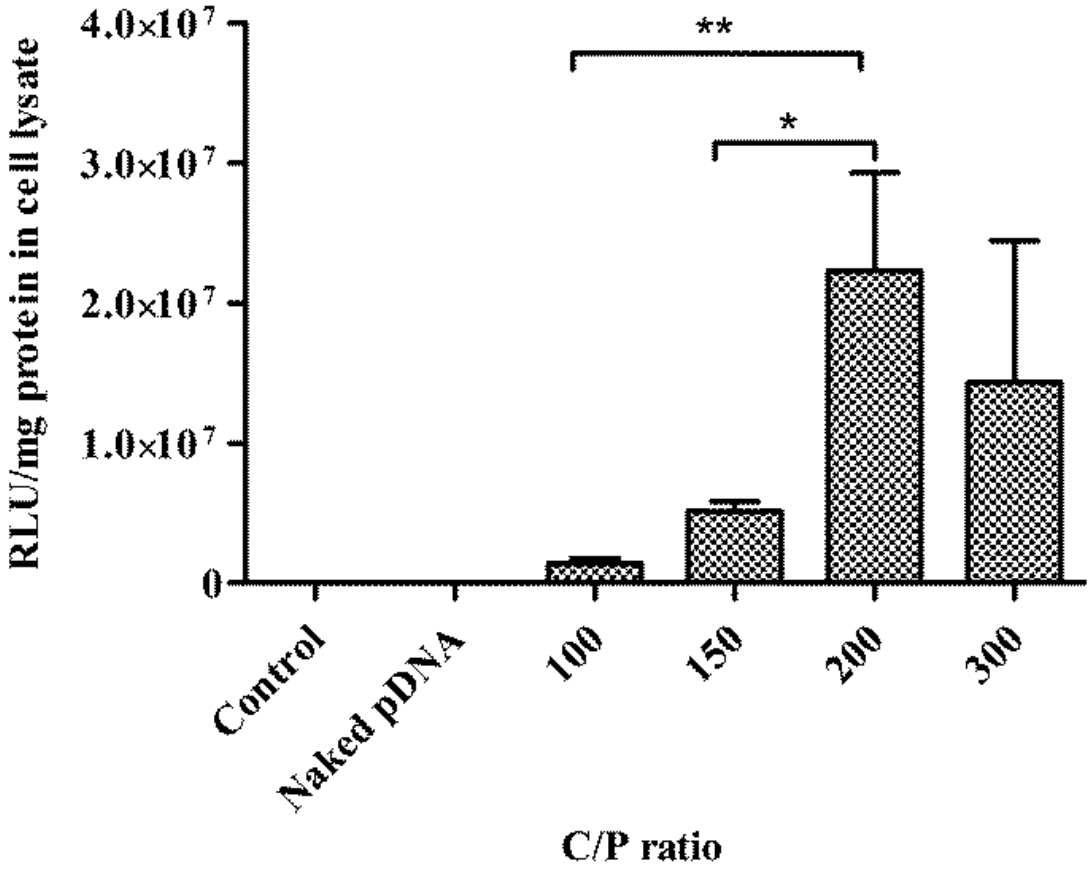

Figure 3.2. Characterization of PEI-based gene delivery system. Schematic showing the formation of PEI-pDNA complexes (a); effect of the various N/P ratios on size of PEI-pDNA (LUC) complexes; Inset: Table displaying average size (diameter, d in nm) of the complexes (with standard deviation) corresponding to different N/P ratios (b); surface charge of PEI-pDNA (LUC) complexes; Inset: Table displaying average surface charge (zeta potential) of the complexes (with standard deviation) corresponding to different N/P ratios (c); and TEM images of PEI-pDNA (LUC) complexes prepared at a N/P ratio of 10 (arrows) (d). Scale bar, 100 nm (*p < 0.05; ***p < 0.001).

(a)

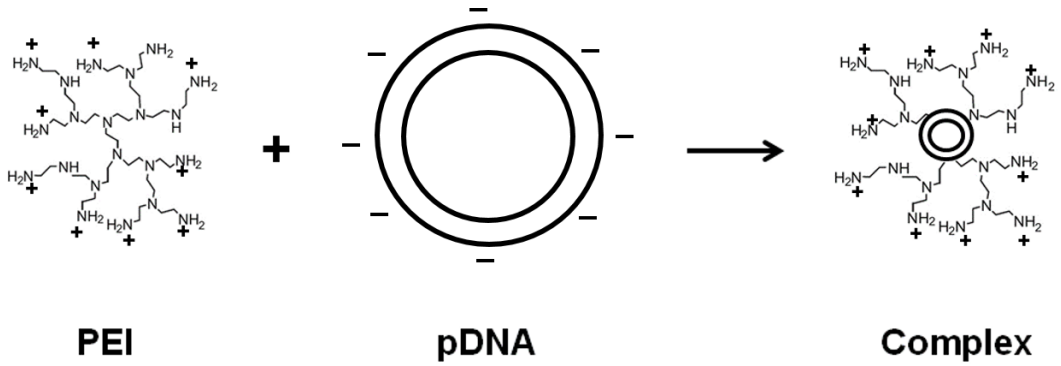

Figure 3.2. Continued

(b)

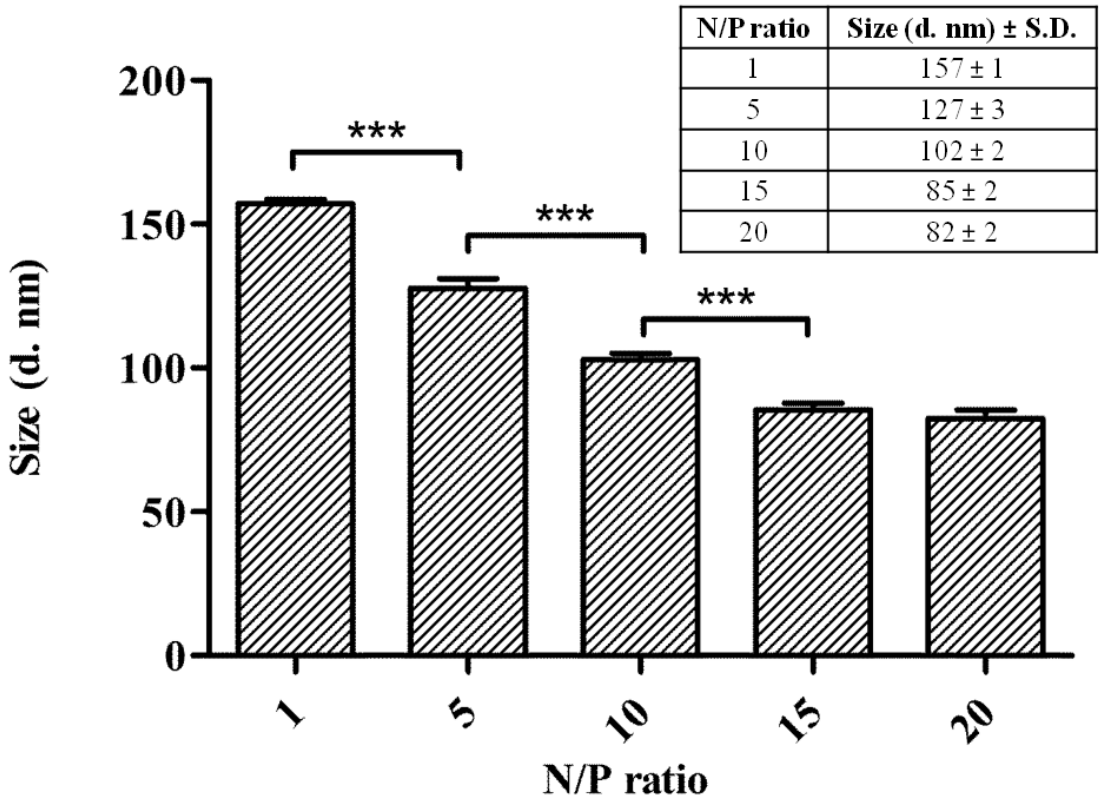

Figure 3.2. Continued

(c)

N/P ratio	Surface charge (mV) ± S.D.
pDNA	- 47 ± 1
1	- 22 ± 2
5	35 ± 0.8
10	37 ± 1
15	40 ± 1
20	45 ± 0.3

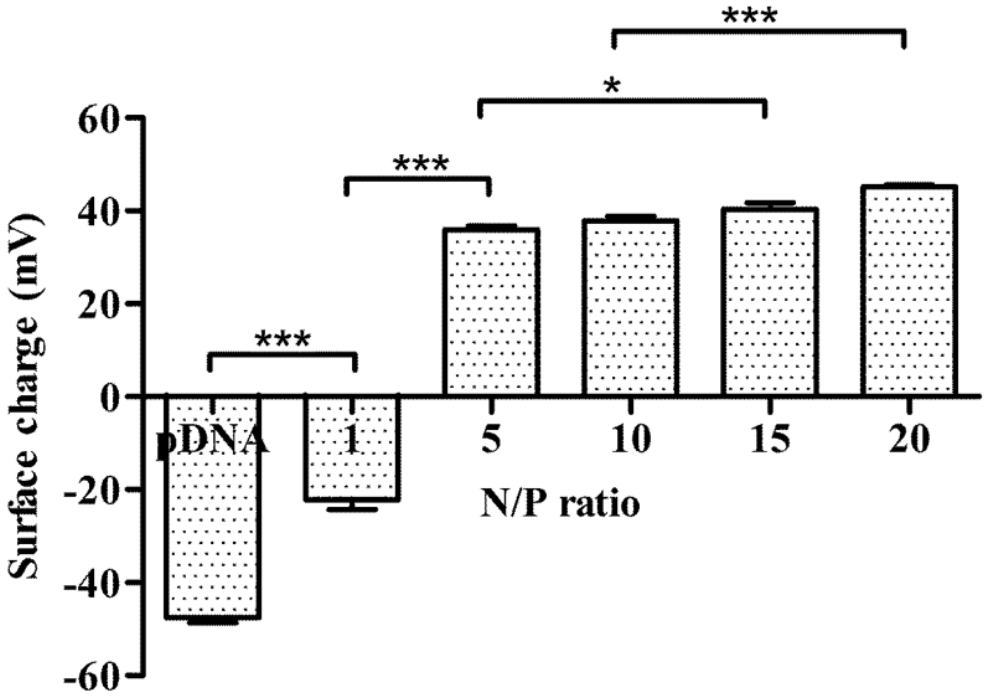

Figure 3.2. Continued

(d)

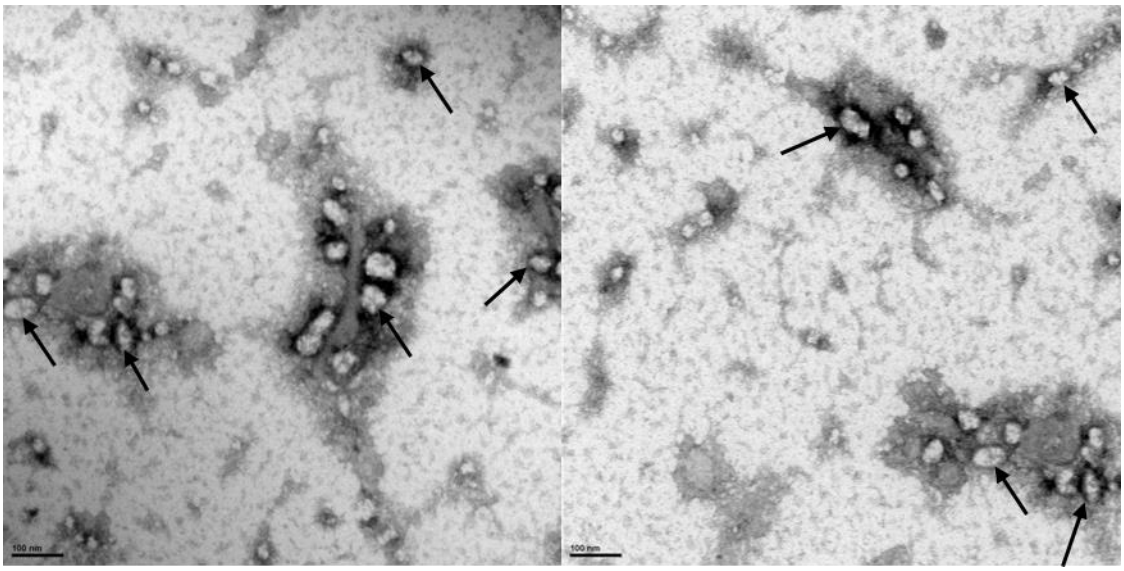

Figure 3.3. Transfection efficiency (a) and cell viability from MTS assay (PEI toxicity) (b) of PEI-pDNA (LUC) complexes fabricated at different N/P ratios in HEPM cells at 4 h or 24 h (*p < 0.05; **p < 0.01; ***p < 0.001).

(a)

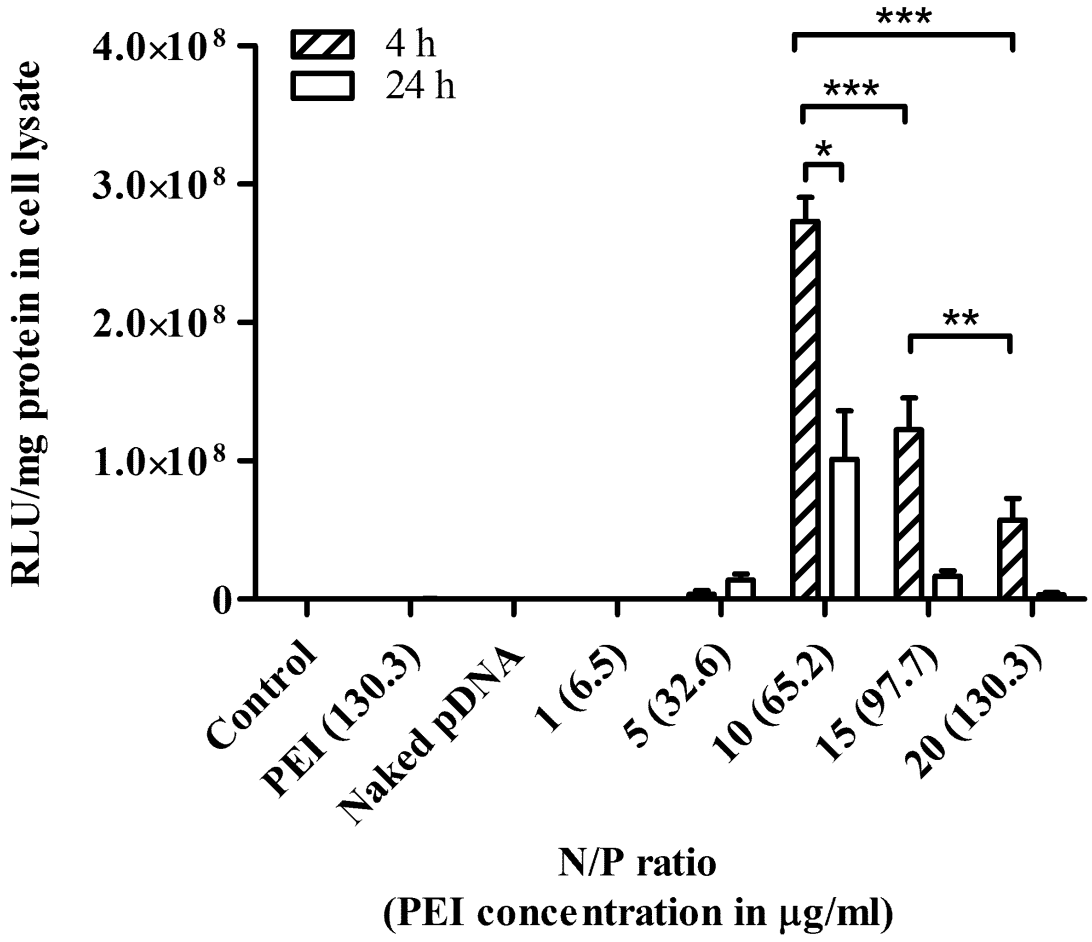

Figure 3.3. Continued

(b)

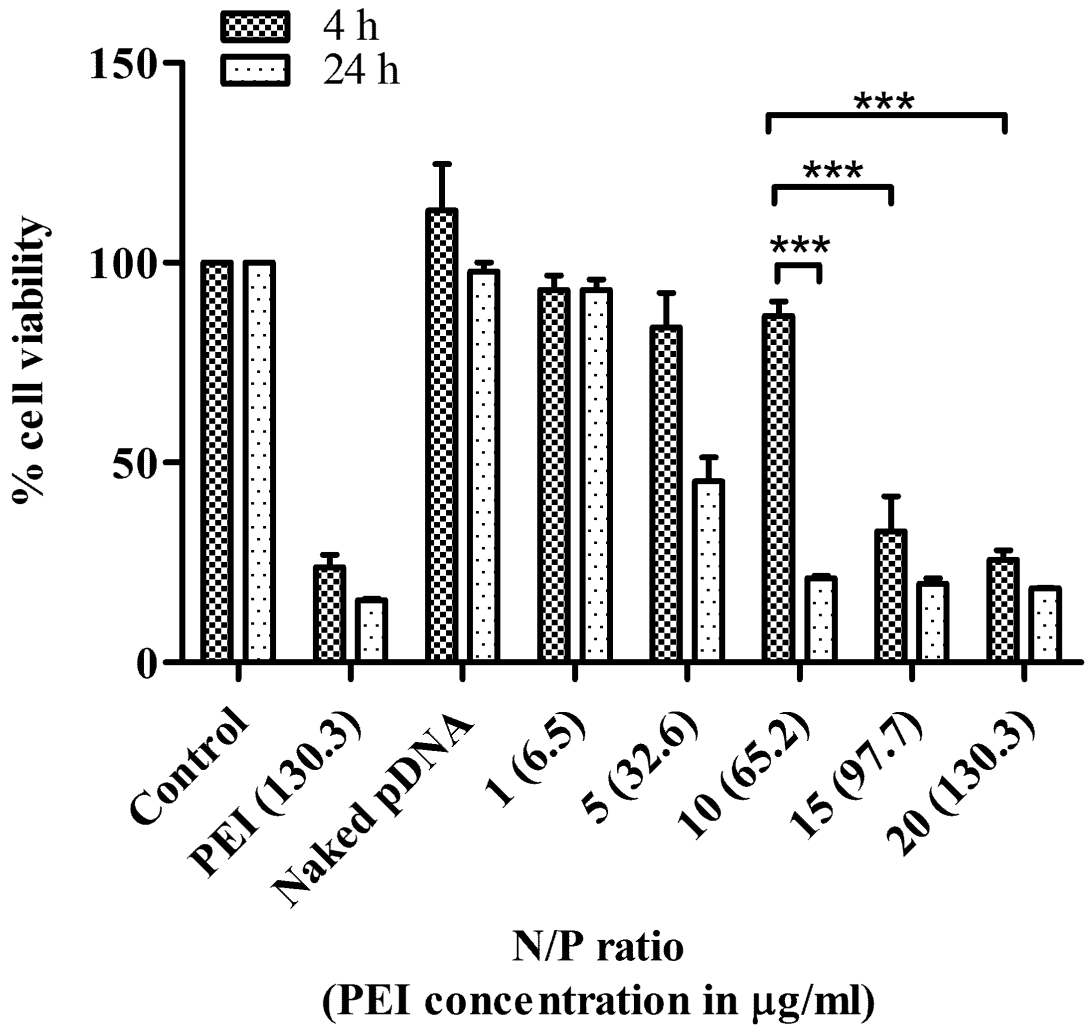

Figure 3.4. Confocal laser scanning microscopic images (Z-series, 63 X) demonstrating EGFP-N1 protein expression in HEPM cells at 4 h or 24 h after transfection with plasmids alone (a) and PEI-pDNA (EGFP-N1) complexes prepared at a N/P ratio of 10 after 4 h (b) or 24 h (c) of transfection: nuclei (blue, DAPI-stained); cytoplasm and cell membrane (red, phalloidin-stained); and EGFP-N1 (green). Scale bar, 20μm.

(a)

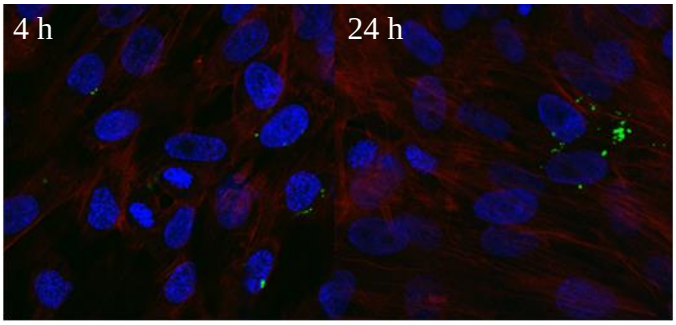

(b)

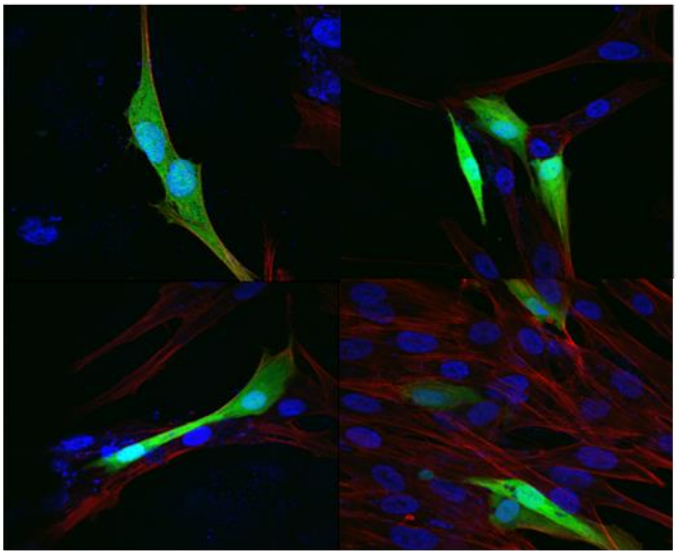

(c)

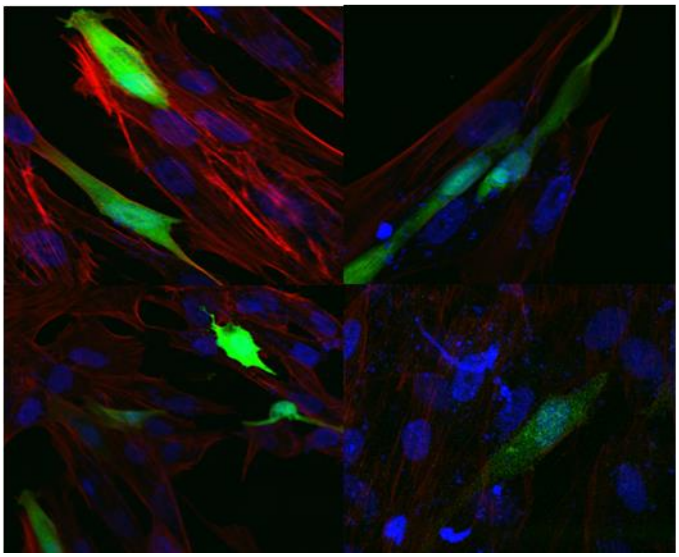

Figure 3.5. Expression of PDGF-BB protein in HEPM cells at 4 h after transfection of the cells with PEI-pDNA (PDGF-B) complexes prepared at a N/P ratio of 10 (**p < 0.01).

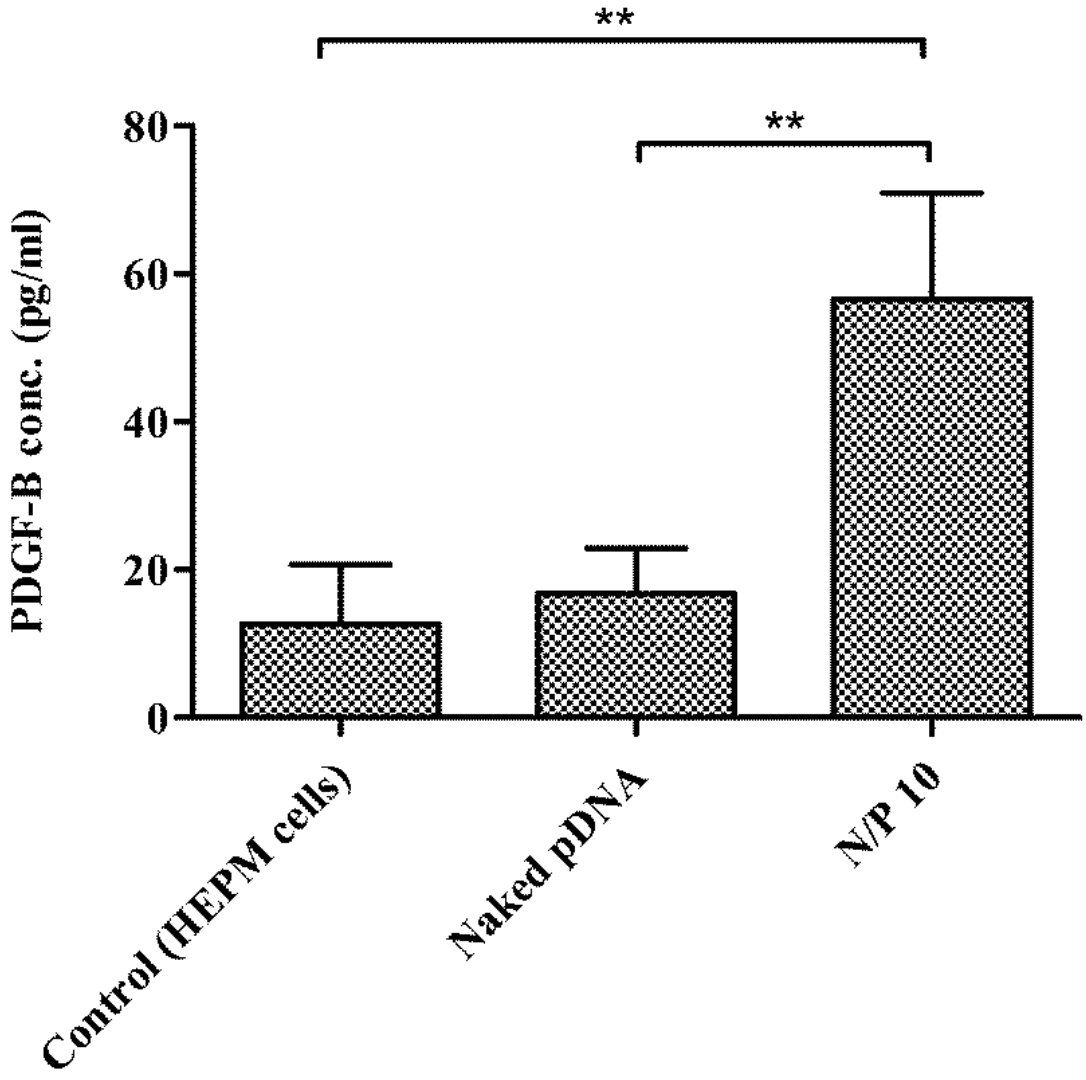

Figure 3.6. Agarose gel electrophoresis images of pDNA and PEI-pDNA (LUC) complexes prepared at a N/P ratio of 10.

CHAPTER IV

GENE ACTIVATED MATRIX ENCODING FOR PLATELET DERIVED GROWTH FACTOR ENHANCES BONE REGENERATION

Introduction

Identification of key molecules involved in bone formation and fracture healing has led to the development of biomimetic materials for clinical applications [165, 166]. One such development in dentistry is the introduction and usage of recombinant growth factors and morphogenetic proteins [167]. Major barriers with protein therapy are cost, low bioavailability and requirements for supraphysiological doses for therapeutic efficacy [168]. One strategy to overcome these drawbacks is gene therapy [72, 169]. There are two primary methods of gene therapy for bone regeneration: 1) transfection of cells *in vitro* and subsequent transplantation into the site of the bone defect [134], and 2) direct delivery of osteogenic plasmid genes immobilized in a scaffold matrix [170]. The latter approach has been shown to be more advantageous in generating a persistent expression of the growth factors by the transfected wound repair cells, is potentially more cost-effective, and may be more safe for clinical use [75, 170-172].

The first set of *in vivo* studies involving non-viral gene activated matrices for bone regeneration utilized plasmids encoding bone morphogenetic protein-2 (BMP-2) and/or human parathyroid hormone peptide [170, 171]. Non-viral gene delivery vectors are relatively safe compared to viral vectors but have lower transfection efficiencies that can often limit their potential [173]. One non-viral gene delivery system showing strong transfection capabilities is cationic polymer, polyethylenimine (PEI). In previous studies,

the branched form of PEI has shown significantly higher gene transfer efficiency than the linear form of PEI [174]. Branched PEI exhibits considerable buffering capacity over a wide pH range due to its protonability, has the highest cationic-charge potential, and condenses plasmid DNA (pDNA) to a greater extent than the linear PEI. This protects the DNA from serum DNases, cytosolic nuclease digestion, facilitates endocytosis and promotes the 'proton sponge effect' [141, 144, 175, 176]. Different molecular weights of branched PEI have been investigated *in vivo* for their transfection efficiencies with 25 kDa PEI yielding the highest transfection efficiency. Low molecular weight PEIs resulted in weak PEI-pDNA complexes that readily dissociated, thus reducing the transfection efficiency relative to 25 kDa PEI [38, 177-179].

Platelet derived growth factor (PDGF) is a potent mitogen and chemoattractant for mesenchymal and osteogenic cells and a stimulant for the expression of angiogenic molecules that play a pivotal role in bone healing [180]. There are several preclinical and clinical reports that have shown the safety and efficacy of PDGF in achieving bone regeneration [181-183]. Past studies on the use of PDGF have been through viral vector delivery or as a recombinant protein [181-183]. The objective of this study was to develop, optimize and test a non-viral based gene delivery system for bone regeneration utilizing a collagen scaffold loaded with cationic PEI-pDNA [encoding PDGF-B] complexes.

Materials and methods

Materials

Branched PEI (mol. wt. 25 kDa) was purchased from Sigma-Aldrich® (St. Louis, MO). The GenElute™ HP endotoxin-free plasmid maxiprep kit was obtained from Sigma-Aldrich®. The luciferase assay system was purchased from Promega Corporation (Madison, WI). The microBCA™ protein assay kit was purchased from Pierce (Rockford, IL). The PDGF-BB ELISA kit was purchased from Quantikine® (R & D Systems®, Minneapolis, MN). Plasmid DNA (6.4 Kb) encoding for firefly luciferase reporter protein (pLUC) driven by cytomegalovirus (CMV) promoter/enhancer (VR1255 pDNA) was obtained from Vical®, Inc. (San Diego, CA). Plasmid DNA (4.7 Kb) coding for the enhanced green fluorescent protein (pEGFP-N1) driven by CMV promoter/enhancer was obtained from Elim Biopharmaceuticals, Inc. (Hayward, CA). Plasmid DNA (4.9 Kb) encoding PDGF-B protein (pPDGF-B) driven by CMV promoter/enhancer was obtained from Origene Technologies, Inc. (Rockville, MD). Absorbable type-I bovine collagen plug was obtained from Zimmer Dental Inc. (Carlsbad, CA). All other chemicals and solvents used were of reagent grade. Human bone marrow stromal cells (BMSCs) and Dulbecco's modified eagle medium (DMEM) were purchased from American Type Culture Collection (ATCC®, Manassas, VA). Trypsin-EDTA (0.25%, 1X solution) and Dulbecco's phosphate buffered saline (PBS) was purchased from Gibco® (Invitrogen™, Grand Island, NY). Fetal bovine serum (FBS) was obtained from Atlanta Biologicals® (Lawrenceville, GA). Gentamycin sulfate (50 mg/ml) was purchased from Mediatech Inc. (Manassas, VA). MTS cell growth assay reagent (Cell Titer 96® AQueous One Solution cell proliferation assay) was purchased

from Promega Corporation. Alexa Fluor® 568 phalloidin was purchased from Invitrogen. Triton X-100 was obtained from Sigma-Aldrich®. Vectashield® Hardset™ mounting medium with 4',6-diamidino-2-phenylindole (DAPI, H-1500) was obtained from Vector Labs Inc. (Burlingame, CA).

Preparation of pDNA encoding different proteins: pLUC, pEGFP-N1 or pPDGF-B

The chemically competent DH5α™ bacterial strain (*Escherichia coli* species) was transformed with pDNA to amplify the commercial plasmids. The pDNA in the transformed cultures was then expanded in *E. coli* in Lennox L Broth (LB Broth) overnight at 37 ^{o}C in an incubator shaker at 300 rpm. Plasmid DNA was extracted using GenElute™ HP endotoxin-free plasmid maxiprep kit and was analyzed for purity using a NanoDrop 2000 UV-Vis Spectrophotometer (Thernoscientific, Wilmington, DE) by measuring the ratio of absorbance (A260 nm/A280 nm). The concentration of pDNA solution was determined by absorbance at 260 nm.

Fabrication of PEI-pDNA complexes

Complexes were prepared by adding 500 µl PEI solution dropwise to 500 µl pDNA (pLUC/pEGFP-N1/pPDGF-B) solution containing 50 µg pDNA and mixed by vortexing for 20 s. The mixture was incubated at room temperature for 30 min to allow complex formation between the positively charged PEI (amine groups) and the negatively charged pDNA (phosphate groups) [176, 184]. Complexes were fabricated using different N (nitrogen) to P (phosphate) ratios (molar ratio of amine groups of PEI to phosphate groups in pDNA backbone) by varying the PEI amounts and maintaining the amount of

pDNA constant (N/P ratios of 5, 10, 15 and 20, Table 4.1). Final volume of the complexes used in the transfection and cytotoxicity experiments was 20 µl containing 1µg of pDNA.

Size and surface charge of the PEI-pPDGF-B complexes

Measurements were carried out using a Zetasizer Nano-ZS (Malvern Instruments, Westborough, MA). The particle size and size distribution by intensity was determined by dynamic laser light scattering (4mW He-Ne laser with a fixed wavelength of 633 nm, 173° backscatter at 25 °C) in 10 mm diameter cells. Surface charge (zeta potential) was measured electrophoretically by the laser scattering technique using folded capillary cells. All measurements were done in triplicate. The mean value was recorded as the average of three different measurements.

Cell culture

Human BMSCs were maintained in DMEM supplemented with 10 % FBS and 50 µg/ml gentamycin in a humidified incubator at 37 ^{o}C containing 95 % air and 5 % CO_2 (Sanyo Scientific, Wood Dale, IL). Cells were grown as a monolayer on 75 cm^2 polystyrene cell culture flasks (Corning Incorporated, Corning, NY) and subcultured (subcultivation ratio of 1:9) after 80-90 % confluence. Cell lines were started from frozen stocks and the medium was changed every 2-3 days. Cell passage numbers used in the experiments were between 4 and 10.

In vitro evaluation of the transfection efficiency of PEI-pLUC complexes in BMSCs

The PEI-pLUC complexes were prepared using N/P ratios of 1, 5, 10, 15 and 20. Cells were seeded at a density of 80,000 cells/well in 24-well plates (Costar®, Corning Inc, NY). The next day, at ~ 80 % cell confluence, the cell culture medium was changed to serum-free medium and the treatments were gently vortexed and added dropwise into the wells. Each well was treated with 20 µl complexes containing 1 µg pLUC. Untreated cells were the controls while cells treated with PEI alone were the negative controls. Cells treated with uncomplexed pDNA served as a control comparison with complex-treated cells. Complexes were incubated with cells for 4 h or 24 h. At the end of each treatment period, cells were washed with 1X phosphate buffered saline (PBS) followed by addition of fresh complete medium. After a total incubation time of 48 h, cells were washed with 1X PBS, treated with 1X lysis buffer and subjected to two freeze-thaw cycles whereupon cells were scraped and centrifuged at 14,000 rpm for 5 min. Luciferase expression was detected by a standard luciferase assay system. The relative light units (RLU) values per mg of the total cell protein, indicative of the transfection efficiency, were normalized against the protein concentration in cell extracts using a microBCA protein assay kit.

In vitro evaluation of toxicity of PEI- pLUC complexes in BMSCs

Cell survival assays were conducted to demonstrate the effect of N/P ratio of the PEI-pLUC complexes on the biocompatibility of complexes in BMSCs. Cells were seeded in clear polystyrene, flat bottom, 96-well plates (Costar®, Corning Inc.) at a density of 10,000 cells/well and allowed to attach overnight and further processed as

described above. Untreated BMSCs were used as controls. Cells treated with PEI alone or uncomplexed pLUC alone served as additional controls. The complexes were incubated with the cells for 4 h or 24 h to mimic the conditions used in the transfection experiments. At the end of the incubation period, the cells were washed with 1X PBS and fresh complete medium was added to the cells followed by addition of 20 µL MTS (3-(4,5-dimethylthiazol-2-yl)-5-(3-carboxymethoxyphenyl)-2-(4-sulfophenyl)-2H-tetrazolium) cell growth assay reagent. The plates were then incubated at 37^{o}C in a humidified 5 % CO_2 atmosphere for 4 hours. The amount of soluble formazan produced by reduction of MTS reagent by viable cells was measured spectrophotometrically using SpectraMax® Plus^{384} (Molecular Devices, Sunnyvale, CA) at 490 nm. The cell viability was expressed by the following equation: cell viability (%) = (absorbance intensity of treated cells / absorbance intensity of untreated cells (control)) x 100.

In vitro visualization of transfection of BMSCs with PEI-pEGFP-N1 complexes

To determine the *in vitro* qualitative fluorescence expressed by EGFP-N1, BMSCs were plated at a density of 50,000 cells/well in clear, flat-bottom, 8-chambered glass slides with cover (Lab-Tek, Nunc™, NY) previously coated with 0.1 % poly-L-lysine and allowed to attach overnight. The next day, cell culture medium was removed and cells were incubated with complexes fabricated at a N/P ratio of 10 containing 1 µg pEGFP-N1 in serum-free medium for 4 h or 24 h and processed as described above. Untreated cells, cells treated with uncomplexed pEGFP-N1 and cells treated with PEI alone were used as controls. After a total incubation time of 48 h, cells were fixed with 4 % paraformaldehyde (Hatfield, PA), followed by permeabilization of cells with 0.2 %

Triton® X-100. Cellular actin was fluorescently tagged by treating the cells with Alexa Fluor® 568 phalloidin. The specimen was mounted with Vectashield® Hardset™ medium containing DAPI. Cells were washed with PBS during every step in the process. The cellular fluorescence was observed using confocal laser scanning microscopy (60X, Carl Zeiss 710, Germany) equipped with Zen 2009 imaging software. The images were processed using ImageJ® open access software (National Institutes of Health, MD).

In vitro evaluation of transfection of BMSCs with PEI-pPDGF-B complexes

The transfection in BMSCs was further evaluated by using pDNA encoding for the PDGF-B protein. Cells were plated at a seeding density of 80,000 cells/well in 24-well plates. The PEI-pPDGF-B complexes containing 1 μg pPDGF-B were prepared at a N/P ratio of 10, incubated with cells for 4 h and the experiment processed as above. After a total incubation time of 48 h, the cell culture supernatants were then harvested by centrifugation after 4 h of incubation with medium supplemented with 10 μg/ml heparin to prevent retention of PDGF-BB on the cell surface. The amounts of PDGF-BB in cell culture supernatants were quantified using a PDGF-BB ELISA kit. Untreated cells and cells treated with naked, uncomplexed plasmids were employed as controls.

Fabrication and characterization of PEI-pPDGF-B complex-loaded scaffolds

Polyethylenimine was mixed with pPDGF-B to prepare complexes at an N/P ratio of 10 according to the method described above. Complexes were then injected into the collagen scaffolds that were previously cut into 5 mm x 2 mm discs and were freeze-dried for subsequent use. The surface characteristics of the scaffolds, before and after

loading with complexes and lyophilization, were studied using scanning electron microscopy (SEM, Hitachi Model S-4800, Japan). The scaffolds were either empty or loaded with the PEI-pPDGF-B complexes. These scaffolds discs were mounted on aluminum specimen stubs using adhesive carbon tape and coated by ion sputtering with conductive gold (10 mA for 2.5 min) (K550 Emitech Sputter Coater, TX). The surface morphology was examined using the microscope operated at 3 kV accelerating voltage.

Attachment and proliferation of BMSCs on collagen scaffolds

The interaction and proliferation of BMSCs within the scaffolds loaded with PEI-pPDGF-B complexes prepared at a N/P ratio of 10 was evaluated *in vitro* using SEM and confocal microscopy, respectively. Empty scaffolds and complex-loaded scaffolds incorporating 50 μg pPDGF-B were placed into the wells of a 48-well plate. For the SEM analysis of cell attachment, 100 μl of cell culture medium containing 90,000 cells were seeded onto a single scaffold per well. After 3 to 4.5 h, 400 μl of culture medium was added to cover the scaffold completely and kept in culture for 6 days. For cell proliferation analysis, 390,000 cells were seeded onto each scaffold in a single well and cultured for 3 days. At the end of the experiment, the scaffolds were washed and fixed overnight in 2.5 % glutaraldehyde in 0.1 M sodium cacodylate buffer (pH 7.2) for SEM and in zinc formalin for confocal microscopy.

SEM sample preparations

Standard methods for SEM were employed. Briefly, after aldehyde fixation, the scaffolds were post-fixed for 1 h at room temperature with a 1 % solution of osmium

tetroxide in 0.1 M sodium cacodylate buffer. The samples were dehydrated through a series of ethanol washes up to 100 % ethanol before being submitted to critical point drying with CO_2 for 2 h. The samples were then mounted onto aluminum stubs, sputter-coated and examined with a Hitachi S-4800.

Immunocytochemical staining

The fixed samples were cryo-embedded and cryo-sectioned at 10 μm thickness along the vertical plane of the scaffolds. Cryo-sections were collected on Superfrost Plus Slides (Fisher Scientific®, Fairlawn, NJ) and were post-fixed before incubating for 10 min with a 0.1 % solution of Triton X-100. After endogenous biotin block, the background staining was blocked by treating the samples with 5 % normal goat sera diluted in PBS (Sigma) for 1 h. This was followed by an incubation of the samples for 30 min with 5 μg/ml mouse anti-proliferating cell nuclear antigen (PCNA) primary antibody (Invitrogen) against PCNA. The samples were then treated with biotinylated anti-mouse IgG secondary antibody (Vector Laboratories, Inc.) for 10 min. Finally, the sections were incubated for 45 min with Streptavidin-Alexa Fluor 488 conjugate (Invitrogen). Negative controls were treated as described above but the specific primary antibody was replaced by a normal mouse IgG match at the same final concentration (Jackson Immunoresearch Laboratories, Inc. West Grove, PA). The washes between each step were performed with 1X PBS. The sections were mounted under coverglasses with Vectashield® containing DAPI and observed for the fluorescently-labeled antigen using a Zeiss 710 laser scanning microscope.

In vivo implantation of complex-loaded collagen scaffolds

Inbred 14 week-old male Fisher (CDF®) white rats (F344/DuCrl, ~ 250 g) were obtained from Charles River Laboratories International, Inc (Wilmington, MA) and housed and cared for in University of Iowa animal facilities. The surgical procedures were approved by and performed according to guidelines established by the University of Iowa Institutional Animal Care and Use Committee. The animals were anaesthetized by intra-peritoneal injection of ketamine (80 mg/kg)-xylazine (8mg/kg) mixture. A sagittal incision, ~ 1.5-2 cm, was made on the scalp of each rat, and the calvaria was exposed by blunt dissection. Two, 5 mm diameter x 2 mm thickness critical-sized defects were generated using a round carbide bur on the parietal bone, on both sides of the sagittal suture. The defects were randomly allocated into the following study groups: (1) empty defects (n = 3); (2) empty scaffolds (n = 5); and (3) PEI-pPDGF-B complex-loaded scaffolds (n = 5). Where applicable, the scaffold was cut into cylinders with a diameter of 5 mm and a thickness of 2 mm and implanted into the defect region. The incision was closed in layers using sterile silk sutures. Buprenorphine (0.15 mg, intramuscular), as an analgesic, was administered to each rat thereafter and the animals were carefully monitored during post-operative recovery. The rats were able to function normally after this procedure. After 4 weeks, all the animals were euthanized and the bony segments containing the regions of interest were cut from the calvarial bone and fixed in 10 % neutral buffered formalin.

micro-CT measurement

Three-dimensional microfocus x-ray microcomputed tomography (μCT) imaging was performed on the specimens using a cone-beam μCT system (μCT40, Scanco Medical AG, Switzerland). Specimens were scanned in 70% ethanol at 55 kVp and 145 μA with a voxel size of 10 μm and an integration time of 300 ms. Analysis was performed using a constant 3.5 mm diameter circular region of interest that was placed in the center of the machined defect and spanned a total of 50 reconstructed slices, such that a total cylindrical volume of interest of ~3.8 mm^3 oriented perpendicular to the outer table of the calvarium was analyzed for each specimen using the instrument's software (sigma = 0.8, support = 1.0, and threshold = 250). Bone volume (BV) per total volume (TV) and connectivity density (Conn.D.) in the bone defect were obtained.

Histological observation of rat bone samples

After treatment, the bone samples underwent a decalcification (Surgipath, Decalcifier II) procedure. When the decalcification end point test returned negative for the presence of calcium, the rat bone specimens (n = 3 for empty defect, n = 5 for empty scaffolds, n = 5 for complex-loaded scaffolds) were introduced into a paraffin processor, paraffin embedded, and blocks were sectioned in the sagittal plane for each specimen. Histological analysis was performed on the 5 μm sections in the central portion of the wound. The sections were collected on Superfrost Plus Slides (Fisher Scientific®), deparaffinized and stained with Harris hematoxylin and eosin (H & E staining) according to standard protocols. Five to six sections, representing the central area of each defect, were used to observe the presence of collagen, new bone formation, and cells in order to

evaluate bone regeneration after 4 weeks *in vivo* implantation. The brightfield examination of the slides was done with an Olympus Stereoscope SZX12 and an Olympus BX61 microscope, both equipped with a digital camera.

Data presentation and statistical analysis

Nonparametric methods were employed to avoid inappropriate distributional assumptions, and exact tests were used whenever feasible. The Kruskal-Wallis procedure was used to assess differences in the outcome of interest among groups; the Wilcoxon Rank Sum test is the equivalent procedure for comparisons of two groups. A Type I error level of 0.05 was utilized throughout, and adjustment for multiple pairwise group comparisons was primarily made using an adaptation of the Tukey method due to Conover in conjunction with an overall 5% level of significance [185]. This asymptotic approach was used for all but the *in vivo* studies, where it was feasible to adjust for multiple pairwise comparisons using exact Wilcoxon Rank Sum tests and a standard Bonferroni correction, again specifying an experiment-wise Type I error of 0.05. Spearman rank correlations were used to evaluate the relationship between N/P ratio and cell viability. Statistical analyses were carried out using SAS® software, version 9.3 (SAS Institute Inc., Cary, NC). Graphs were generated using Prism 5.0 (GraphPad Software Inc., San Diego, CA); numerical data were represented as means with bars representing standard deviations.

Results and discussion

This report investigates the effects of delivery of PEI-complexed pDNA encoding for PDGF-B from porous 3-D collagen scaffolds on bone tissue regeneration. This form of gene-activated matrix (GAM) provides localized transient gene therapy since the *PDGF-B* gene will not be integrated into the host chromosome [48, 139]. The transfection efficiencies of PEI-condensed pDNA complexes are significantly affected by the type of cells being transfected, therefore making it necessary to optimize the gene delivery method for every cell line used. As a result, we first optimized the amine to phosphate (N/P) ratio of the PEI-pPDGF-B complexes so as to generate the maximum transfection in BMSCs with minimal cytotoxicity. We prepared complexes at different N/P ratios and evaluated the influence of the ratio stoichiometry on transfection efficiency and toxicity in BMSCs. It is critical for gene therapy applications that clinical amounts of proteins are produced by the transfected cells and that the gene expression levels are tightly regulated. To address the feasibility and potency concerns, GAMs containing physically entrapped *PDGF-B* plasmid genes were implanted in a rat calvarial defect model and the bone regenerative capacity was assessed. In this study, it is also important to note that the amounts of PEI and pDNA utilized were significantly lower than the amounts used in other studies evaluating GAMs [45, 122].

Generation of pDNA encoding LUC, EGFP-N1 or PDGF-B proteins

The purity of extracted pDNA as determined by the ratio of absorbance (A260 nm/A280 nm) was within the range of 1.8 to 2.0 (recommended by the manufacturer's protocol). The concentration of pDNA solution was determined by UV absorbance at

260nm and was further concentrated as needed. Agarose gel electrophoresis confirmed the size and quality of pDNA without any signs of degradation.

Size and surface charge of PEI-pPDGF-B complexes

The PEI-pPDGF-B complexes at a N/P ratio of 10 were prepared as described above. The complexes were 102 ± 2 nm in size with a net surface charge of +37 ± 1 mV. The polydispersity index (PDI) was approximately 0.1, thus indicating a narrow size distribution, high uniformity in particle size distribution and overall general homogeneity of the sample. The size and surface charge of the complexes are both important parameters for their interaction and entry into cells [149, 186]. The small size of the polycation-condensed pDNA complexes is critical for both efficient *in vitro* cellular uptake by clathrin-mediated endocytosis [187] as well as *in vivo* distribution and diffusion in the tissues [188]. With regards to the surface charge of the complexes, there has to be a balance between the maximal transfection efficiency and the amount of cell death associated with transfection [141, 189]. In this study, we focused on localized gene therapy, and therefore the effects of the net positive charge on binding and inactivation of the cationic polymer-pDNA complexes by the circulating proteins and the subsequent complement activation, along with the induced recognition by cells of the reticuloendothelial system [190], are of lesser concern.

In vitro gene expression by PEI-pLUC complexes

One microgram of pLUC was combined with different amounts of PEI (Table 4.1) to generate complexes with varying N/P ratios. We quantified the luciferase protein

formation due to gene expression after incubating the complexes with BMSCs for 4 h or 24 h (Figure 4.1). The levels of *LUC* gene expression were significantly affected by the transfection efficiencies of the different N/P ratios of the complexes. The values are expressed as mean ± SD for each treatment (n = 3). A Kruskal-Wallis procedure indicated that the distribution of transfection outcomes differed among the treatment groups at both 4 h ($p = 0.0019$) or 24 h ($p = 0.0024$). The transfection efficiency of the PEI-pLUC complexes increased as the N/P ratio at which PEI-pLUC complexes were prepared increased from 1 (0.13 μg PEI) to 10 (1.30 μg PEI). The transfection efficiency then dropped in cells treated with PEI-pLUC complexes prepared at a N/P ratio of 15 (1.95 μg PEI) and dropped further in cells treated with PEI-pLUC complexes prepared at a N/P ratio of 20 (2.6 μg PEI). At 24 h of incubation with the cells, complexes prepared at a N/P ratio of 5 showed an increase in the amount of transgene expression obtained compared to only 4 h incubation. This may be due to higher uptake and entry of the complexes into the cells over a period of time. The factors contributing to low transfection efficiencies of complexes prepared at N/P ratios < 10 include size and surface charge, pDNA binding and condensation capacity, and stability of the complexes. The mean response for complexes prepared at a N/P ratio of 10 at 4 h of treatment was significantly greater (more efficient transfection of BMSCs) than that for complexes prepared at all other N/P ratios considered after adjustment for all multiple pairwise comparisons. However, the LUC protein expression obtained in cells decreased at 24 h of incubation with complexes prepared at a N/P ratio of 10 as a result of cytotoxicity induced by PEI (see section below). The toxicity of PEI in BMSCs also led to a decline in the levels of protein expression achieved when the cells were treated with complexes

prepared at higher N/P ratios of 15 and 20 at 4 h or 24 h of treatment. The gene expression generated by complexes prepared at a N/P ratio of 15 was found to be lower than the transfection resulting from complexes prepared at a N/P ratio of 10 at 4 h of treatment which reduced further at 24 h of treatment. At 4 h of incubation with BMSCs, the transgene expression generated by complexes prepared at a N/P ratio of 20 was lower when compared to complexes prepared at a N/P ratio of 15, and in a manner similar to complexes at N/P ratios of 10 and 15, the transfection efficiency decreased at 24 h of incubation time. This result is comparable to the transfection data from treatment of the HEPM cells with the PEI-pDNA complexes as discussed in Chapter III.

In vitro cell viability assay for PEI-pLUC complexes

The toxicity of PEI-pLUC complexes prepared at various N/P ratios containing 1 µg of pLUC (Table 4.1) was assessed in BMSCs treated with the complexes for 4 h or 24 h. The amount of PEI in the complexes prepared at different N/P ratios was found to have a significant effect on cell viability (Figure 4.2). Values are expressed as mean ± SD for each treatment performed in triplicate. Results of the Kruskal-Wallis test provided evidence that the distribution of cell viability outcomes differed significantly among the treatment groups assayed at both 4 h ($p = 0.0057$) or 24 h ($p = 0.0024$). A strong and highly significant negative correlation between N/P carrier ratio and % cell viability was detected using the Spearman rank correlation at both 4 h ($r = -0.88$, $p < 0.0001$) or 24 h ($r = -0.97$, $p < 0.0001$). Approximately 82 % of BMSCs were viable at 4 h when treated with PEI-pLUC complexes prepared at a N/P ratio of 10. However, cell viability decreased to 34 % when complexes were incubated with cells for 24 h, leading to a

corresponding decrease in the transgene expression (Figures 4.1 and 4.2). Complexes of PEI-pLUC prepared at N/P ratios higher than 10 resulted in elevated cytotoxicity and therefore lower transgene expressions following incubation in cells at both 4 h or 24 h. These data clearly suggest that high amounts of PEI and prolonged cell-PEI exposure times are cytotoxic. These findings are in agreement with previously reported results showing successful non-viral gene delivery with PEI-pDNA complexes as a critical balance between sufficient PEI to ensure high transfection efficiency without causing high cytotoxicity [177, 191]. The PEI-pLUC complexes prepared at N/P ratios of 1 and 5 were relatively non-toxic, but demonstrated low transfection efficiencies in BMSCs. In our study, only the PEI-pLUC complexes prepared at N/P ratio of 10 displayed a balance between relatively high transgene expression and low cytotoxicity. Accordingly, the PEI-pDNA complexes used in the subsequent *in vitro* and *in vivo* experiments were fabricated at a N/P ratio of 10.

In vitro gene expression by PEI-pEGFP-N1 complexes

The transfection in BMSCs was further evaluated using confocal microscopy with fluorescent probes. Cells were transfected with complexes prepared at N/P ratio of 10 containing 1 μg of pEGFP-N1 at the treatment time points of 4 h or 24 h (Figure 4.3). Confocal images (Z-series, 63X) showed the characteristic green fluorescence in the transfected cells at both 4 h or 24 h due to expression of the gene and formation of the EGFP-N1 protein. In these fixed cells, phalloidin permeated the plasma membrane to stain the cytoplasmic F-actin in red. The cell nuclei were stained blue by DAPI. The cells in the control groups (untreated cells, cells treated with uncomplexed pEGFP-N1 and

PEI-treated cells) did not show any green fluorescence (data not shown). Confocal microscopy imaging, along with the quantitative results obtained earlier, thus confirmed the capability of the PEI-pDNA complexes to efficiently transfect BMSCs.

In vitro investigation of gene expression by PEI-pPDGF-B complexes

Since this study was targeted towards bone regeneration in a defect, we evaluated the gene delivery efficacy of the PEI-pPDGF-B complexes through expression of PDGF-BB. Platelet-derived growth factor is a required element in angiogenesis, is a potent mitogen for mesenchymal and progenitor cells and drives the chemotaxis of osteoblast and vascular endothelial cells [162, 192]. It also stimulates osteoblast type-1 collagen synthesis and extracellular matrix secretion. Based on the N/P ratio optimization experiments performed previously, we assessed the transfection efficiency of PEI-pPDGF-B complexes prepared at a N/P ratio of 10 containing 1 μg pPDGF-B in BMSCs for 4 h. The PDGF-BB ELISA quantified PDGF-BB protein formation further confirming the transfection potential of the PEI-pDNA complexes in our target cells. The data is represented as mean ± SD for each treatment carried out in triplicate. After the transfection of cells with the PEI-pPDGF-B complexes, PDGF-BB levels in cell culture medium supernatants (83 pg/ml) were approximately 6-fold higher than in cells treated with the naked, uncomplexed pPDGF-B (14 pg/ml) (Figure 4.4). The highest PDGF-BB protein expression levels (83 pg/ml) were obtained by treating the cells with 1 μg pPDGF-B for 4 h, followed by further incubation for 44 h. Initial attempts at detecting PDGF-BB using ELISA resulted in low levels of detectable PDGF-BB. Heparin can prevent the reuptake of secreted proteins, thereby allowing for a more accurate estimation

of its secretion but has never been evaluated for its potential to improve detection of proteins following PEI-pDNA complex transfections [193]. We showed that heparin, when added to the cells 4 h prior to the analysis, resulted in an increased detection in the protein levels of PDGF-BB (132 pg/ml). The data provided strong evidence that the distribution of PDGF-BB concentrations differed among the treatment groups ($p = 6.5 \times 10^{-5}$, Kruskal-Wallis test). After adjustment for multiple pairwise comparisons, significantly more PDGF-BB was found to be produced by the cells transfected with PEI-pPDGF-B complexes or PEI-pPDGF-B complexes followed by heparin treatment relative to that produced by control or naked pDNA groups. Furthermore, significantly more PDGF-BB was secreted by the cells transfected with PEI-pPDGF-B complexes following heparin treatment versus without heparin treatment. These results also verified the ability of PEI-pDNA complexes to efficiently transfect BMSCs with therapeutically relevant genes.

SEM analysis of collagen scaffolds

The collagen scaffold was characterized using SEM. The resorbable collagen scaffold showed a highly interconnecting porous structure, with pore diameters ranging from 100-200 μm (Figure 4.5a). The incorporation of complexes within the scaffolds and the subsequent lyophilization procedure did not appear to have any significant effect on the morphology or the microarchitecture of the final scaffold biomaterial (Figure 4.5b). Three-dimensional porous polymer scaffolds, such as the collagen scaffold utilized here can create and maintain a space within the defect *in vivo*. This helps recruit the healthy pre-osteoblasts and osteoblasts to the wound site, enhances their proliferation and

differentiation and forms a space-filling tissue [49]. These important processes ultimately help control the size and shape of the regenerated bone tissue within the defect.

SEM and confocal analysis of attachment and proliferation of BMSCs on collagen scaffolds

In order to provide a favorable environment for bone regeneration, the scaffold must provide sites for cellular attachment and support cell survival and growth. It is desirable that the implanted scaffold is inert and biodegradable when the new tissue is regenerated by the osteogenic cells [194, 195]. Type I collagen constitutes the main protein component of natural extracellular matrices and plays an important role in the process of repair of damaged tissue [196, 197]. It is particularly important for bone regeneration involving this guided bone-growth approach that the collagen scaffold has sufficient physical and mechanical properties to provide physical support and retain its original geometry following *in vivo* implantation in order to fill-in specific critical-sized defects. Type I collagen matrices have been previously reported to serve as a platform for cell adhesion and migration, and direct the growth of cells [170, 196, 198, 199]. After 6 days in cell culture, we found that the scaffold surface was vastly different from the images obtained earlier in this study prior to incubating it with cells and the cell culture medium (Figures 4.5a-c). This may possibly be due to the degradation of collagen. Morphological changes were observed on the surface of the porous scaffold material and inner walls of the pores after cell culture treatment. High magnification SEM imaging demonstrated the recruitment and attachment of BMSCs into the scaffold containing PEI-pPDGF-B complexes (Figure 4.5d). We observed BMSCs adhering to the scaffolds via

various cell processes. The cell morphology was found to be spindle-shaped with branched cytoplasm. These highly porous scaffolds supported cell anchorage and with pore sizes greater than the size of cells, provided adequate space within the scaffold to allow migration of cells into the scaffold through the pores. The complex-loaded scaffolds would therefore be expected to allow cells from the surrounding tissues into the wound site to stimulate their growth and differentiation, thus promoting tissue development [53].

It has been determined from the experiment above that PEI-pPDGF-B complexes are able to transfect BMSCs efficiently, which then allows for expression of the PDGF-BB protein. Platelet derived growth factor is a cytokine that regulates cell growth and cellular division for bone-forming cells and functions as a mitogenic and chemotactic agent [192, 200, 201]. The complex-loaded scaffold matrix was therefore evaluated for its ability to promote *in vitro* cell proliferation next, by detecting and quantifying the presence of dividing cells in culture using indirect immunocytochemistry and immunofluorescence assays [202]. Immunofluorescence staining was utilized to investigate cellular proliferation by the indirect fluorescent labeling of the nuclear protein, PCNA. This was accomplished using mouse anti-PCNA primary antibody expressed against PCNA, to detect the levels of expression of PCNA in the proliferating cells. PCNA plays an integral role in the eukaryotic cell cycle and is essential for cellular DNA synthesis [203]. This unconjugated, monoclonal, IgG2a antibody is specific to multiple PCNAs which are expressed during DNA synthesis, and hence are a useful tool for studying the proliferating healthy cells. As a control for the experiment, negative staining done using normal IgG in place of the specific primary antibody did not show

any green fluorescence (data not shown). After incubating the complex-loaded scaffolds for 3 days in culture medium with BMSCs, the scaffolds were harvested, stained and observed under a confocal microscope to detect proliferating cells (green fluorescence). The nuclei of cells were stained by DAPI (blue fluorescence). Cells were counted under the same magnification (20X). At day 3, significantly higher numbers of proliferating BMSCs were observed with scaffolds containing PEI-pPDGF-B complexes compared to empty scaffolds ($p = 0.0079$, Wilcoxon Rank Sum test) (Figures 4.6a-b). The number of proliferating cells in the scaffolds was 3.4-fold higher with the complex-treated group than that obtained with the untreated group (Figure 4.6c). Confocal imaging confirmed the recruitment of BMSCs into the scaffold containing PEI-pPDGF-B complexes and their subsequent proliferation compared to empty scaffolds, therefore validating the important role of PDGF-BB in chemotaxis and growth of cells potentially capable of osteogenesis.

In vivo bone regeneration

The collagen scaffold matrix containing PEI-pPDGF-B complexes was evaluated *in vivo* for its efficacy as a bone regenerative biomaterial unit. Critical-sized calvarial defects were created in rats and were utilized as a model to test the *in vivo* efficacy of three different treatment groups: (1) empty defects (untreated) as a control, (2) defect filled with empty collagen scaffolds, and (3) defect filled with PEI-pPDGF-B complexes entrapped in collagen scaffolds. The rats were sacrificed after 4 weeks and newly-formed bone tissue was evaluated for its volume and connectivity density using micro-CT scans. The micro-CT scan imaged the circular bone defects induced and the regenerated bone

tissue in the defects as a result of various treatments (Figures 4.7a-f). The defect site was most significantly bridged with bone when treated with the scaffolds containing PEI-pPDGF-B complexes compared to other groups tested. The amount of bone tissue regenerated was quantified by analyzing the bone formation parameters, trabecular bone volume fraction of the total tissue volume of interest (BV/TV) and the degree of trabecular connectivity (connectivity density or thickness). The BV/TV was 44-fold and 14-fold higher in defects treated with complex-embedded scaffolds when compared to the empty scaffold and empty defect control groups, respectively (Figure 4.7g). The data provided evidence that the distribution of BV/TV differed significantly among the three comparison groups ($p = 0.0025$, Kruskal-Wallis test). When pairwise group comparisons were made using exact Wilcoxon Rank Sum tests, a significant difference was found in the distribution of BV/TV between the complex-embedded scaffold and the empty scaffold groups ($p = 0.0079$); this remained significant after Bonferroni adjustment for multiple comparisons. The difference between the complex-embedded scaffold and the empty defect groups, after adjustment for multiple comparisons, gave a p value that was equal to 0.0357. The connectivity density of the regenerated bone was 36-fold and 52-fold greater for the complex-loaded scaffold group than for the empty scaffold group and empty defect control group, respectively (Figure 4.7h). The distribution of connectivity density also differed significantly among the three comparison groups ($p = 0.0016$, Kruskal-Wallis test). Pairwise comparisons via exact the Wilcoxon Rank Sum test provided strong evidence of a difference in connectivity density between the complex-embedded scaffold and the empty scaffold groups ($p = 0.0079$) which was significant after Bonferroni adjustment for multiple comparisons; a difference was also seen between

the complex-embedded scaffold and the empty defect control groups ($p = 0.0357$). Histology images with H & E staining further validated the μCT results (Figure 4.8). The empty defect images showed that the gap between the healthy native bone edges was unfilled, while the empty scaffold group showed only loose, soft tissue formation with a thin rim of new bone forming at the edges of the defect (Figures 4.8a-b). For the complex-loaded scaffold group, we observed complete bridging of the defect by the mature, mineralized bone tissue indicated by the arrows (Figure 4.8c). We hypothesize that the complexes may have released from the degrading matrix, which then will transfect the surrounding cells. It is also possible that the cells could have migrated into the porous matrix containing the complexes followed by their transfection by the complexes. These transfected cells produce PDGF-BB which stimulates cellular proliferation, cell growth and division, and angiogenesis [162]. Platelet derived growth factor signaling is also involved in cell migration, tissue remodeling and cellular differentiation of pre-osteoblasts into osteoblasts that initiate bone formation by secreting the osteoid matrix that mineralizes to form mature bone tissue [204]. The chemotactic action of PDGF further augments these processes. Ultimately, new bone material is laid down by the osteogenic cells by communication through cytokine PDGF signaling.

Conclusions

In summary, BMSCs were efficiently transfected with a variety of reporter or therapeutic genes when using PEI-pDNA complexes prepared at an optimal N/P ratio of 10. These PEI-pDNA complexes were stable and nanometer-sized, with a net positive surface charge. The PEI-pPDGF-B complex-activated collagen scaffolds favored cellular

attachment and promoted cellular proliferation *in vitro*. The complex-loaded scaffolds promoted osteogenesis and demonstrated superior tissue regeneration efficacy in calvarial defects in rats when compared to the empty defect and empty scaffold groups. This system efficaciously delivered pDNA into the cells without any apparent adverse effects. Gene activated matrices encoding for PDGF-B protein therefore have a strong potential for clinical applications that require enhanced bone regeneration.

Table 4.1. PEI amount in different N/P ratios used for formulating PEI-pDNA complexes (using 1 µg pDNA).

N/P ratio	PEI amount (µg)
1	0.13
5	0.65
10	1.30
15	1.95
20	2.6

Figure 4.1. Luciferase assay assessing the effect of N/P ratio on the transfection capability of PEI-pLUC complexes in BMSCs at 4 h or 24 h (n = 3).

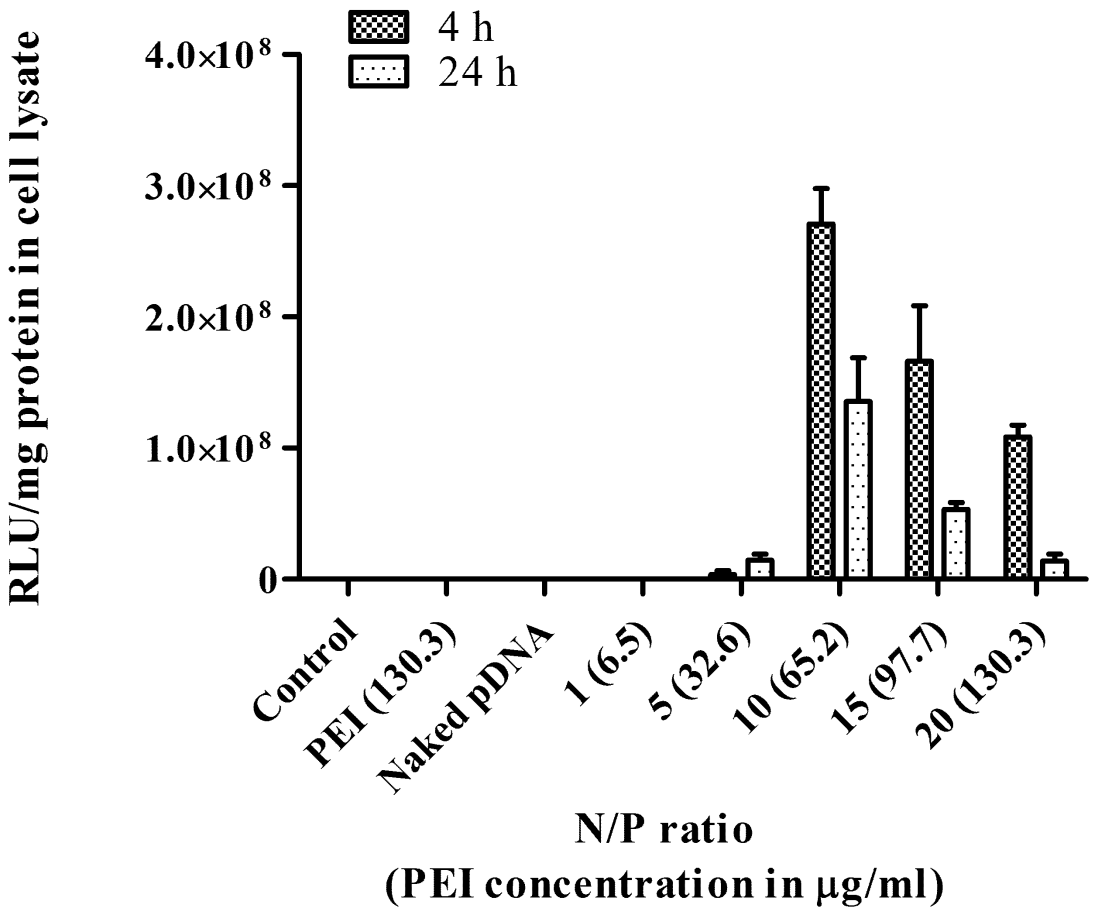

Figure 4.2. MTS assay assessing the effect of N/P ratio on the biocompatibility of PEI-pLUC complexes in BMSCs at 4 h or 24 h (n = 3).

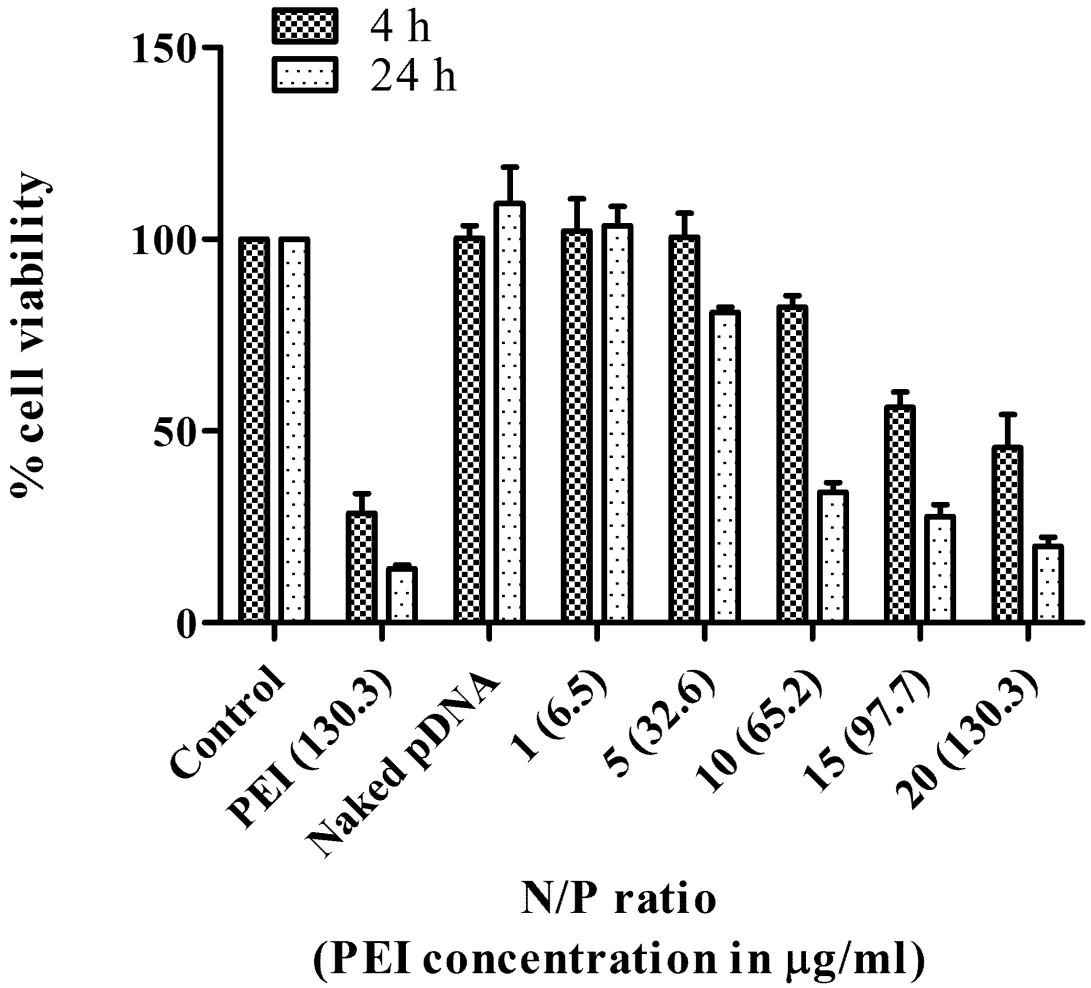

Figure 4.3. Confocal micrographs demonstrating transfection in BMSCs after 4 h or 24 h of treatment with PEI-pEGFP complexes fabricated at a N/P ratio of 10: nuclei (blue, DAPI-stained); cytoplasm and cell membrane (red, phalloidin-stained); and EGFP-N1 (green). Scale bar, 20µm.

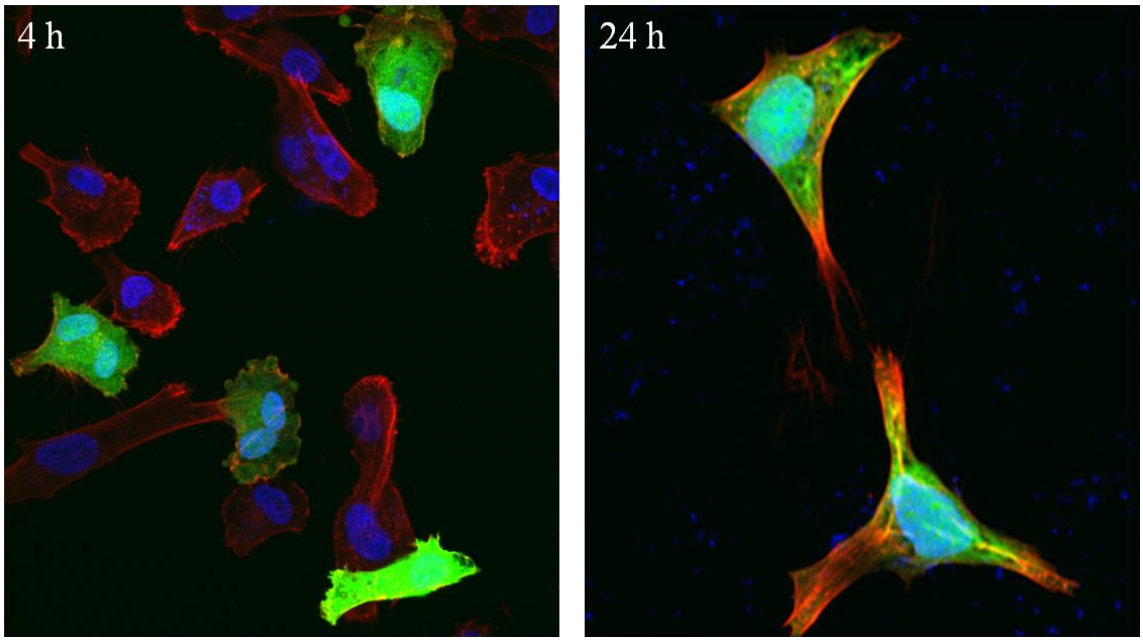

Figure 4.4. ELISA assay demonstrating the expression of PDGF-BB protein as a result of transfection of BMSCs with PEI-pPDGF-B complexes for 4 h (n = 3).

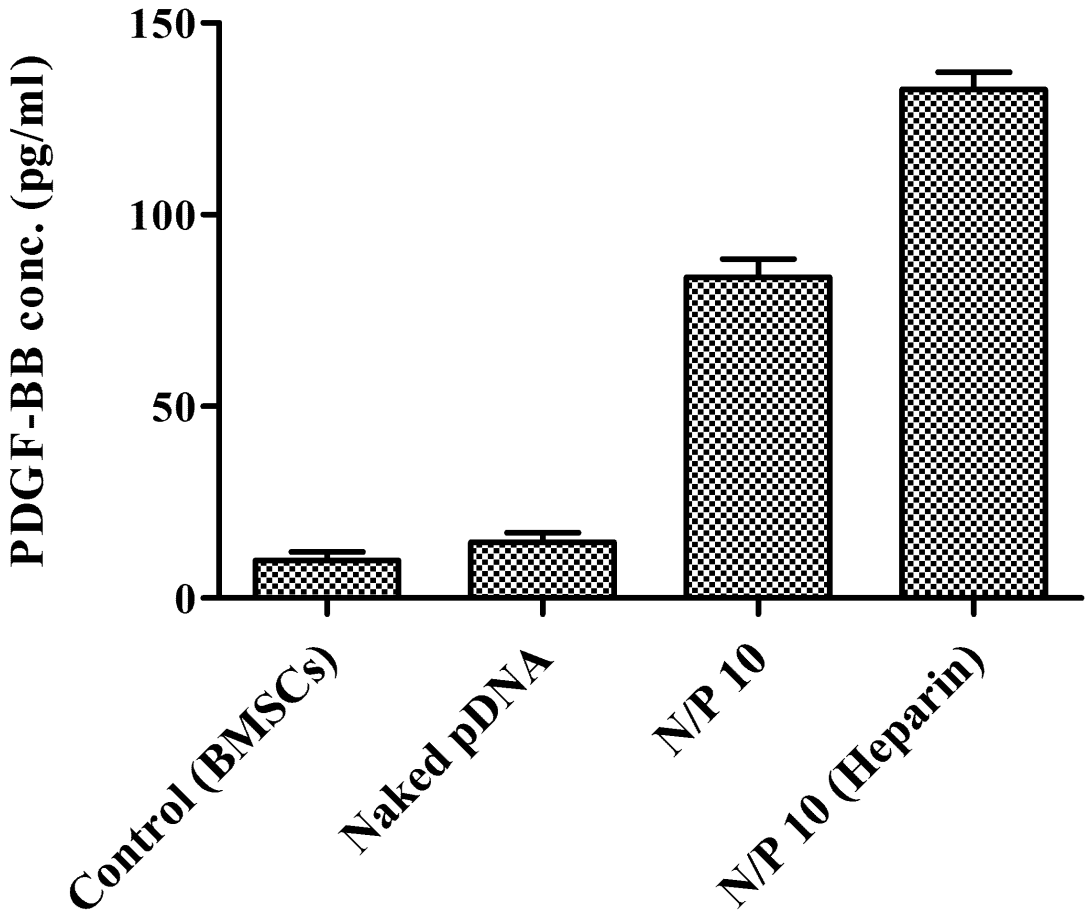

Figure 4.5. SEM images of empty collagen scaffolds (a) and collagen scaffolds embedded with PEI-pPDGF-B complexes (b); SEM images showing complex-loaded scaffolds seeded with BMSCs, low magnification (200X) (c) and adhesion of BMSCs to the complex-loaded scaffolds (arrows), high magnification (3500X) (d) at day 6 of incubation.

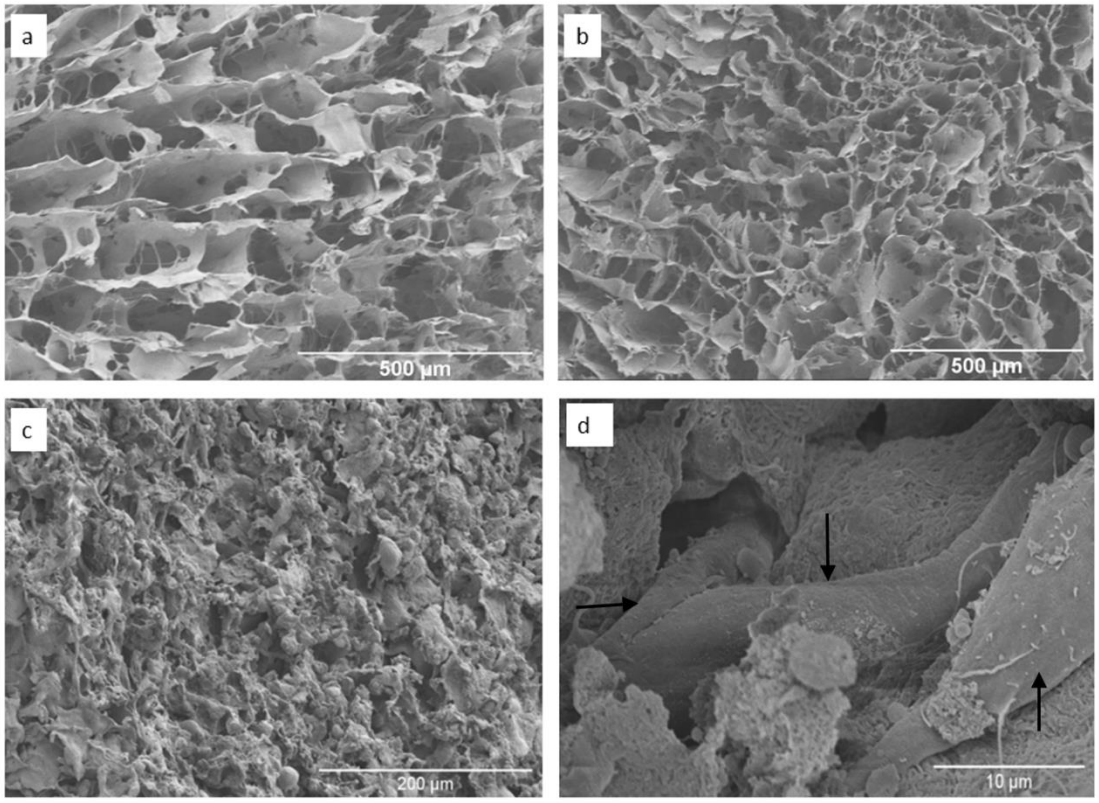

Figure 4.6. Influence of the complex-loaded scaffolds on proliferation of BMSCs: confocal image demonstrating proliferating cells [DAPI (blue)- and PCNA (green)-positive cells] on empty scaffolds (20X) (a) and on PEI-pPDGF-B complex-loaded scaffolds (20X) (b); measurement of proliferation of BMSCs seeded on empty scaffolds compared to complex-loaded scaffolds (c) at day 3 of culture (n = 6). Scale bar, 20 µm.

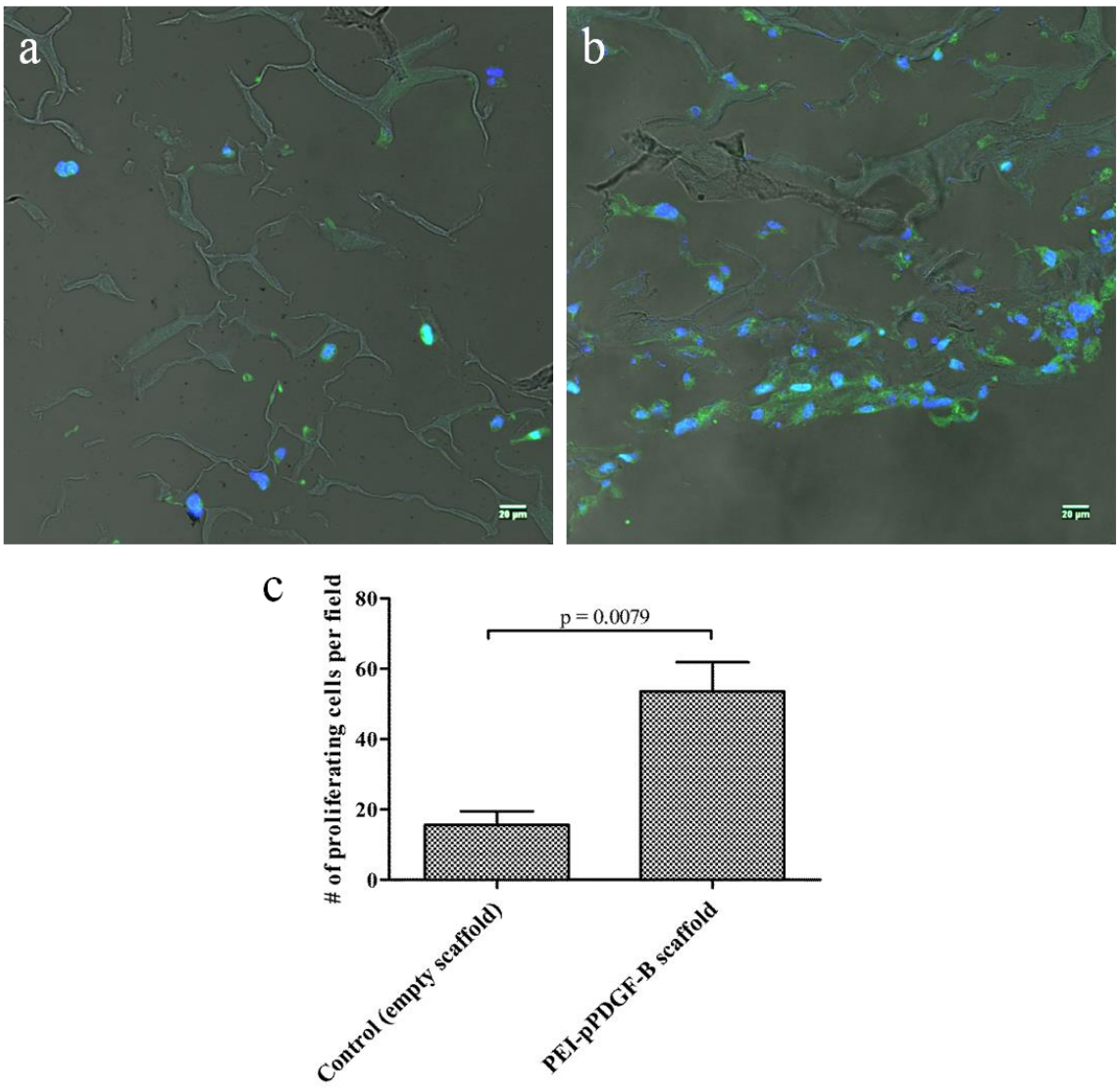

Figure 4.7. Evaluation of *in vivo* bone formation: representative micro-CT scans showing the level of regenerated bone tissue after 4 weeks in empty defects (a, d, n = 3); empty scaffolds (b, e, n = 5); and PEI-pPDGF-B complex-loaded scaffolds (c, f, n = 5); assessment of regenerated bone volume fraction (g) and bone connectivity density (h) in different groups. Scale bar, 1 mm.

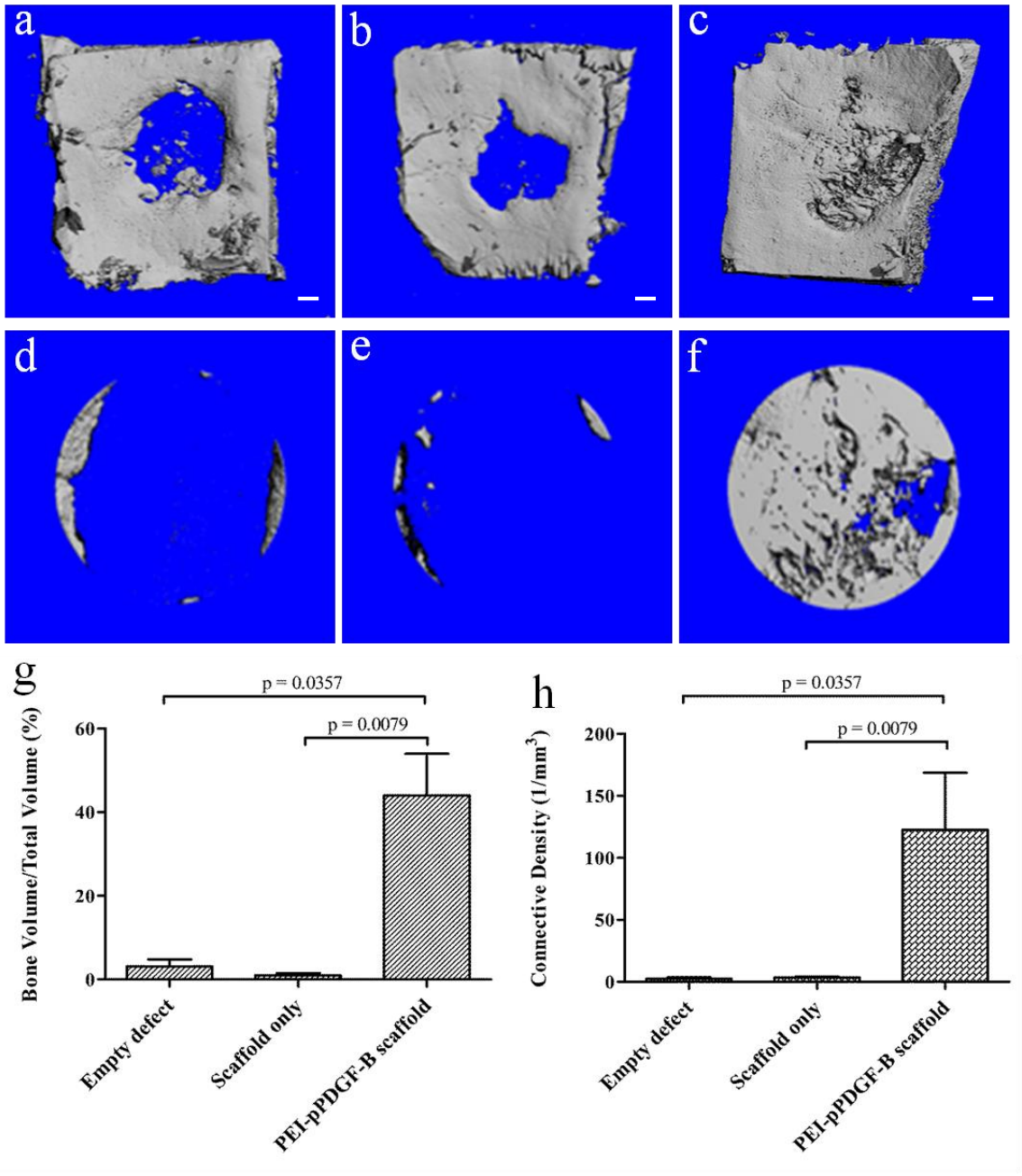

Figure 4.8. Representative histology sections demonstrating the extent of new bone formation in the defects at 4 weeks due to various treatments: empty defects (a); empty scaffolds (b); and PEI-pPDGF-B complex-loaded scaffolds (c). OB = old bone and NB = new bone. Note the complete bridging of new bone in the PEI-pPDGF-B complex-loaded test group indicated by the arrows. Scale bar, 50 μm.

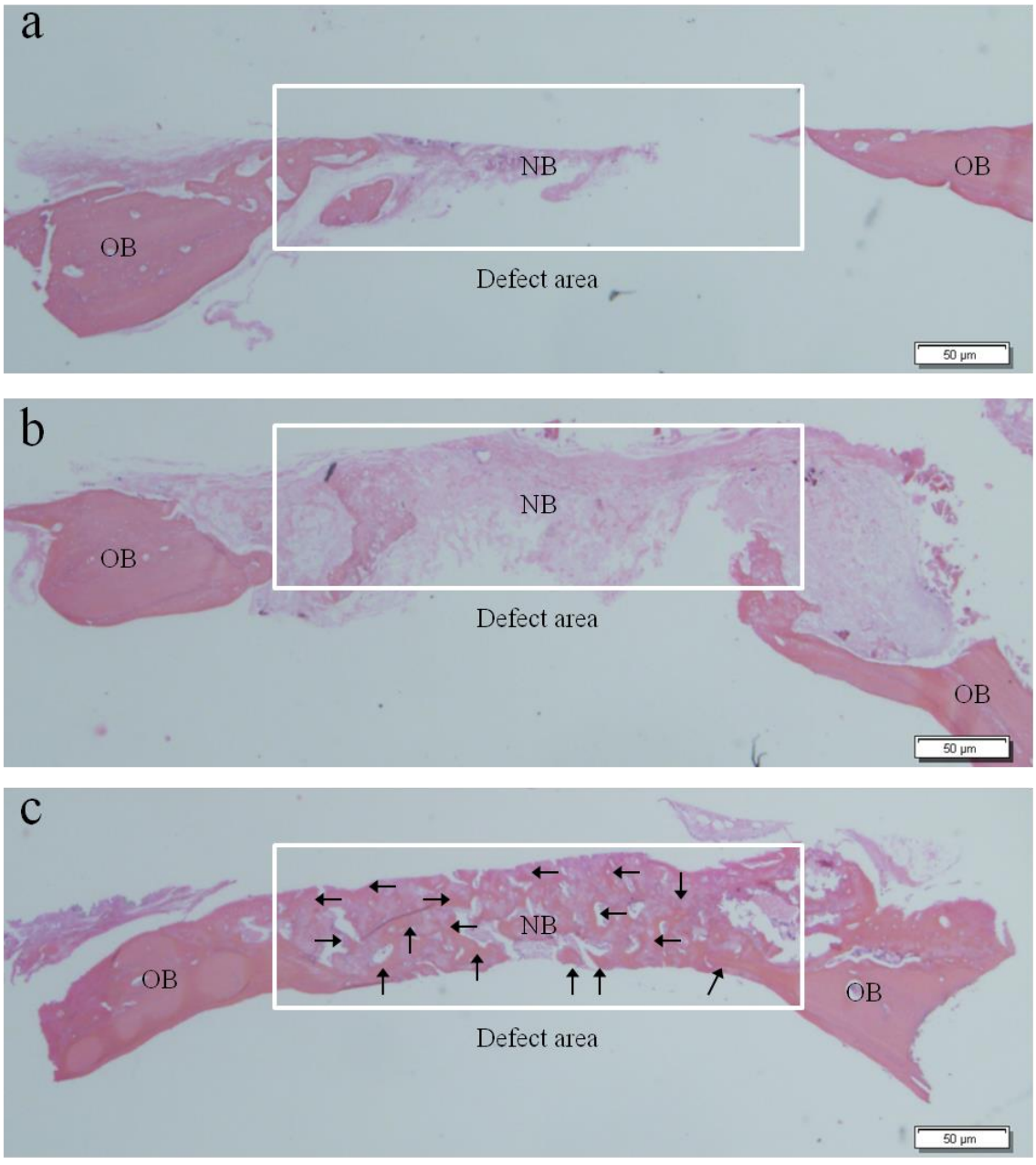

CHAPTER V

COMBINATORIAL NON-VIRAL GENE DELIVERY FOR BONE REGENERATION

Introduction

Both in orthopedics as well as in dentistry, there is an enormous need for developing novel biomaterials with improved bone regenerative capacity and predictability [205]. In dentistry, there are a multitude of conditions (periodontitis, ridge resorption, fracture or bone tumors) affecting the craniofacial complex in which bone loss is inevitable and predictable bone regeneration is required in order to restore both function and esthetics [206]. Bone replacement grafts currently available for predictable bone regeneration are either overly expensive or require harvesting from a distant donor site leading to significant morbidity [207]. Moreover, their predictability is restricted to select clinical indications. Over the last few decades, identification of key molecules involved in bone development and fracture healing has led to the introduction and rapid expansion of bone biomimetic materials in dentistry [208]. One such advancement is the introduction and current usage of growth factors or morphogens such as platelet derived growth factor-BB (PDGF-BB) and bone morphogenetic protein-2 (BMP-2) in clinical dentistry. Several studies including *in vitro*, *in vivo* and human clinical trials testing the efficacy of growth factors had clearly underscored their potential in regenerating lost bone or periodontium, leading to their approval for select clinical use [68].

Following tissue injury, platelets release PDGF at the site of the injury that act on specific cell surface receptors enhancing cell migration (chemotaxis) and proliferation

(mitogenesis) [68]. The chemotactic ability of PDGF has been demonstrated on several cell types including osteoblasts [209]. Vascular endothelial growth factor (VEGF), a growth factor known for its role in angiogenesis, is also involved in both intra-membranous and endochondral ossification [55]. This property has led to the development of delivery systems that release these factors for bone tissue engineering applications [210]. Combining PDGF with VEGF was shown to enhance the maturation of the blood vessels and to dramatically reverse experimentally induced ischemia in animals [211, 212]. Furthermore, there is growing evidence that delivery of PDGF along with VEGF has a synergistic effect on bone regeneration that is greater than either factor alone [213, 214].

Growth factors, though promising, are not without drawbacks. Being recombinant proteins, they are expensive and the supraphysiological dosage in which they are used (to compensate for their shorter duration of activity in the *in vivo* milieu) raises serious concerns regarding their safety. Increasingly, side effects of delivering proteins such as BMP-2 in higher doses for both indicated and off-label use are being reported [17]. One approach to overcome the shortcomings of protein-based approaches is gene therapy [215]. Gene delivery allows targeted synthesis of gene products in a controlled fashion and proteins produced endogenously by this approach have been shown to be less altered and therefore less immunogenic [79]. Gene therapy studies conducted in animals using viral vectors delivered through a traditional *ex vivo* or an *in vivo* approach successfully demonstrated the feasibility and effectiveness of delivering *PDGF-B* genes in animal models [216-218]. In addition to periodontal regeneration, delivery of *PDGF-B* genes using viral vectors in animals was shown to accelerate bone regeneration around dental

implants in a peri-implant bone loss model [219]. In spite of its proven efficacy in animals, conducting human clinical trials and ultimately translating viral gene therapy into clinical settings, especially for non-lethal conditions, can be extremely challenging [79]. In spite of lower transfection efficiency, non-viral vectors are safer and potentially more clinically translatable for bone regeneration applications. Once inside the target cells, the plasmid DNA (pDNA) containing the non-viral vector is processed in the endosome and/or lysosome, and pDNA is released into the cytoplasm by a mechanism called endosomal escape [220]. The released pDNA translocates from the cytoplasm to the nucleus through the nuclear pores reaching the extra chromosomal space whereupon it acts as local protein machinery [221].

In our recent study, we reported that delivering pDNA encoding PDGF-B using non-viral vectors (PEI-condensed pDNA) resulted in significant bone regeneration [47]. The new bone formation was 44x and 14x more, when the collagen scaffold carriers containing polyethylenimine (PEI)-pPDGF-B complexes were implanted into artificially created calvarial defects in rats, when compared to scaffold alone or empty defect groups, respectively. As a next step, in this study we explored the possibility of delivering both PDGF-B and VEGF plasmids from the same carrier system to evaluate their potential synergistic effects in bone regeneration, when delivering these key growth factors simultaneously within the created bone defect. To our knowledge, this is the first attempt to deliver multiple plasmids from a completely non-viral gene delivery system for bone regeneration.

Materials and methods

To gain insights into the synergistic effects of delivering PDGF-B (~ 4.9 Kb pDNA, Origene Technologies, Inc., Rockville, MD) and VEGF (~ 4.9 Kb pDNA, Origene Technologies, Inc.) plasmids, we utilized the same calvarial defect model in rats as in our study in Chapter IV and incorporated the following five groups: (a) empty defects, (b) empty collagen scaffolds, (c) PEI-pPDGF-B complex-loaded scaffolds, (d) PEI-pVEGF complex-loaded scaffolds, and (e) PEI-(pPDGF-B + pVEGF) complex-loaded scaffolds in a 1:1 ratio of plasmid amounts. The PDGF-B and VEGF plasmids were prepared as described in Chapters III and IV. Synthesis and *in vitro* characterization of PEI-pDNA complexes were performed as described in Chapter IV and in [47]. Briefly, PEI (branched, 25 kDa, Sigma-Aldrich, St. Louis, MO)-pDNA (6.4 Kb pDNA encoding *luciferase* reporter gene, *Vical*, Inc., San Diego, CA) complexes were fabricated at amine (N) to phosphate (P) ratios of 1, 5, 10, 15, and 20, and characterized for size, surface charge, and *in vitro* cytotoxicity and transfection efficacy in human bone marrow stromal cells (BMSCs; American Type Culture Collection, ATCC, Manassas, VA). The complexes prepared at an N/P ratio of 10 were 102 ± 2 nm in size with a positive surface charge of 37 ± 1 mV as measured using a Zetasizer Nano-ZS (Malvern Instruments, Westborough, MA). It was found that the transfection efficiency of pDNA complexes with PEI prepared at N/P ratio of 10 in BMSCs (1 μg pDNA, seeding density of 80,000 cells/well in 24-well plates) was significantly greater than that for complexes prepared at all other N/P ratios as determined by luciferase expression using a standard luciferase assay system (Promega Corporation, Madison, WI) (Elangovan et al., 2014). Complexes prepared at an N/P ratio of 10 also displayed low cytotoxicity in BMSCs (1 μg pDNA,

seeding density of 10,000 cells/well in 96-well plates) as assessed by the MTS (3-(4,5-dimethylthiazol-2-yl)-5-(3-carboxymethoxyphenyl)-2-(4-sulfophenyl)-2H-tetrazolium) cell viability assay (Cell Titer 96 AQueous One Solution cell proliferation assay, Promega Corporation). In our study, only the PEI-pDNA complexes prepared at N/P ratio of 10 displayed efficient transfection of BMSCs with relatively lower cell toxicity when compared to complexes prepared at other N/P ratios. As a result, the PEI-pDNA complexes used in the further *in vivo* experiments were prepared at N/P ratio of 10 (Elangovan et al., 2014). The transgene nuclear delivery potential of the PEI-pPDGF-B and PEI-pVEGF complexes prepared at N/P ratio of 10 and the subsequent expression of PDGF-BB and VEGF was assessed in BMSCs (1 μg pDNA each, seeding density of 80,000 cells/well in 24-well plates) using PDGF-BB and VEGF ELISA kits (Quantikine, R & D Systems, Minneapolis, MN). The fabrication of PEI-pPDGF-B complex-loaded scaffolds, PEI-pVEGF complex-loaded scaffolds, and PEI-(pPDGF-B + pVEGF) complex-loaded scaffolds in a 1:1 ratio of the plasmids was carried out as described in Chapter IV.

The surgical procedures were approved by and performed according to guidelines established by the University of Iowa Institutional Animal Care and Use Committee. The *in vivo* bone regenerative capacity of the gene delivery system was investigated in two 5 mm diameter × 2 mm thickness critical-sized calvarial defects in fourteen week-old male Fisher 344 rats (Charles River Laboratories International, Inc., Wilmington, MA). Prior to implantation into the defects, the scaffolds were cut to fit the diameter of the defect. The skin wound was then sutured and post-operative care followed as per the protocol. The animals were euthanized after four weeks and the parietal bone fractions

containing the regions of interest (5 mm diameter) were analyzed for bone volume (BV) per total volume (TV) and connectivity density (Conn.D.) in the bone defect using three-dimensional microfocus x-ray microcomputed tomography (micro-CT) imaging (cone-beam micro-CT40, Scanco Medical AG, Switzerland) as described in Chapter IV (Elangovan et al., 2014). For histological observations, the bone specimens were stained with Harris hematoxylin and eosin (H & E staining) in order to evaluate bone regeneration after four weeks *in vivo* implantation. The light microscopic (bright-field) examination of the sections was performed with an Olympus Stereoscope SZX12 as described in Chapter IV (Elangovan et al., 2014).

Results and discussion

As demonstrated in Figure 5.1, BMSCs transfected with PEI-pPDGF-B and PEI-pVEGF complexes resulted in significantly higher levels of PDGF-BB and VEGF in the cell culture medium supernatants compared to cells treated with naked, uncomplexed PDGF-B and VEGF plasmids. These results confirmed the efficiency of PEI-pDNA complexes to transfect BMSCs with therapeutic genes for bone regeneration. It is also clear that a ~3x higher concentration of VEGF was secreted into the supernatant, when compared to PDGF-BB, when the cells were transfected separately with the same starting amounts of plasmids. Figure 5.2 is a schematic of the proposed mechanism of treatment for bone regeneration. The PEI-pDNA complexes are formed as a result of electrostatic interactions between the positively charged PEI and the negatively charged pDNA. The net positively charged complexes (prepared at N/P ratio of 10, with sizes approximately 100 nm as observed by transmission electron microscopy (TEM) images) are then

injected into the porous collagen scaffolds and lyophilized. The complexes may then be released from the degrading matrix, transfecting the surrounding cells (Figure 5.2). In addition, cells may migrate into the porous matrix containing the immobilized complexes followed by their transfection by the complexes. Ultimately, these transfected cells produce PDGF-BB and VEGF which stimulates further cell migration (via chemotaxis), proliferation, differentiation, angiogenesis, tissue remodeling and mature bone formation [163, 222]. In further experiments, we evaluated the capacity of different treatments to initiate and form mature bone tissue. After four weeks of *in vivo* implantation of the scaffolds, the regions of interest were examined using micro-CT scans and the bone formation parameters such as regenerated bone tissue volume fraction of the total tissue volume of interest (BV/TV) and the degree of trabecular connectivity (connectivity density) were quantitated. As depicted in Figure 5.3, treatment with the collagen scaffold matrix containing PEI-pPDGF-B complexes showed complete coverage of the defect by the newly-formed bone tissue, compared to other groups evaluated. The combined therapy with pPDGF-B and pVEGF and defects implanted with PEI-pVEGF complexes alone exhibited only partial bone regeneration along the edges of the created defects. Patchy, irregularly-shaped, minimal mineralized regions were observed within the defects. A significant difference was found in the distribution of BV/TV between the PEI-pPDGF-B complex-embedded scaffolds and the remaining treatments. Similarly, connectivity density of the regenerated bone was significantly higher for the PEI-pPDGF-B complex-loaded scaffold group than for the other groups. The amount of bone tissue regenerated and the distribution of mineralization observed with this analysis was further validated using histological analysis with standard H & E stained sections of the defect

regions at four weeks post-implantation (Figure 5.4). Histology data showed that, while the gap between the healthy native bone edges was unfilled within the empty defects, the other groups, with the exception of PEI-pPDGF-B complex-loaded scaffolds, revealed bridging of the defect by both soft and hard tissue formation indicated by the presence of collagen fibrils, blood vessels, cells (most likely fibroblasts, osteogenic and/or inflammatory), extracellular matrix, and some new bone at the edges. For the PEI-pPDGF-B complex-loaded scaffold treatments, complete bridging of the defect by new bone (arrows) was observed. We hypothesize that the decreased bone formation seen in the defects treated with PEI-(pPDGF-B + pVEGF) complex-loaded scaffolds might be due to several reasons. Combining the two different pDNA encoding PDGF-B and VEGF vectors respectively, doubled the PEI concentration which may have increased the cytotoxicity *in vivo* via an apoptotic cell death pathway [223]. In addition, it has been reported that VEGF is a potential ligand for PDGF α and β receptors in mesenchymal stems cells (MSCs, undifferentiated osteoprogenitor cells) and can signal through PDGF receptors [224]. Therefore, it is also possible that VEGF significantly suppressed the osteogenic differentiation of MSCs by PDGF-BB via competitive receptor binding. Moreover, during the bone healing, PDGF is secreted first by the platelets as well the inflammatory cells followed by the release of VEGF. Therefore, in conjunction with our findings, it is clear that sequential delivery of these growth factors will be necessary for optimal bone regeneration.

Bone tissue engineering and development is a dynamic, highly regulated and organized process that is typically driven by the action of multiple growth factors for mediation of different cellular activities such as cellular recruitment, mitosis and

differentiation of MSCs into osteoblasts [225-227]. In the sequential cascade of events involved in bone regeneration, transient PDGF action is critical for chemotaxis, growth, and differentiation of MSCs in the early healing phase [228]. This can later be followed by prolonged, sustained angiogenic action of VEGF throughout the bone tissue healing process. Because PDGF-BB and VEGF each have distinct actions in bone formation, controlling their sequence of release may promote and induce improved bone regeneration. This can be accomplished by delivering PDGF-B and VEGF plasmids, each with different release kinetics from a single, structural collagen scaffold. This proposed novel delivery strategy, through the virtue of controlled dose and rate of plasmid delivery, might be able to abolish or reduce the aforementioned concerns regarding simultaneous dual delivery of PDGF-BB and VEGF.

Conclusions

In light of the results obtained in the present study, we showed that a non-viral gene delivery system was able to successfully transfect *PDGF-B* and *VEGF* genes into BMSCs. However, the bone regeneration efficacy was superior when the calvarial defects were treated with PEI-pPDGF-B complexes alone rather than those treated with PEI-(pPDGF-B + pVEGF) complexes. This study gains new insights into the possibility of developing combinatorial non-viral gene delivery system for bone regeneration and highlights the likely importance of temporal control of delivery of specific growth factors at specific time points in the healing process.

Figure 5.1. Detection of PDGF-BB and VEGF proteins in cell supernatants by ELISA after BMSC transfection with PEI-pPDGF-B and PEI-pVEGF complexes, respectively (n = 3, ***p < 0.001). The data were compared by ANOVA, followed by a Tukey post-test analysis (Prism 5.0, GraphPad Software Inc., San Diego, CA). The differences between the groups were considered to be statistically significant at p < 0.05.

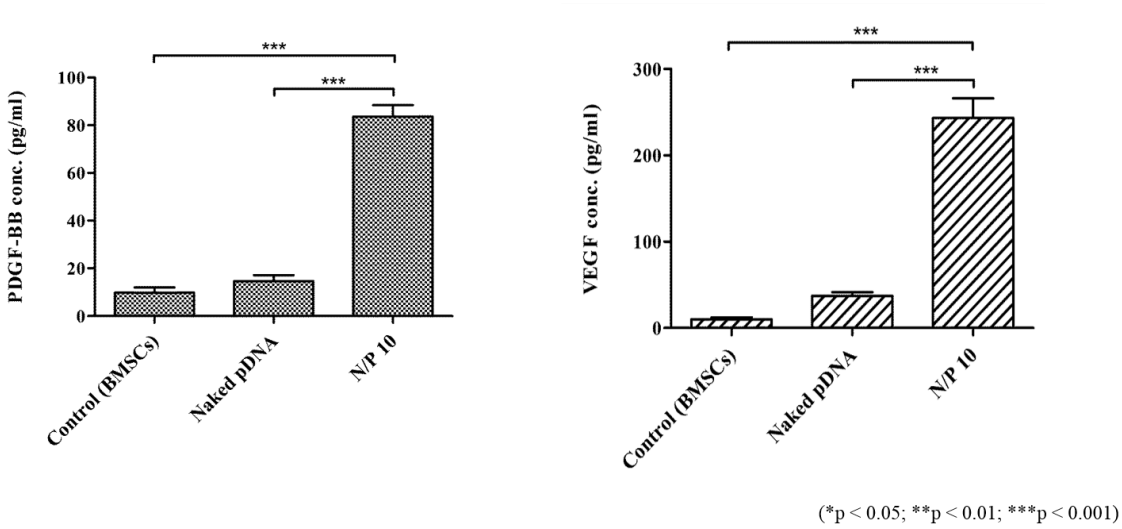

(*p < 0.05; **p < 0.01; ***p < 0.001)

Figure 5.2. Schematic of the gene delivery system along with TEM of the complexes prepared at N/P ratio of 10 along with the proposed mechanism of action for bone defect repair.

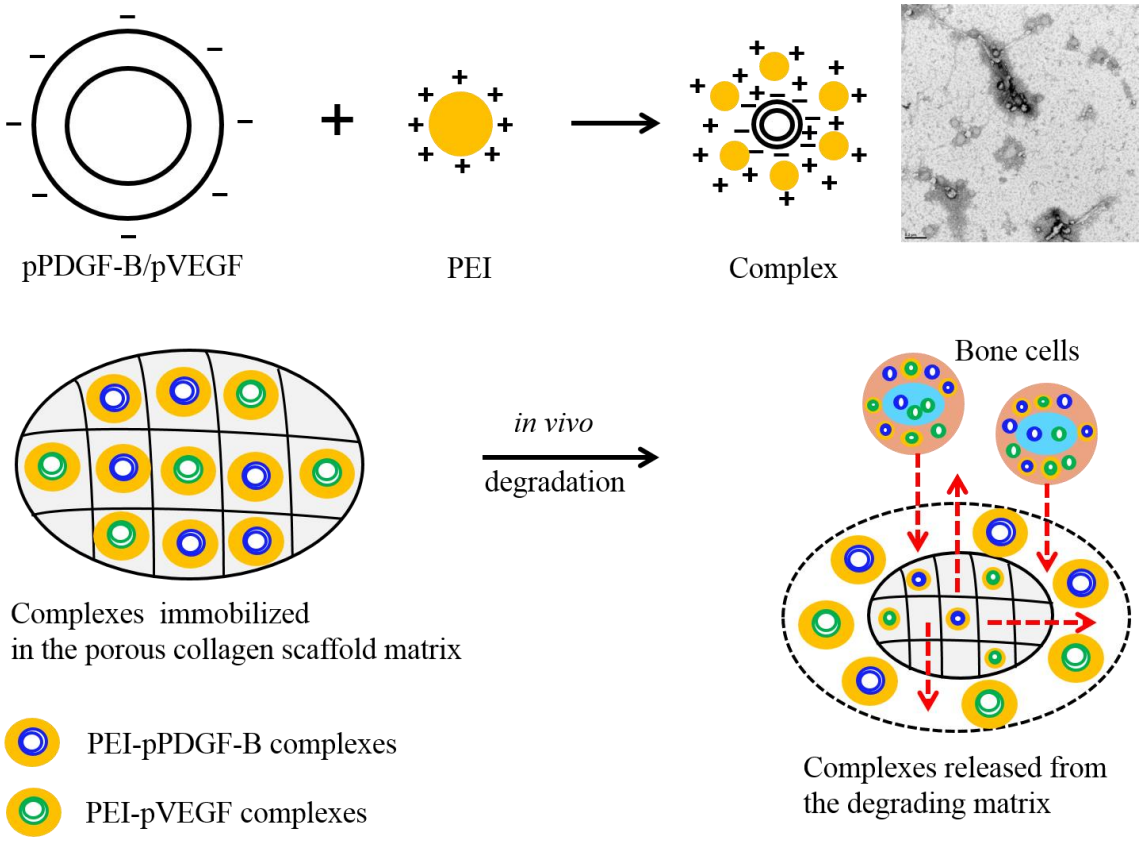

Figure 5.3. Representative micro-CT images of bone specimens demonstrating the extent of regenerated bone in the calvarial defects at four weeks in untreated, open defects (a); defects filled with empty collagen scaffolds (b); defects filled with PEI-pPDGF-B complex-loaded scaffolds (c); defects filled with PEI-pVEGF complex-loaded scaffolds (d); defects filled with PEI-(pPDGF-B + pVEGF) complex-loaded scaffolds (e); regenerated bone volume fraction (f); and connectivity density across different groups (g). Each defect within an animal was considered as being independent (n = 3, *p < 0.05; **p < 0.01; ***p < 0.001). The data were compared by ANOVA, followed by a Tukey post-test analysis (Prism 5.0, GraphPad Software Inc., San Diego, CA). The differences between the groups were considered to be statistically significant at p < 0.05. Scale bar, 1 mm.

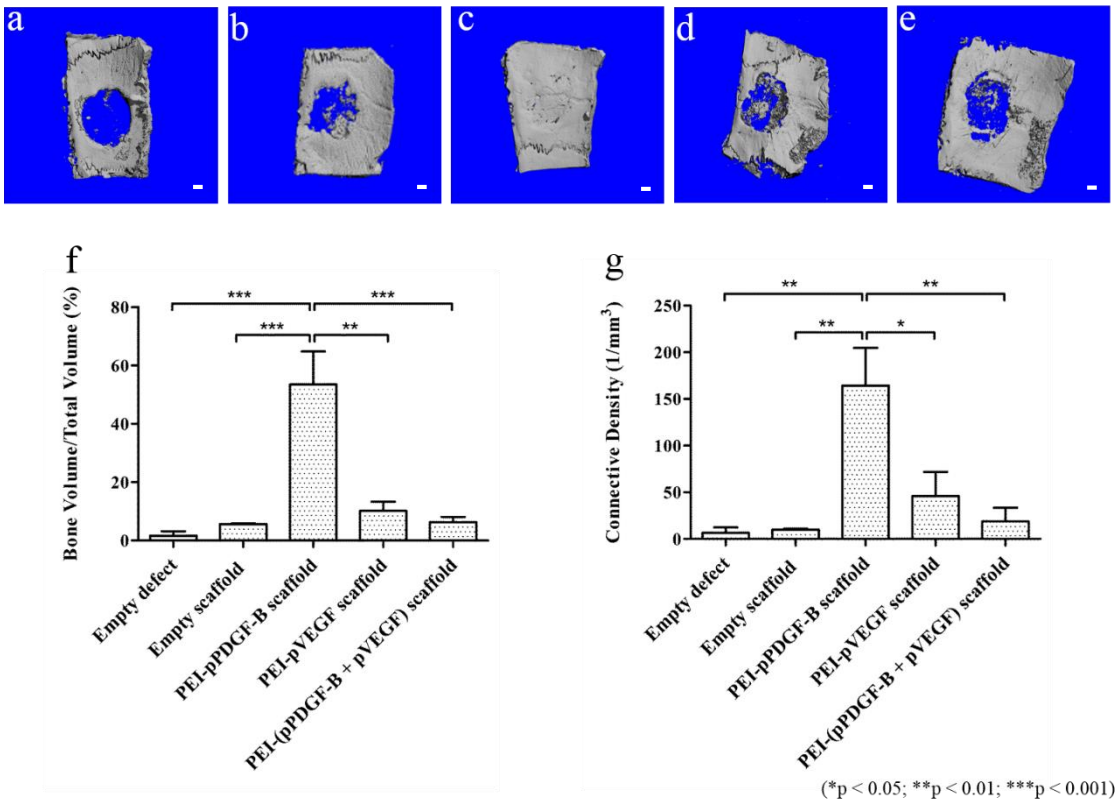

Figure 5.4. Representative histology sections of bone specimens showing the extent of regenerated bone in the calvarial defects at four weeks in untreated, open defects (a); defects filled with empty collagen scaffolds (b); defects filled with PEI-pPDGF-B complex-loaded scaffolds (c); defects filled with PEI-pVEGF complex-loaded scaffolds (d); and defects filled with PEI-(pPDGF-B + pVEGF) complex-loaded scaffolds (e). OB = old bone and NB = new bone. Note the complete bridging of the bone defects by the regenerated tissue in the group treated with the PEI-pPDGF-B complex-loaded scaffolds as indicated by the arrows. Scale bar, 50 μm.

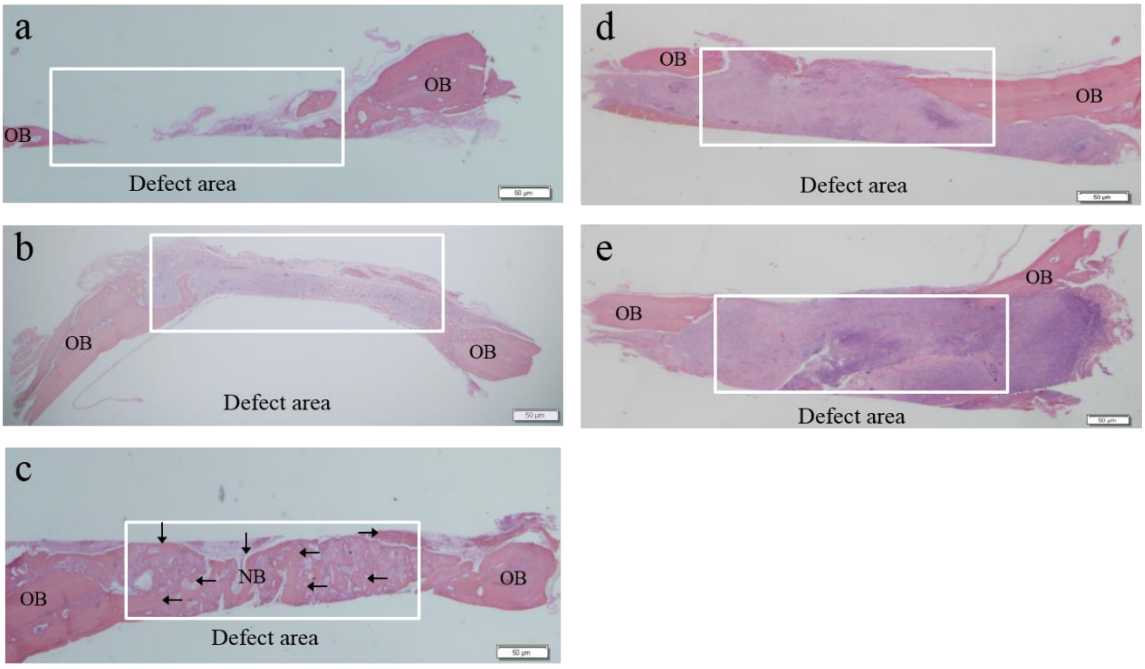

CHAPTER VI

COPPER-LOADED CHITOSAN SCAFFOLDS FOR BONE REGENERATION

Introduction

Bone defects resulting from tumor resection, periodontal disease, skeletal deficiency/disorder, abnormal development, and trauma, present significant health risks and are challenging to treat. Various approaches have been undertaken to treat bone defects with the goal of regenerating the lost osseous tissue thereby regaining function. Current treatments to treat bone defects are only partially effective and are often accompanied by major drawbacks such as limited supply and transplant rejection/incompatibility along with surgical side effects from harvesting bone such as infection, disease transmission or neurovascular injury [229-232]. Limitations of the current strategies of bone regeneration or replacement have led to tissue engineering approaches for repairing skeletal defects [233-235]. In orthopedics and dentistry, guided bone regeneration in combination with osteoconductive scaffolds is an alternative [236-238]. As such, there is a great need for biomaterials with higher bone regenerative capacity and predictability that favors complete bone regeneration without the aforementioned drawbacks.

Chitosan is an abundantly available natural biopolymer; it is biodegradable and biocompatible [239]. It undergoes enzymatic degradation to glucosamine and N-acetylglucosamine copolymers, substances naturally found in the body which are excreted or used in the amino sugar pool [240]. Chitosan aids in hemostasis and plays a role in activation of macrophages and cytokine stimulation [240]. Chitosan has also been

reported to induce collagen synthesis and angiogenesis in the early wound healing and tissue remodeling phases of wound repair [241, 242]. Owing to these attributes, chitosan has generated significant interest as a biomaterial for a broad range of wound healing applications [243-245]. It has been shown that chitosan forms a chelate complex with metal ions and that copper ions strongly interact with chitosan [246]. The chelation between chitosan and copper ions that occurs through the four nitrogen ligands in a square-planar geometrical manner is responsible for the formation of tightly packed chitosan gel [247, 248].

Apart from the known physiological roles of copper in enzymatic reactions and protein functions, it has also been reported to act as an endogenous stimulator of angiogenesis by inducing the migration and proliferation of endothelial cells [249-251]. Copper has been demonstrated to induce vascular endothelial growth factor (VEGF) expression *in vitro* and *in vivo* [252]. The quality of regenerating tissue was also shown to be distinctly improved as observed by a high density of cells in the granulation layer of copper-treated wounds. Copper-sensitive pathways are implicated to be involved in the regulation of key mediators of wound healing such as angiogenesis and tissue extracellular matrix remodeling. The primary objective of this proof of concept study was to develop chitosan scaffolds complexed with copper and test their *in vivo* bone regeneration capacity. This study, to our knowledge, is the first to develop and investigate the effect of copper crosslinked chitosan scaffold on bone tissue engineering in critical-sized calvarial defects.

Materials and methods

Materials

Chitosan (high purity, M_v 110,000-150,000) and copper (II) sulfate were purchased from Sigma–Aldrich® (St. Louis, MO). All other chemicals and solvents used were of reagent grade.

Scaffold fabrication

To prepare the chitosan sponges, chitosan was dissolved in 0.3 M acetate buffer, pH 4.5 at a concentration of 2 % w/v and freeze-dried for 5 h (FreezeZone 4.5, Labconco®, MO). The copper-chitosan scaffolds were prepared by slowly adding 450 µl of 2 % w/v chitosan solution to 50 µl of 0.625 mM copper sulfate solution in acetate buffer. The concentration of copper used in this study was based on reports that have demonstrated copper-induced VEGF expression, stimulation of cell proliferation, and wound healing [249, 252]. The mixture was vortexed for 30 s-1 min for homogeneity, incubated at room temperature for 4 h and later freeze-dried to completely remove the solvent (Figure 6.1). Addition of chitosan solution to the copper solution led to the spontaneous formation of a chitosan gel without any leakage.

Morphological characterization of the scaffolds

Standard protocols for scanning electron microscopy (SEM, Hitachi Model S-4800, Japan) were employed. Briefly, the scaffolds were mounted on aluminum stubs, sputter-coated with gold and examined using 3 kV accelerating voltage and a current of

10 μA. The surface characteristics of the scaffolds, including pore interconnectivity and scaffold integrity were analyzed.

Surgical procedure: In vivo implantation of scaffolds

Inbred 14 week-old male Fisher (CDF®) white rats (F344/DuCrl, ~250 g) were obtained from Charles River Laboratories International, Inc (Wilmington, MA) and housed and cared for in University of Iowa animal facilities. The surgical procedures were approved by and performed according to guidelines established by the University of Iowa Institutional Animal Care and Use Committee, Iowa. The animals were anaesthetized by intra-peritoneal injection of ketamine (80 mg/kg)-xylazine (8 mg/kg) mixture (provided by the Office of Animal Resources, University of Iowa). A sagittal incision, ~1.5 - 2 cm, was made on the scalp of each rat, and the calvaria was exposed by blunt dissection. Two 5 mm diameter × 2 mm thickness critical-sized defects were generated using a round carbide bur on the parietal bone, on both sides of the sagittal suture. The defects were randomly allocated into the following study groups: (1) empty defects (n = 3); (2) chitosan scaffolds (n = 2); and (3) copper-loaded chitosan scaffolds (n = 2). The shape and size of the cylindrical scaffold discs was adjusted to fit into the defects with a diameter of 5 mm and a thickness of 2 mm and implanted into the rats. The incision was closed in layers using sterile silk sutures. Buprenorphine (0.15 mg, intramuscular), as an analgesic, was administered to each rat thereafter and the animals were carefully monitored during post-operative recovery. The rats were able to function normally after this procedure. After 4 weeks, all the animals were euthanized and the

bony segments containing the regions of interest were harvested from the calvarial bone and fixed in 10 % neutral buffered formalin.

Micro-CT analysis

Three-dimensional microfocus x-ray microcomputed tomography imaging was performed on the specimens using a cone-beam micro-CT system (micro-CT40, Scanco Medical AG, Switzerland). Specimens were scanned in 70 % ethanol at 55 kVp and 145 μA with a voxel size of 10 μm and an integration time of 300 ms. Analysis was performed using a constant 5 mm diameter circular region of interest that was placed in the center of the machined defect and spanned a total of 50 reconstructed slices such that a total cylindrical volume of interest of ~9.8 mm^3 oriented perpendicular to the outer table of the calvarium was analyzed for each specimen using Scanco's provided software (sigma = 0.8, support = 1.0, and threshold = 250). Bone volume (BV) per total volume (TV) in the bone defect was obtained.

Histological analysis of rat bone defects

The bone samples underwent a decalcification (Surgipath Decalcifier II®) procedure. When the decalcification end point test returned negative for the presence of calcium, the rat bone specimens were introduced into a paraffin processor, paraffin embedded, and the blocks were sectioned in the sagittal plane for each specimen. Histological analysis was performed on the 5 μm sections in the central portion of the wound. The sections were collected on Superfrost Plus Slides (Fisher Scientific®), deparaffinized and stained with Harris hematoxylin and eosin (H & E staining) according

to standard protocols. Sections representing the central area of each defect were used to observe the presence of collagen, new bone formation, and cells in order to evaluate bone regeneration after 4 weeks *in vivo* implantation. The bright field examination of the slides was performed with an Olympus Stereoscope SZX12 and an Olympus BX61 microscope, both equipped with a digital camera.

Data presentation

Numerical data were reported as means with bars representing standard error of the mean (SEM) from replicate samples. Graphs were generated using Prism 5.0 (GraphPad Software Inc., San Diego, CA). The data were compared by ANOVA followed by a Tukey post-test analysis. The differences between the groups were considered to be statistically significant when the p value was < 0.05. Statistical analyses were performed using Prism 5.0 software.

Results and discussion

SEM analysis of chitosan scaffolds and chitosan-copper scaffolds

The three-dimensional porous polymer scaffold design creates and maintains a three-dimensional space within the defect *in vivo for tissue regeneration*. This facilitates the recruitment of healthy bone cells and other appropriate cell types from the surrounding tissue to the wound site, favors cellular attachment, and promotes the growth and differentiation of these cells. Subsequently, a space-filling tissue is formed over time as a result of cell localization facilitated by the scaffold [47]. Thus, within the defect, the three-dimensional scaffolds help control the size and shape of the regenerated, functional

bone tissue. The crosslinking and gelation of polymeric chitosan chains induced by copper (II) ions may also improve the mechanical strength and degradation rate of these scaffold matrices.

The freeze-drying technique was utilized in the preparation of scaffolds to obtain a three-dimensional structure with a spongy texture. In this method, the frozen solvent was removed by sublimation, and the now empty spaces once occupied by the frozen solvent crystals formed the pores of the scaffold. The chitosan scaffolds showed a highly-porous, interconnecting network with pore sizes of 104 ± 5 μm (Figure 6.2a). The incorporation of copper within the scaffolds did not appear to have any adverse effect on the morphology or the micro-structural aspects of the final scaffold (Figure 6.2b).

In vivo bone regeneration: Micro-CT scans

The chitosan scaffold matrix containing copper was evaluated *in vivo* for its efficacy as a bone regenerative biomaterial. Critical-sized calvarial defects were created in rats and were utilized as a model to test the *in vivo* efficacy of three different treatment groups: (1) empty defects (untreated) as a control, (2) defect filled with chitosan scaffolds, and (3) defect filled with copper entrapped in the chitosan scaffolds. The rats were sacrificed after 4 weeks and newly-formed bone tissue was evaluated for its volume using micro-CT scans. The micro-CT scan imaged the induced circular bone defects and the regenerated bone tissue in the defects as a result of various treatments (Figures 6.3a-c, the circles superimposed on each of the representative images indicate the original bone defect edges). The empty, untreated defect displayed minimal irregular, patchy bone formation, while the chitosan scaffold exhibited a much more organized mineralized

regions towards the defect edge. In contrast, the scaffolds incorporating copper demonstrated remarkable mineralized tissue formation within the defect area, when compared to the other groups evaluated. The new bone tissue also appeared to be synthesized more towards periphery of the defect, and patterning to close in on the defect. This treatment was observed to have more hard tissue ingrowth from the edges of the defect within the implant region compared to the empty defects or chitosan scaffolds. The addition of chitosan solution to the copper sulfate solution results in the chelation of copper (II) ions with the amino groups of chitosan. This causes the gelation of chitosan solution and the retention of the copper (II) ions within the gel as well as the subsequent freeze-dried scaffolds [247]. We hypothesize that the presence of copper in the scaffold matrix may have accelerated the proliferation of epithelial and endothelial cells [253]. These functions, together with growth factor signaling, could have then promoted regeneration of the osseous tissue [219, 222, 254].

In vivo bone regeneration: new bone volume fraction

The amount of bone tissue regenerated was quantified by analyzing bone volume fraction of the total tissue volume of interest - bone volume / total volume (BV/TV). The BV/TV was two-fold and eleven-fold higher in defects treated with copper-embedded chitosan scaffolds, when compared to the chitosan scaffold and empty defect control groups, respectively (Figure 6.3d). Results of the ANOVA test provided evidence that the distribution of BV/TV outcomes differed significantly among the three treatment groups ($p = 0.0418$). These highly macro-porous scaffolds most likely caused the cells in the vicinity to migrate into the scaffold and through its pores. The walls of the porous matrix

then act as a support for the attachment and anchoring of cells. Since the pores are larger in size than the cells, there is sufficient room within the scaffolds for tissue development. This structure facilitates the processes of cell growth and proliferation, differentiation, and angiogenesis, thereby enhancing local tissue repair [255]. The chitosan biomaterial surface together with copper may possibly be osteoconductive for progenitors and give rise to such processes. In addition, the incorporation of copper may have allowed more cells to enter the scaffold through angiogenesis. Later, as the chitosan matrix biodegrades away, it is replaced by the newly-formed bone tissue.

In vivo bone regeneration: H & E staining

Histology further confirmed the differences observed with micro-CT analysis. The pattern of distribution of mineralization across the defect regions as a result of different treatments observed in micro-CT images is consistent with histological examination using H & E stains. The image from the untreated, open defect showed that the defect created between the old bone edges was unfilled, while the chitosan scaffold group demonstrated more bone formation in the defect peripheries than empty defects (Figures 6.4a-b). In the defect implanted with chitosan-copper scaffolds, we found significantly more bone formation in the defect than the other two groups. The bone formation is pronounced at the edges of the defects gradually protruding towards the center of the defect (Figure 6.4c). The histology data demonstrated that the cells begin to regenerate the tissue and mineralization begins to occur around 4 weeks *in vivo*. We hypothesize that the copper is released gradually from the degrading chitosan matrix, which then results in endothelial cell proliferation leading to new blood vessel growth

and osteoprogenitor recruitment into the scaffold. Copper has been studied to stimulate cell growth and division and promoting angiogenesis [249, 250]. Along with oxygen and nutrients, new blood vessels help in the transportation of inflammatory cells and osteoprogenitors to the wound site, thus accelerating/improving bone healing, repair and regeneration [55].

To our knowledge, this is the first report to explore the effect of adding copper (II) ions to scaffolds to enhance bone tissue regeneration. This proof of concept experiment clearly demonstrates the safety, feasibility and efficacy of chitosan copper scaffolds (relative to the controls or chitosan scaffolds) for bone tissue engineering. No biologics were employed in this study to make this scaffold osteoinductive and we relied completely on the osteoconductivity of the scaffold. In more comprehensive future studies, it will be necessary to carry out detailed physicochemical characterizations of the chitosan scaffolds with and without copper, determine if using higher concentrations of copper in the scaffolds generates any toxicity, quantify the degree of vascularization that occurs using chitosan copper scaffolds versus chitosan scaffolds alone and determine the kinetics of bone regeneration over time using chitosan scaffolds with and without copper. We anticipate that in future studies, this scaffold could promote complete bone regeneration when the experiments are extended to more than 4 weeks and potentially synergistic morphogens such as bone morphogenetic proteins (BMPs) are simultaneously incorporated into the scaffold.

Conclusions

Our results demonstrated that the copper-loaded chitosan scaffolds promoted osseous defect healing in calvarial defects in rats. This study demonstrated the feasibility and capability of copper-loaded chitosan scaffolds in enhancing the bone repair and regeneration process.

Figure 6.1. Diagrammatic showing the formulation approach of copper-chitosan scaffolds.

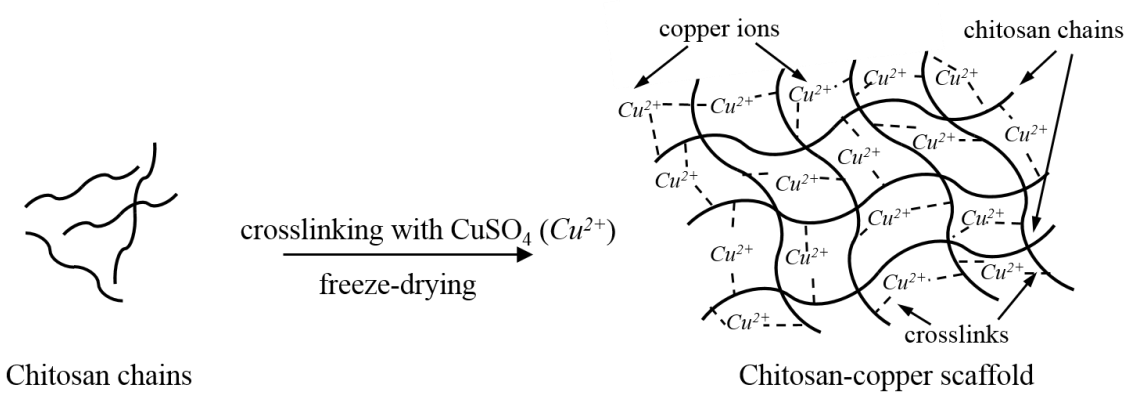

Figure 6.2. SEM images of chitosan scaffolds (a) and chitosan scaffolds containing copper (b).

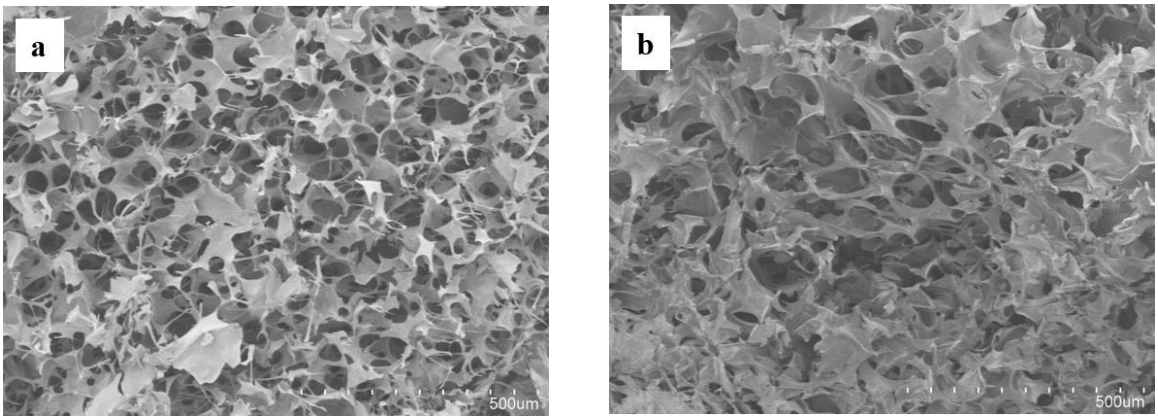

Figure 6.3. Evaluation of *in vivo* bone formation: representative micro-CT scans showing the level of regenerated tissue after 4 weeks in empty defects (a, n = 3); chitosan scaffolds (b, n = 2); and copper-loaded chitosan scaffolds (c, n = 2); assessment of regenerated bone volume fraction in defects treated with different groups (d). Scale bar, 1 mm.

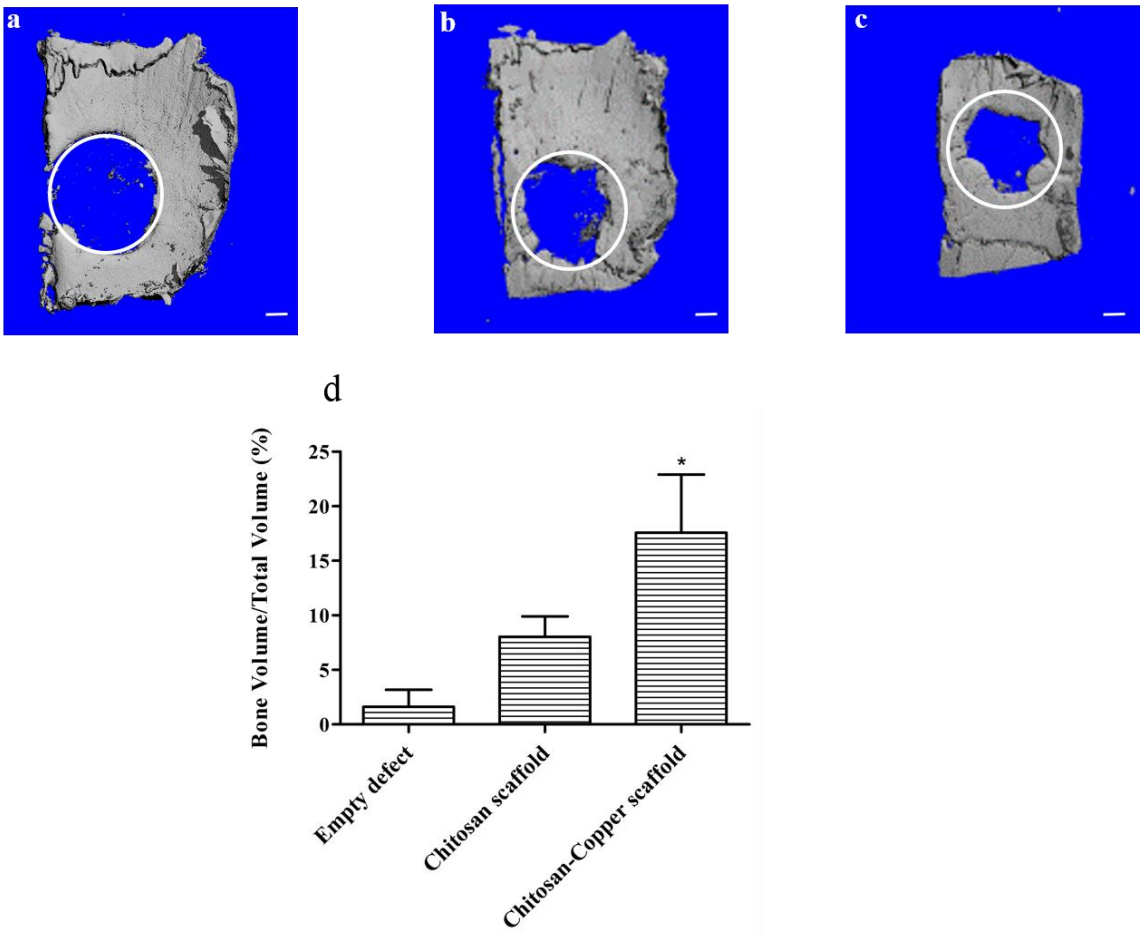

Figure 6.4. Representative histology sections demonstrating the extent of new bone formation in the defects at 4 weeks due to various treatments: empty defects (a); chitosan scaffolds (b); and copper-loaded chitosan scaffolds (c). OB = old bone and NB = new bone. Note the partial bridging of new bone in the copper-loaded chitosan test group indicated by the arrows. Scale bar, 50 μm.

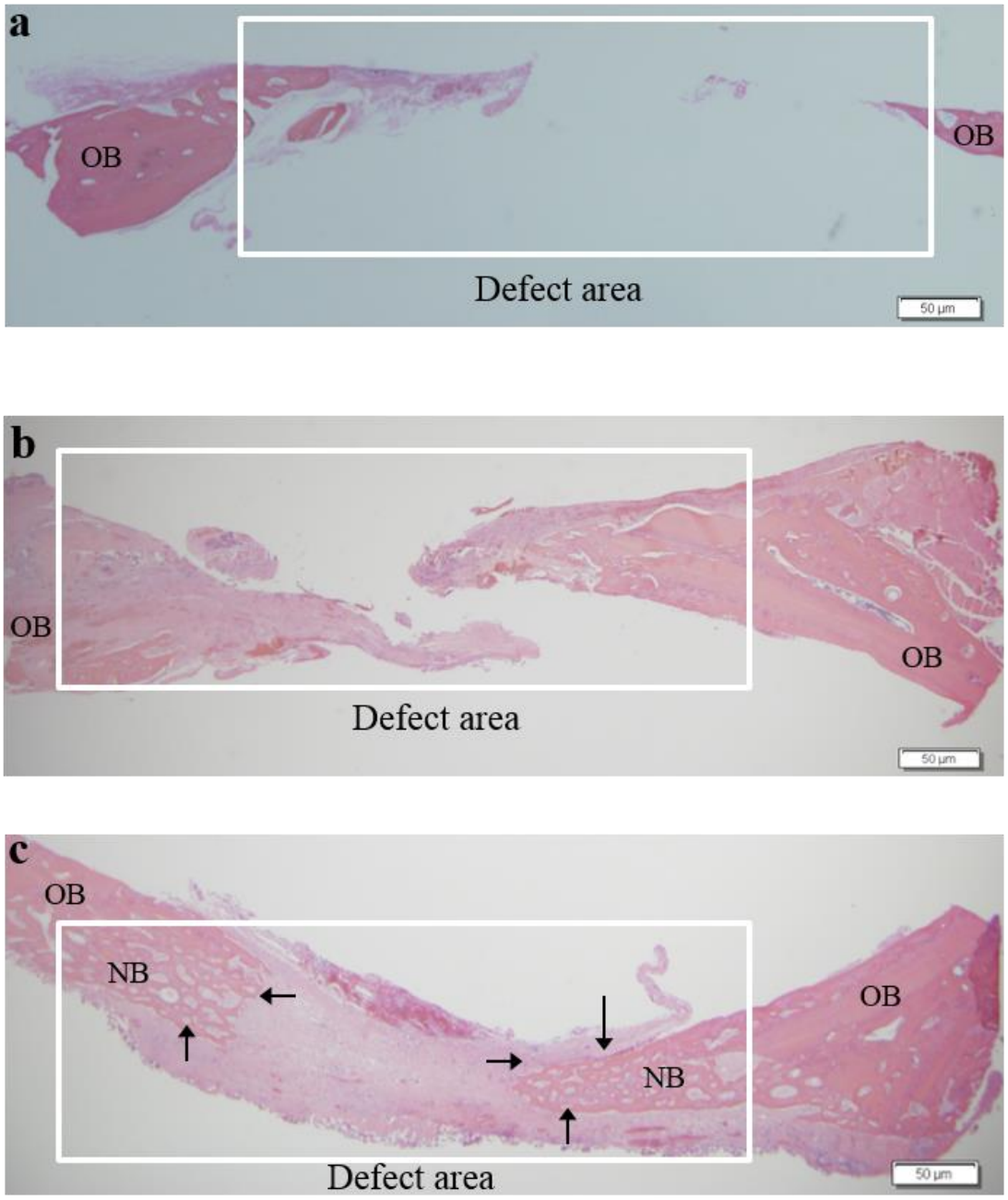

CHAPTER VII

CONCLUSIONS AND FUTURE WORK

Introduction of growth factors into clinical practice has improved the prognosis of complex clinical scenarios, but with a high degree of variability. This, in part, is due to a lack of a continual supply of these proteins for a prolonged period of time. One method to overcome this drawback is gene therapy. Gene therapy is an effective approach to overcome the shortcomings of protein therapy such as rapid clearance and high cost. The use of non-viral vectors that are safe and efficient in transfecting target cells has very high potential for clinical translation in periodontal, bone and other orthopedic applications. The major limitation of non-viral gene delivery is its lower transfection efficiency, which when addressed will have a wide array of applications in dental and craniofacial fields. The purpose of our study was to develop and test a non-viral gene delivery system for bone regeneration that utilizes collagen scaffold to deliver PEI-pDNA (encoding platelet derived growth factor (PDGF-B) complexes. Cationic complexes incorporating pDNAs encoding the LUC, EGFP-N1 or PDGF-B proteins were successfully prepared. Two different non-viral vectors, PEI and calcium phosphate, were evaluated as gene delivery vectors. It was found that PEI is a more effective vector for delivering genes of interest to pre-osteoblastic HEPM cells than calcium phosphate. In order to achieve efficient transfections, the cell-complex incubation time, amount of PEI in complexes, size and surface charge of the complexes were found to be very crucial parameters. *In vitro* experiments demonstrated that PEI-pDNA complexes prepared at a N/P ratio of 10 were able to transfect *LUC, EGFP-N1* and *PDGF-B* genes efficiently into HEPM cells with relatively lower cytotoxicity than complexes prepared at other N/P ratios.

In the second study, the *in vivo* transfection efficacy of PEI-pDNA complexes prepared at a N/P ratio of 10 for the purpose of bone regeneration was explored. BMSCs were efficiently transfected with a variety of reporter or therapeutic genes when using PEI-pDNA complexes prepared at an optimal N/P ratio of 10. These PEI-pDNA complexes were stable and nanometer-sized, with a net positive surface charge. The PEI-pPDGF-B complex-activated collagen scaffolds favored cellular attachment and promoted cellular proliferation *in vitro*. The complex-loaded scaffolds promoted osteogenesis and demonstrated superior tissue regeneration efficacy in calvarial defects in rats when compared to the empty defect and empty scaffold groups. This system efficaciously delivered pDNA into the cells without any apparent adverse effects. Gene activated matrices encoding for PDGF-B protein were shown to have a strong potential for clinical applications that require enhanced bone regeneration.

This study was then followed up with combinatorial *in vivo* non-viral gene delivery of growth factors with the aim of enhancing bone regeneration due to synergistic effect. Herein, we showed that the non-viral gene delivery system was able to successfully transfect *PDGF-B* and *VEGF* genes into BMSCs as detected by the ELISA assay. However, the bone regeneration efficacy was superior when the calvarial defects were treated with PEI-pPDGF-B complexes alone, than those treated with PEI-(pPDGF-B + pVEGF) complexes. This study gains new insights into the possibility of developing combinatorial non-viral gene delivery system for bone regeneration and highlights the probable importance of temporal delivery of specific growth factors at specific time points in the healing process.

Another interesting result was the promotion of osseous defect healing in calvarial defects in rats implanted with the copper-loaded chitosan scaffolds. This study demonstrated the feasibility and capability of copper-loaded chitosan scaffolds in enhancing the bone repair and regeneration process.

The long term goal of this project is to develop a safe and efficient non-viral gene delivery system that may be utilized for several biomedical applications including hard bone formation and soft tissue engineering. Our further studies are proposed to build on the knowledge derived so far. We need to investigate the effect of sequential delivery of plasmid DNA encoding the two growth factors, PDGF-B and VEGF, on bone regeneration. The copper-loaded chitosan scaffolds, either in combination with tissue inductive/conductive growth factors or with genes encoding these factors need to be studied for their bone regenerative capacity. Copper-chitosan scaffolds incorporating the *PDGF-B* gene should be developed and evaluated *in vivo* as a comparison to the collagen scaffolds. An ongoing study utilizes chemically modified messenger RNA (mRNA) as an attractive and promising alternative to plasmid DNA-based gene therapy for tissue regeneration.

REFERENCES

[1] Hsiong SX, Mooney DJ. Regeneration of vascularized bone. Periodontol 2000. 2006;41:109-22.

[2] Ai-Aql ZS, Alagl AS, Graves DT, Gerstenfeld LC, Einhorn TA. Molecular mechanisms controlling bone formation during fracture healing and distraction osteogenesis. J Dent Res. 2008;87:107-18.

[3] Tsiridis E, Upadhyay N, Giannoudis P. Molecular aspects of fracture healing: which are the important molecules? Injury. 2007;38 Suppl 1:S11-25.

[4] McAllister BS, Haghighat K. Bone augmentation techniques. J Periodontol. 2007;78:377-96.

[5] Deschaseaux F, Sensebe L, Heymann D. Mechanisms of bone repair and regeneration. Trends Mol Med. 2009;15:417-29.

[6] Darby I. Periodontal materials. Aust Dent J. 2011;56 Suppl 1:107-18.

[7] Langer R, Vacanti JP. Tissue engineering. Science. 1993;260:920-6.

[8] Zegzula HD, Buck DC, Brekke J, Wozney JM, Hollinger JO. Bone formation with use of rhBMP-2 (recombinant human bone morphogenetic protein-2). J Bone Joint Surg Am. 1997;79:1778-90.

[9] Fang J, Zhu YY, Smiley E, Bonadio J, Rouleau JP, Goldstein SA, et al. Stimulation of new bone formation by direct transfer of osteogenic plasmid genes. Proc Natl Acad Sci USA. 1996;93:5753-8.

[10] Lieberman JR, Daluiski A, Stevenson S, Wu L, McAllister P, Lee YP, et al. The effect of regional gene therapy with bone morphogenetic protein-2- producing bone-marrow cells on the repair of segmental femoral defects in rats. J Bone Joint Surg Am. 1999;81:905-17.

[11] Shea LD, Wang D, Franceschi RT, Mooney DJ. Engineered bone development from a pre-osteoblast cell line on three-dimensional scaffolds. Tissue Eng. 2000;6:605-17.

[12] Hirschi KK, Skalak TC, Peirce SM, Little CD. Vascular assembly in natural and engineered tissues. Ann N Y Acad Sci. 2002;961:223-42.

[13] Chen RR, Mooney DJ. Polymeric growth factor delivery strategies for tissue engineering. Pharm Res. 2003;20:1103-12.

[14] Zhao GQ. Consequences of knocking out BMP signaling in the mouse. Genesis. 2003;35:43-56.

[15] Reyes R, De la Riva B, Delgado A, Hernandez A, Sanchez E, Evora C. Effect of triple growth factor controlled delivery by a brushite-PLGA system on a bone defect. Injury. 2012;43:334-42.

[16] De la Riva B, Sanchez E, Hernandez A, Reyes R, Tamimi F, Lopez-Cabarcos E, et al. Local controlled release of VEGF and PDGF from a combined brushite-chitosan system enhances bone regeneration. J Control Release. 2010;143:45-52.

[17] Woo EJ. Adverse events reported after the use of recombinant human bone morphogenetic protein 2. J Oral Maxillofac Surg. 2012;70:765-7.

[18] Young HE, Mancini ML, Wright RP, Smith JC, Black AC, Jr., Reagan CR, et al. Mesenchymal stem cells reside within the connective tissues of many organs. Dev Dyn. 1995;202:137-44.

[19] Chang SC-N, Wei FC, Chuang H, Chen YR, Chen JK, Lee KC, et al. Ex Vivo Gene Therapy in Autologous Critical-Size Craniofacial Bone Regeneration. Plast Reconstr Surg. 2003;112:1841-50.

[20] Quarto R, Mastrogiacomo M, Cancedda R, Kutepov SM, Mukhachev V, Lavroukov A, et al. Repair of Large Bone Defects with the Use of Autologous Bone Marrow Stromal Cells. N Engl J Med. 2001;344:385-6.

[21] Kon E, Muraglia A, Corsi A, Bianco P, Marcacci M, Martin I, et al. Autologous bone marrow stromal cells loaded onto porous hydroxyapatite ceramic accelerate bone repair in critical-size defects of sheep long bones. J Biomed Mater Res. 2000;49:328-37.

[22] Zara JN, Siu RK, Zhang X, Shen J, Ngo R, Lee M, et al. High doses of bone morphogenetic protein 2 induce structurally abnormal bone and inflammation in vivo. Tissue Eng Part A. 2011;17:1389-99.

[23] Shimer AL, Oner FC, Vaccaro AR. Spinal reconstruction and bone morphogenetic proteins: open questions. Injury. 2009;40 Suppl 3:S32-8.

[24] Mindea SA, Shih P, Song JK. Recombinant human bone morphogenetic protein-2-induced radiculitis in elective minimally invasive transforaminal lumbar interbody fusions: a series review. Spine (Phila Pa 1976). 2009;34:1480-4.

[25] Kimelman Bleich N, Kallai I, Lieberman JR, Schwarz EM, Pelled G, Gazit D. Gene therapy approaches to regenerating bone. Adv Drug Deliv Rev. 2012;64:1320-30.

[26] Bonadio J, Smiley E, Patil P, Goldstein S. Localized, direct plasmid gene delivery in vivo: Prolonged therapy results in reproducible tissue regeneration. Nat Med. 1999;5:753-9.

[27] Holladay C, Keeney M, Greiser U, Murphy M, O'Brien T, Pandit A. A matrix reservoir for improved control of non-viral gene delivery. J Control Release. 2009;136:220-5.

[28] Hosseinkhani H, Azzam T, Kobayashi H, Hiraoka Y, Shimokawa H, Domb AJ, et al. Combination of 3D tissue engineered scaffold and non-viral gene carrier enhance in vitro DNA expression of mesenchymal stem cells. Biomaterials. 2006;27:4269-78.

[29] Pack DW, Hoffman AS, Pun S, Stayton PS. Design and development of polymers for gene delivery. Nat Rev Drug Discov. 2005;4:581-93.

[30] D'Mello S, Salem AK, Hong L, Elangovan S. Characterization and evaluation of the efficacy of cationic complex mediated plasmid DNA delivery in human embryonic palatal mesenchyme cells. J Tissue Eng Regen Med. 2014; doi: 10.1002/term.1873.

[31] Boussif O, LezoualC'H F, Zanta MA, Mergny MD, Scherman D, Demeneix B, et al. A versatile vector for gene and oligonucleotide transfer into cells in culture and in vivo: Polyethylenimine. Proc Natl Acad Sci USA. 1995;92:7297-301.

[32] Huang YC, Riddle K, Rice KG, Mooney DJ. Long-term in vivo gene expression via delivery of PEI-DNA condensates from porous polymer scaffolds. Hum Gene Ther. 2005;16:609-17.

[33] Huang YC, Simmons C, Kaigler D, Rice KG, Mooney DJ. Bone regeneration in a rat cranial defect with delivery of PEI-condensed plasmid DNA encoding for bone morphogenetic protein-4 (BMP-4). Gene Ther. 2005;12:418-26.

[34] Akinc A, Thomas M, Klibanov AM, Langer R. Exploring polyethylenimine-mediated DNA transfection and the proton sponge hypothesis. J Gene Med. 2005;7:657-63.

[35] Behr JP. The proton sponge: A trick to enter cells the viruses did not exploit. Chimia. 1997;51:34-6.

[36] Deng R, Yue Y, Jin F, Chen Y, Kung HF, Lin MCM, et al. Revisit the complexation of PEI and DNA - How to make low cytotoxic and highly efficient PEI gene transfection non-viral vectors with a controllable chain length and structure? J Control Release. 2009;140:40-6.

[37] Schäfer J, Höbel S, Bakowsky U, Aigner A. Liposome-polyethylenimine complexes for enhanced DNA and siRNA delivery. Biomaterials. 2010;31:6892-900.

[38] Abdallah B, Hassan A, Benoist C, Goula D, Behr JP, Demeneix BA. A powerful nonviral vector for in vivo gene transfer into the adult mammalian brain: Polyethylenimine. Hum Gene Ther. 1996;7:1947-54.

[39] Undale AH, Westendorf JJ, Yaszemski MJ, Khosla S. Mesenchymal stem cells for bone repair and metabolic bone diseases. Mayo Clin Proc. 2009;84:893-902.

[40] Chamberlain G, Fox J, Ashton B, Middleton J. Concise review: Mesenchymal stem cells: Their phenotype, differentiation capacity, immunological features, and potential for homing. Stem Cells. 2007;25:2739-49.

[41] Mooney DJ, Vandenburgh H. Cell Delivery Mechanisms for Tissue Repair. Cell Stem Cell. 2008;2:205-13.

[42] Undale AH, Westendorf JJ, Yaszemski MJ, Khosla S. Mesenchymal stem cells for bone repair and metabolic bone diseases. Mayo Clin Proc. 2009;84:893-902.

[43] Steinert AF, Noth U, Tuan RS. Concepts in gene therapy for cartilage repair. Injury. 2008;39 Suppl 1:S97-113.

[44] Bonadio J. Review: local gene delivery for tissue regeneration. e-biomed: J Regen Med. 2000;1:25-9.

[45] Huang YC, Connell M, Park Y, Mooney DJ, Rice KG. Fabrication and in vitro testing of polymeric delivery system for condensed DNA. J Biomed Mater Res A. 2003;67:1384-92.

[46] Shea LD, Smiley E, Bonadio J, Mooney DJ. DNA delivery from polymer matrices for tissue engineering. Nat Biotechnol. 1999;17:551-4.

[47] Elangovan S, D'Mello SR, Hong L, Ross RD, Allamargot C, Dawson DV, et al. The enhancement of bone regeneration by gene activated matrix encoding for platelet derived growth factor. Biomaterials. 2014;35:737-47.

[48] Evans CH. Gene delivery to bone. Adv Drug Deliv Rev. 2012;64:1331-40.

[49] Putnam AJ, Mooney DJ. Tissue engineering using synthetic extracellular matrices. Nat Med. 1996;2:824-6.

[50] Chvapil M. Collagen sponge: theory and practice of medical applications. J Biomed Mater Res. 1977;11:721-41.

[51] Even-Ram S, Yamada KM. Cell migration in 3D matrix. Curr Opin Cell Biol. 2005;17:524-32.

[52] Zeltinger J, Sherwood JK, Graham DA, Mueller R, Griffith LG. Effect of pore size and void fraction on cellular adhesion, proliferation, and matrix deposition. Tissue Eng. 2001;7:557-72.

[53] Wake MC, Patrick CW, Jr., Mikos AG. Pore morphology effects on the fibrovascular tissue growth in porous polymer substrates. Cell Transplant. 1994;3:339-43.

[54] Yannas IV. Tissue and organ regeneration in adults: Springer; 2001.

[55] Hankenson KD, Dishowitz M, Gray C, Schenker M. Angiogenesis in bone regeneration. Injury. 2011;42:556-61.

[56] Tonnesen MG, Feng X, Clark RA. Angiogenesis in wound healing. J Investig Dermatol Symp Proc. 2000;5:40-6.

[57] Jang JH, Rives CB, Shea LD. Plasmid delivery in vivo from porous tissue-engineering scaffolds: transgene expression and cellular transfection. Mol Ther. 2005;12:475-83.

[58] Doukas J, Blease K, Craig D, Ma C, Chandler LA, Sosnowski BA, et al. Delivery of FGF genes to wound repair cells enhances arteriogenesis and myogenesis in skeletal muscle. Mol Ther. 2002;5:517-27.

[59] Guo T, Zhao J, Chang J, Ding Z, Hong H, Chen J, et al. Porous chitosan-gelatin scaffold containing plasmid DNA encoding transforming growth factor-beta1 for chondrocytes proliferation. Biomaterials. 2006;27:1095-103.

[60] Berry M, Gonzalez AM, Clarke W, Greenlees L, Barrett L, Tsang W, et al. Sustained effects of gene-activated matrices after CNS injury. Mol Cell Neurosci. 2001;17:706-16.

[61] Kim A, Checkla DM, Dehazya P, Chen W. Characterization of DNA-hyaluronan matrix for sustained gene transfer. J Control Release. 2003;90:81-95.

[62] Tyrone JW, Mogford JE, Chandler LA, Ma C, Xia Y, Pierce GF, et al. Collagen-embedded platelet-derived growth factor DNA plasmid promotes wound healing in a dermal ulcer model. J Surg Res. 2000;93:230-6.

[63] Pannier AK, Shea LD. Controlled release systems for DNA delivery. Mol Ther. 2004;10:19-26.

[64] Jones E, Yang X. Mesenchymal stem cells and bone regeneration: current status. Injury. 2011;42:562-8.

[65] Weissman IL. Translating stem and progenitor cell biology to the clinic: barriers and opportunities. Science. 2000;287:1442-6.

[66] Endo M, Kuroda S, Kondo H, Maruoka Y, Ohya K, Kasugai S. Bone regeneration by modified gene-activated matrix: effectiveness in segmental tibial defects in rats. Tissue Eng. 2006;12:489-97.

[67] Winn SR, Hu Y, Sfeir C, Hollinger JO. Gene therapy approaches for modulating bone regeneration. Adv Drug Deliv Rev. 2000;42:121-38.

[68] Kaigler D, Avila G, Wisner-Lynch L, Nevins ML, Nevins M, Rasperini G, et al. Platelet-derived growth factor applications in periodontal and peri-implant bone regeneration. Expert Opin Biol Ther. 2011;11:375-85.

[69] Sluzky V, Tamada JA, Klibanov AM, Langer R. Kinetics of insulin aggregation in aqueous solutions upon agitation in the presence of hydrophobic surfaces. Proc Natl Acad Sci USA. 1991;88:9377-81.

[70] Bowen-Pope DF, Malpass TW, Foster DM, Ross R. Platelet-derived growth factor in vivo: levels, activity, and rate of clearance. Blood. 1984;64:458-69.

[71] Edelman ER, Nugent MA, Karnovsky MJ. Perivascular and intravenous administration of basic fibroblast growth factor: vascular and solid organ deposition. Proc Natl Acad Sci USA. 1993;90:1513-7.

[72] Cotrim AP, Baum BJ. Gene therapy: Some history, applications, problems, and prospects. Toxicol Pathol. 2008;36:97-103.

[73] Ramseier CA, Abramson ZR, Jin Q, Giannobile WV. Gene therapeutics for periodontal regenerative medicine. Dent Clin North Am. 2006;50:245-63.

[74] Goldstein SA, Bonadio J. Potential role for direct gene transfer in the enhancement of fracture healing. Clin Orthop Relat Res. 1998:S154-S62.

[75] Patil P, Graziano G, Bonadio J, Goldstein S. Interbody fusion augmentation using localized gene delivery. Trans Orthop Res Soc. 2000;25:360.

[76] Langer R. Drug delivery and targeting. Nature. 1998;392:5-10.

[77] Terrell TG, Working PK, Chow CP, Green JD. Pathology of recombinant human transforming growth factor-beta 1 in rats and rabbits. Int Rev Exp Pathol. 1993;34 Pt B:43-67.

[78] Horn NA, Meek JA, Budahazi G, Marquet M. Cancer gene therapy using plasmid DNA: purification of DNA for human clinical trials. Hum Gene Ther. 1995;6:565-73.

[79] Evans C. Gene therapy for the regeneration of bone. Injury. 2011;42:599-604.

[80] Orsi S, De Capua A, Guarnieri D, Marasco D, Netti PA. Cell recruitment and transfection in gene activated collagen matrix. Biomaterials. 2010;31:570-6.

[81] Avilés MO, Lin CH, Zelivyanskaya M, Graham JG, Boehler RM, Messersmith PB, et al. The contribution of plasmid design and release to in vivo gene expression following delivery from cationic polymer modified scaffolds. Biomaterials. 2010;31:1140-7.

[82] Yang X, Walboomers XF, Van Den Dolder J, Yang F, Bian Z, Fan M, et al. Non-viral bone morphogenetic protein 2 transfection of rat dental pulp stem cells using calcium phosphate nanoparticles as carriers. Tissue Eng Part A. 2008;14:71-81.

[83] Evans CH, Ghivizzani SC, Robbins PD. Orthopedic gene therapy--lost in translation? J Cell Physiol. 2012;227:416-20.

[84] Marquez L, de Abreu FA, Ferreira CL, Alves GD, Miziara MN, Alves JB. Enhanced bone healing of rat tooth sockets after administration of epidermal growth factor (EGF) carried by liposome. Injury. 2013;44:558-64.

[85] Caplan AI, Correa D. PDGF in bone formation and regeneration: new insights into a novel mechanism involving MSCs. J Orthop Res. 2011;29:1795-803.

[86] Moore DC, Ehrlich MG, McAllister SC, Machan JT, Hart CE, Voigt C, et al. Recombinant human platelet-derived growth factor-BB augmentation of new-bone formation in a rat model of distraction osteogenesis. J Bone Joint Surg Am. 2009;91:1973-84.

[87] Lind M, Schumacker B, Soballe K, Keller J, Melsen F, Bunger C. Transforming growth factor-beta enhances fracture healing in rabbit tibiae. Acta Orthop Scand. 1993;64:553-6.

[88] Rosier RN, O'Keefe RJ, Hicks DG. The potential role of transforming growth factor beta in fracture healing. Clin Orthop Relat Res. 1998:S294-300.

[89] Azad V, Breitbart E, Al-Zube L, Yeh S, O'Connor JP, Lin SS. rhBMP-2 enhances the bone healing response in a diabetic rat segmental defect model. J Orthop Trauma. 2009;23:267-76.

[90] Rao SM, Ugale GM, Warad SB. Bone morphogenetic proteins: periodontal regeneration. N Am J Med Sci. 2013;5:161-8.

[91] Street J, Bao M, deGuzman L, Bunting S, Peale FV, Jr., Ferrara N, et al. Vascular endothelial growth factor stimulates bone repair by promoting angiogenesis and bone turnover. Proc Natl Acad Sci USA. 2002;99:9656-61.

[92] Wang DS, Miura M, Demura H, Sato K. Anabolic effects of 1,25-dihydroxyvitamin D3 on osteoblasts are enhanced by vascular endothelial growth factor produced by

osteoblasts and by growth factors produced by endothelial cells. Endocrinology. 1997;138:2953-62.

[93] Nakamura T, Hara Y, Tagawa M, Tamura M, Yuge T, Fukuda H, et al. Recombinant human basic fibroblast growth factor accelerates fracture healing by enhancing callus remodeling in experimental dog tibial fracture. J Bone Miner Res. 1998;13:942-9.

[94] Schmid GJ, Kobayashi C, Sandell LJ, Ornitz DM. Fibroblast growth factor expression during skeletal fracture healing in mice. Dev Dyn. 2009;238:766-74.

[95] Centrella M, McCarthy TL, Canalis E. Activin-A binding and biochemical effects in osteoblast-enriched cultures from fetal-rat parietal bone. Mol Cell Biol. 1991;11:250-8.

[96] Hashimoto M, Shoda A, Inoue S, Yamada R, Kondo T, Sakurai T, et al. Functional regulation of osteoblastic cells by the interaction of activin-A with follistatin. J Biol Chem. 1992;267:4999-5004.

[97] Sakai R, Eto Y. Involvement of activin in the regulation of bone metabolism. Mol Cell Endocrinol. 2001;180:183-8.

[98] Shen FH, Visger JM, Balian G, Hurwitz SR, Diduch DR. Systemically administered mesenchymal stromal cells transduced with insulin-like growth factor-I localize to a fracture site and potentiate healing. J Orthop Trauma. 2002;16:651-9.

[99] Trippel SB. Potential role of insulinlike growth factors in fracture healing. Clin Orthop Relat Res. 1998:S301-13.

[100] Murphy CM, Haugh MG, O'Brien FJ. The effect of mean pore size on cell attachment, proliferation and migration in collagen-glycosaminoglycan scaffolds for bone tissue engineering. Biomaterials. 2010;31:461-6.

[101] O'Brien FJ, Harley BA, Yannas IV, Gibson L. Influence of freezing rate on pore structure in freeze-dried collagen-GAG scaffolds. Biomaterials. 2004;25:1077-86.

[102] Tierney CM, Haugh MG, Liedl J, Mulcahy F, Hayes B, O'Brien FJ. The effects of collagen concentration and crosslink density on the biological, structural and mechanical properties of collagen-GAG scaffolds for bone tissue engineering. J Mech Behav Biomed Mater. 2009;2:202-9.

[103] Campoccia D, Doherty P, Radice M, Brun P, Abatangelo G, Williams DF. Semisynthetic resorbable materials from hyaluronan esterification. Biomaterials. 1998;19:2101-27.

[104] Lisignoli G, Zini N, Remiddi G, Piacentini A, Puggioli A, Trimarchi C, et al. Basic fibroblast growth factor enhances in vitro mineralization of rat bone marrow stromal cells

grown on non-woven hyaluronic acid based polymer scaffold. Biomaterials. 2001;22:2095-105.

[105] Radice M, Brun P, Cortivo R, Scapinelli R, Battaliard C, Abatangelo G. Hyaluronan-based biopolymers as delivery vehicles for bone-marrow-derived mesenchymal progenitors. J Biomed Mater Res. 2000;50:101-9.

[106] Bruder SP, Kurth AA, Shea M, Hayes WC, Jaiswal N, Kadiyala S. Bone regeneration by implantation of purified, culture-expanded human mesenchymal stem cells. J Orthop Res. 1998;16:155-62.

[107] Hiraoka Y, Kimura Y, Ueda H, Tabata Y. Fabrication and biocompatibility of collagen sponge reinforced with poly(glycolic acid) fiber. Tissue Eng. 2003;9:1101-12.

[108] Hosseinkhani H, Yamamoto M, Inatsugu Y, Hiraoka Y, Inoue S, Shimokawa H, et al. Enhanced ectopic bone formation using a combination of plasmid DNA impregnation into 3-D scaffold and bioreactor perfusion culture. Biomaterials. 2006;27:1387-98.

[109] Banerjee I, Mishra D, Maiti TK. PLGA Microspheres Incorporated Gelatin Scaffold: Microspheres Modulate Scaffold Properties. Int J Biomater. 2009;2009:143659.

[110] Sheridan MH, Shea LD, Peters MC, Mooney DJ. Bioabsorbable polymer scaffolds for tissue engineering capable of sustained growth factor delivery. J Control Release. 2000;64:91-102.

[111] Murphy WL, Dennis RG, Kileny JL, Mooney DJ. Salt fusion: an approach to improve pore interconnectivity within tissue engineering scaffolds. Tissue Eng. 2002;8:43-52.

[112] Liu X, Won Y, Ma PX. Porogen-induced surface modification of nano-fibrous poly(L-lactic acid) scaffolds for tissue engineering. Biomaterials. 2006;27:3980-7.

[113] Liu Y, Shu XZ, Gray SD, Prestwich GD. Disulfide-crosslinked hyaluronan–gelatin sponge: Growth of fibrous tissue in vivo. J Biomed Mater Res A. 2004;68A:142-9.

[114] Avilés MO, Lin C-H, Zelivyanskaya M, Graham JG, Boehler RM, Messersmith PB, et al. The contribution of plasmid design and release to in vivo gene expression following delivery from cationic polymer modified scaffolds. Biomaterials. 2010;31:1140-7.

[115] Al-Munajjed AA, O'Brien FJ. Influence of a novel calcium-phosphate coating on the mechanical properties of highly porous collagen scaffolds for bone repair. J Mech Behav Biomed Mater. 2009;2:138-46.

[116] Al-Munajjed AA, Plunkett NA, Gleeson JP, Weber T, Jungreuthmayer C, Levingstone T, et al. Development of a biomimetic collagen-hydroxyapatite scaffold for

bone tissue engineering using a SBF immersion technique. J Biomed Mater Res B Appl Biomater. 2009;90:584-91.

[117] Gleeson JP, Plunkett NA, O'Brien FJ. Addition of hydroxyapatite improves stiffness, interconnectivity and osteogenic potential of a highly porous collagen-based scaffold for bone tissue regeneration. Eur Cell Mater. 2010;20:218-30.

[118] Li Y, Danmark S, Edlund U, Finne-Wistrand A, He X, Norgard M, et al. Resveratrol-conjugated poly-epsilon-caprolactone facilitates in vitro mineralization and in vivo bone regeneration. Acta Biomater. 2011;7:751-8.

[119] Shiraishi N, Anada T, Honda Y, Masuda T, Sasaki K, Suzuki O. Preparation and characterization of porous alginate scaffolds containing various amounts of octacalcium phosphate (OCP) crystals. J Mater Sci Mater Med. 2010;21:907-14.

[120] Fang J, Zhu YY, Smiley E, Bonadio J, Rouleau JP, Goldstein SA, et al. Stimulation of new bone formation by direct transfer of osteogenic plasmid genes. Proc Natl Acad Sci USA. 1996;93:5753-8.

[121] Bonadio J, Smiley E, Patil P, Goldstein S. Localized, direct plasmid gene delivery in vivo: prolonged therapy results in reproducible tissue regeneration. Nat Med. 1999;5:753-9.

[122] Huang YC, Simmons C, Kaigler D, Rice KG, Mooney DJ. Bone regeneration in a rat cranial defect with delivery of PEI-condensed plasmid DNA encoding for bone morphogenetic protein-4 (BMP-4). Gene Ther. 2005;12:418-26.

[123] Chew SA, Kretlow JD, Spicer PP, Edwards AW, Baggett LS, Tabata Y, et al. Delivery of plasmid DNA encoding bone morphogenetic protein-2 with a biodegradable branched polycationic polymer in a critical-size rat cranial defect model. Tissue Eng Part A. 2011;17:751-63.

[124] Park J, Lutz R, Felszeghy E, Wiltfang J, Nkenke E, Neukam FW, et al. The effect on bone regeneration of a liposomal vector to deliver BMP-2 gene to bone grafts in peri-implant bone defects. Biomaterials. 2007;28:2772-82.

[125] Patil PV GG, Bonadio J, et al. Interbody fusion augmentation using localized gene delivery. Trans Orthop Res Soc. 2000;25:360.

[126] Geiger F, Bertram H, Berger I, Lorenz H, Wall O, Eckhardt C, et al. Vascular endothelial growth factor gene-activated matrix (VEGF165-GAM) enhances osteogenesis and angiogenesis in large segmental bone defects. J Bone Miner Res. 2005;20:2028-35.

[127] Itaka K, Ohba S, Miyata K, Kawaguchi H, Nakamura K, Takato T, et al. Bone regeneration by regulated in vivo gene transfer using biocompatible polyplex nanomicelles. Mol Ther. 2007;15:1655-62.

[128] Bright C, Park YS, Sieber AN, Kostuik JP, Leong KW. In vivo evaluation of plasmid DNA encoding OP-1 protein for spine fusion. Spine (Phila Pa 1976). 2006;31:2163-72.

[129] Keeney M, van den Beucken JJJP, van der Kraan PM, Jansen JA, Pandit A. The ability of a collagen/calcium phosphate scaffold to act as its own vector for gene delivery and to promote bone formation via transfection with VEGF165. Biomaterials. 2010;31:2893-902.

[130] Ono I, Yamashita T, Jin H-Y, Ito Y, Hamada H, Akasaka Y, et al. Combination of porous hydroxyapatite and cationic liposomes as a vector for BMP-2 gene therapy. Biomaterials. 2004;25:4709-18.

[131] Mulligan R. The basic science of gene therapy. Science. 1993;260:926-32.

[132] Verma IM, Naldini L, Kafri T, Miyoshi H, Takahashi M, Blömer U, et al. Gene Therapy: Promises, Problems and Prospects. In: Boulyjenkov V, Berg K, Christen Y, editors. Genes and Resistance to Disease: Springer Berlin Heidelberg; 2000. p. 147-57.

[133] Zegzula HD, Buck DC, Brekke J, Wozney JM, Hollinger JO. Bone Formation with Use of rhBMP-2 (Recombinant Human Bone Morphogenetic Protein-2). J Bone Joint Surg Am. 1997;79:1778-90.

[134] Lieberman JR, Daluiski A, Stevenson S, Wu L, McAllister P, Lee YP, et al. The effect of regional gene therapy with bone morphogenetic protein-2-producing bone-marrow cells on the repair of segmental femoral defects in rats. J Bone Joint Surg Am. 1999;81:905-17.

[135] Endo M, Kuroda S, Kondo H, Maruoka Y, Ohya K, Kasugai S. Bone regeneration by modified gene-activated matrix: effectiveness in segmental tibial defects in rats. Tissue Eng. 2006;12:489-97.

[136] Yoneda T, Pratt RM. Glucocorticoid receptors in palatal mesenchymal cells from the human embryo: relevance to human cleft palate formation. J Craniofac Genet Dev Biol. 1982;1:411-23.

[137] Elangovan S, Jain S, Tsai PC, Margolis HC, Amiji M. Nano-sized calcium phosphate particles for periodontal gene therapy. J Periodontol. 2013;84:117-25.

[138] Olton D, Li J, Wilson ME, Rogers T, Close J, Huang L, et al. Nanostructured calcium phosphates (NanoCaPs) for non-viral gene delivery: Influence of the synthesis parameters on transfection efficiency. Biomaterials. 2007;28:1267-79.

[139] Parker SE, Vahlsing HL, Serfilippi LM, Franklin CL, Doh SG, Gromkowski SH, et al. Cancer gene therapy using plasmid DNA: safety evaluation in rodents and non-human primates. Hum Gene Ther. 1995;6:575-90.

[140] Anderson WF. Human gene therapy. Nature. 1998;392:25-30.

[141] Boussif O, Lezoualc'h F, Zanta MA, Mergny MD, Scherman D, Demeneix B, et al. A versatile vector for gene and oligonucleotide transfer into cells in culture and in vivo: polyethylenimine. Proc Natl Acad Sci. 1995;92:7297-301.

[142] Intra J, Salem AK. Characterization of the transgene expression generated by branched and linear polyethylenimine-plasmid DNA nanoparticles in vitro and after intraperitoneal injection in vivo. J Control Release. 2008;130:129-38.

[143] Kircheis R, Wightman L, Schreiber A, Robitza B, Rössler V, Kursa M, et al. Polyethylenimine/DNA complexes shielded by transferrin target gene expression to tumors after systemic application. Gene Ther. 2001;8:28-40.

[144] Godbey WT, Wu KK, Mikos AG. Poly(ethylenimine) and its role in gene delivery. J Control Release. 1999;60:149-60.

[145] Abdallah B, Hassan A, Benoist C, Goula D, Behr JP, Demeneix BA. A powerful nonviral vector for in vivo gene transfer into the adult mammalian brain: polyethylenimine. Hum Gene Ther. 1996;7:1947-54.

[146] Godbey WT, Wu KK, Mikos AG. Size matters: molecular weight affects the efficiency of poly(ethylenimine) as a gene delivery vehicle. J Biomed Mater Res. 1999;45:268-75.

[147] Liu Y, Wang T, He F, Liu Q, Zhang D, Xiang S, et al. An efficient calcium phosphate nanoparticle-based nonviral vector for gene delivery. Int J Nanomedicine. 2011;6:721.

[148] O'Mahoney JV, Adams TE. Optimization of experimental variables influencing reporter gene expression in hepatoma cells following calcium phosphate transfection. DNA Cell Biol. 1994;13:1227-32.

[149] Bettinger T, Remy J-S, Erbacher P. Size reduction of galactosylated PEI/DNA complexes improves lectin-mediated gene transfer into hepatocytes. Bioconjug Chem. 1999;10:558-61.

[150] Naoto O, Yamaguchi N, Yamaguchi N, Shibamoto S, Fumiaki I, Nango M. The fusogenic effect of synthetic polycations on negatively charged lipid bilayers. J Biochem. 1986;100:935-44.

[151] Sokolova VV, Radtke I, Heumann R, Epple M. Effective transfection of cells with multi-shell calcium phosphate-DNA nanoparticles. Biomaterials. 2006;27:3147-53.

[152] Welzel T, Radtke I, Meyer-Zaika W, Heumann R, Epple M. Transfection of cells with custom-made calcium phosphate nanoparticles coated with DNA. J Mater Chem. 2004;14:2213-7.

[153] Dunlap DD, Maggi A, Soria MR, Monaco L. Nanoscopic structure of DNA condensed for gene delivery. Nucleic Acids Res. 1997;25:3095-101.

[154] Godbey W, Wu K, Hirasaki G, Mikos A. Improved packing of poly (ethylenimine)/DNA complexes increases transfection efficiency. Gene Ther. 1999;6:1380-8.

[155] Hsu C, Uludağ H. Effects of size and topology of DNA molecules on intracellular delivery with non-viral gene carriers. BMC Biotechnol. 2008;8:23.

[156] Ogris M, Steinlein P, Kursa M, Mechtler K, Kircheis R, Wagner E. The size of DNA/transferrin-PEI complexes is an important factor for gene expression in cultured cells. Gene Ther. 1998;5:1425-33.

[157] Bisht S, Bhakta G, Mitra S, Maitra A. pDNA loaded calcium phosphate nanoparticles: highly efficient non-viral vector for gene delivery. Int J Pharm. 2005;288:157-68.

[158] Jordan M, Wurm F. Transfection of adherent and suspended cells by calcium phosphate. Methods. 2004;33:136-43.

[159] Seelos C. A critical parameter determining the aging of DNA–calcium-phosphate precipitates. Anal Biochem. 1997;245:109-11.

[160] Urabe M, Kume A, Tobita K, Ozawa K. DNA/calcium phosphate precipitates mixed with medium are stable and maintain high transfection efficiency. Anal Biochem. 2000;278:91-2.

[161] Orrantia E, Chang PL. Intracellular distribution of DNA internalized through calcium phosphate precipitation. Exp Cell Res. 1990;190:170-4.

[162] Battegay EJ, Rupp J, Iruela-Arispe L, Sage EH, Pech M. PDGF-BB modulates endothelial proliferation and angiogenesis in vitro via PDGF beta-receptors. J Cell Biol. 1994;125:917-28.

[163] Bolander ME. Regulation of Fracture Repair by Growth Factors. Proc Soc Exp Biol Med. 1992;200:165-70.

[164] He XX, Wang K, Tan W, Liu B, Lin X, He C, et al. Bioconjugated nanoparticles for DNA protection from cleavage. J Am Chem Soc. 2003;125:7168-9.

[165] Canalis E, McCarthy T, Centrella M. Growth factors and the regulation of bone remodeling. J Clin Invest. 1988;81:277-81.

[166] Lynch SE, Colvin RB, Antoniades HN. Growth factors in wound healing. Single and synergistic effects on partial thickness porcine skin wounds. J Clin Invest. 1989;84:640-46.

[167] Elangovan S, Srinivasan S, Ayilavarapu S. Novel regenerative strategies to enhance periodontal therapy outcome. Expert Opin Biol Ther. 2009;9:399-410.

[168] Winn SR, Hu Y, Sfeir C, Hollinger JO. Gene therapy approaches for modulating bone regeneration. Adv Drug Deliv Rev. 2000;42:121-38.

[169] Ramseier CA, Abramson ZR, Jin Q, Giannobile WV. Gene therapeutics for periodontal regenerative medicine. Dent Clin North Am. 2006;50:245-63.

[170] Fang J, Zhu Y-Y, Smiley E, Bonadio J, Rouleau JP, Goldstein SA, et al. Stimulation of new bone formation by direct transfer of osteogenic plasmid genes. Proc Natl Acad Sci. 1996;93:5753-8.

[171] Bonadio J, Smiley E, Patil P, Goldstein S. Localized, direct plasmid gene delivery in vivo: prolonged therapy results in reproducible tissue regeneration. Nat Med. 1999;5:753-9.

[172] Goldstein SA, Bonadio J. Potential role for direct gene transfer in the enhancement of fracture healing. Clin Orthop Relat Res. 1998:S154-62.

[173] Elangovan S, Karimbux N. Review paper: DNA delivery strategies to promote periodontal regeneration. J Biomater Appl. 2010;25:3-18.

[174] Intra J, Salem AK. Characterization of the transgene expression generated by branched and linear polyethylenimine-plasmid DNA nanoparticles in vitro and after intraperitoneal injection in vivo. J Control Release. 2008;130:129-38.

[175] Dash PR, Toncheva V, Schacht E, Seymour LW. Synthetic polymers for vectorial delivery of DNA: characterisation of polymer-DNA complexes by photon correlation spectroscopy and stability to nuclease degradation and disruption by polyanions in vitro. J Control Release. 1997;48:269-76.

[176] Dunlap DD, Maggi A, Soria MR, Monaco L. Nanoscopic structure of DNA condensed for gene delivery. Nucleic Acids Res. 1997;25:3095-101.

[177] Godbey WT, Wu KK, Hirasaki GJ, Mikos AG. Improved packing of poly(ethylenimine)/DNA complexes increases transfection efficiency. Gene Ther. 1999;6:1380-8.

[178] Godbey WT, Wu KK, Mikos AG. Size matters: Molecular weight affects the efficiency of poly(ethylenimine) as a gene delivery vehicle. J Biomed Mater Res. 1999;45:268-75.

[179] Papisov IM, Litmanovich AA. Molecular "recognition" in interpolymer interactions and matrix polymerization. Conducting Polymers/Molecular Recognition: Springer Berlin Heidelberg; 1989. p. 139-79.

[180] Hollinger JO, Hart CE, Hirsch SN, Lynch S, Friedlaender GE. Recombinant human platelet-derived growth factor: biology and clinical applications. J Bone Joint Surg Am. 2008;90:48-54.

[181] Chang P-C, Seol Y-J, Cirelli JA, Pellegrini G, Jin Q, Franco LM, et al. PDGF-B gene therapy accelerates bone engineering and oral implant osseointegration. Gene Ther. 2009;17:95-104.

[182] Javed F, Al-Askar M, Al-Rasheed A, Al-Hezaimi K. Significance of the platelet-derived growth factor in periodontal tissue regeneration. Arch Oral Biol. 2011;56:1476-84.

[183] Lee Y-M, Park Y-J, Lee S-J, Ku Y, Han S-B, Klokkevold PR, et al. The bone regenerative effect of platelet-derived growth factor-BB delivered with a chitosan/tricalcium phosphate sponge carrier. J Periodontol. 2000;71:418-24.

[184] Minagawa K, Matsuzawa Y, Yoshikawa K, Matsumoto M, Doi M. Direct observation of the biphasic conformational change of DNA induced by cationic polymers. FEBS Lett. 1991;295:67-9.

[185] WJ C. Practical Nonparametric Statistics. 3rd ed. New York: Wiley; 1999.

[186] Oku N, Yamaguchi N, Yamaguchi N, Shibamoto S, Ito F, Nango M. The fusogenic effect of synthetic polycations on negatively charged lipid bilayers. J Biochem. 1986;100:935-44.

[187] Wagner E, Cotten M, Foisner R, Birnstiel ML. Transferrin-polycation-DNA complexes: the effect of polycations on the structure of the complex and DNA delivery to cells. Proc Natl Acad Sci USA. 1991;88:4255-9.

[188] Ferkol T, Perales JC, Eckman E, Kaetzel CS, Hanson RW, Davis PB. Gene transfer into the airway epithelium of animals by targeting the polymeric immunoglobulin receptor. J Clin Invest. 1995;95:493-502.

[189] Plank C, Mechtler K, Szoka Jr FC, Wagner E. Activation of the complement system by synthetic DNA complexes: A potential barrier for intravenous gene delivery. Hum Gene Ther. 1996;7:1437-46.

[190] Ferrari S, Moro E, Pettenazzo A, Behr JP, Zacchello F, Scarpa M. ExGen 500 is an efficient vector for gene delivery to lung epithelial cells in vitro and in vivo. Gene Ther. 1997;4:1100-6.

[191] Hsu CY, Uludag H. Effects of size and topology of DNA molecules on intracellular delivery with non-viral gene carriers. BMC Biotechnol. 2008;8:23.

[192] Bolander ME. Regulation of fracture repair by growth factors. Proc Soc Exp Biol Med. 1992;200:165-70.

[193] Banfi A, von Degenfeld G, Gianni-Barrera R, Reginato S, Merchant MJ, McDonald DM, et al. Therapeutic angiogenesis due to balanced single-vector delivery of VEGF and PDGF-BB. FASEB J. 2012;26:2486-97.

[194] Chung HJ, Park TG. Surface engineered and drug releasing pre-fabricated scaffolds for tissue engineering. Adv Drug Deliv Rev. 2007;59:249-62.

[195] Pieper JS, Hafmans T, van Wachem PB, van Luyn MJA, Brouwer LA, Veerkamp JH, et al. Loading of collagen-heparan sulfate matrices with bFGF promotes angiogenesis and tissue generation in rats. J Biomed Mater Res. 2002;62:185-94.

[196] Kim B-S, Mooney DJ. Development of biocompatible synthetic extracellular matrices for tissue engineering. Trends Biotechnol. 1998;16:224-30.

[197] Marks MG, Doillon C, Silvert FH. Effects of fibroblasts and basic fibroblast growth factor on facilitation of dermal wound healing by type I collagen matrices. J Biomed Mater Res. 1991;25:683-96.

[198] Helm GA, Sheehan JM, Sheehan JP, Jane JA, diPierro CG, Simmons NE, et al. Utilization of type I collagen gel, demineralized bone matrix, and bone morphogenetic protein-2 to enhance autologous bone lumbar spinal fusion. J Neurosurg. 1997;86:93-100.

[199] Sweeney TM, Opperman LA, Persing JA, Ogle RC. Repair of critical size rat calvarial defects using extracellular matrix protein gels. J Neurosurg. 1995;83:710-5.

[200] Lynch SE, Williams RC, Polson AM, Howell TH, Reddy MS, Zappa UE, et al. A combination of platelet-derived and insulin-like growth factors enhances periodontal regeneration. J Clin Periodontol. 1989;16:545-8.

[201] Nevins M, Camelo M, Nevins ML, Schenk RK, Lynch SE. Periodontal regeneration in humans using recombinant human platelet-derived growth factor-BB (rhPDGF-BB) and allogenic bone. J Periodontol. 2003;74:1282-92.

[202] Schneider J, Gu W, Zhu L, Mahdavi V, Nadal-Ginard B. Reversal of terminal differentiation mediated by p107 in Rb-/- muscle cells. Science. 1994;264:1467-71.

[203] Cardoso MC, Leonhardt H, Nadal-Ginard B. Reversal of terminal differentiation and control of DNA replication: Cyclin A and cdk2 specifically localize at subnuclear sites of DNA replication. Cell. 1993;74:979-92.

[204] Fathke C, Wilson L, Hutter J, Kapoor V, Smith A, Hocking A, et al. Contribution of bone marrow-derived cells to skin: collagen deposition and wound repair. Stem cells. 2004;22:812-22.

[205] Toolan BC. Current concepts review: Orthobiologics. Foot Ankle Int. 2006;27:561-6.

[206] Darby I. Periodontal materials. Aust Dent J. 2011;56:107-18.

[207] McAllister BS, Haghighat K. Bone augmentation techniques. J Periodontol. 2007;78:377-96.

[208] Deschaseaux F, Sensébé L, Heymann D. Mechanisms of bone repair and regeneration. Trends Mol Med. 2009;15:417-29.

[209] Canalis E, Varghese S, McCarthy T, Centrella M. Role of platelet derived growth factor in bone cell function. Growth Regul. 1992;2:151-5.

[210] Sun Q, Silva EA, Wang A, Fritton JC, Mooney DJ, Schaffler MB, et al. Sustained release of multiple growth factors from injectable polymeric system as a novel therapeutic approach towards angiogenesis. Pharm Res. 2010;27:264-71.

[211] Banfi A, von Degenfeld G, Gianni-Barrera R, Reginato S, Merchant MJ, McDonald DM, et al. Therapeutic angiogenesis due to balanced single-vector delivery of VEGF and PDGF-BB. FASEB J. 2012;26:2486-97.

[212] Chen RR, Silva EA, Yuen WW, Mooney DJ. Spatio–temporal VEGF and PDGF delivery patterns blood vessel formation and maturation. Pharm Res. 2007;24:258-64.

[213] De la Riva B, Sánchez E, Hernández A, Reyes R, Tamimi F, López-Cabarcos E, et al. Local controlled release of VEGF and PDGF from a combined brushite–chitosan system enhances bone regeneration. J Control Release. 2010;143:45-52.

[214] Reyes R, De la Riva B, Delgado A, Hernández A, Sánchez E, Évora C. Effect of triple growth factor controlled delivery by a brushite–PLGA system on a bone defect. Injury. 2012;43:334-42.

[215] Ramseier CA, Abramson ZR, Jin Q, Giannobile WV. Gene therapeutics for periodontal regenerative medicine. Dent Clin North Am. 2006;50:245.

[216] Anusaksathien O, Webb SA, Jin Q-M, Giannobile WV. Platelet-derived growth factor gene delivery stimulates ex vivo gingival repair. Tissue Eng. 2003;9:745-56.

[217] Giannobile WV, Lee CS, Tomala MP, Tejeda KM, Zhu Z. Platelet-derived growth factor (PDGF) gene delivery for application in periodontal tissue engineering. J Periodontol. 2001;72:815-23.

[218] Jin Q, Anusaksathien O, Webb SA, Printz MA, Giannobile WV. Engineering of tooth-supporting structures by delivery of PDGF gene therapy vectors. Mol Ther. 2004;9:519-26.

[219] Chang P-C, Seol Y-J, Cirelli JA, Pellegrini G, Jin Q, Franco LM, et al. PDGF-B gene therapy accelerates bone engineering and oral implant osseointegration. Gene Ther. 2010;17:95-104.

[220] Ledley FD. Nonviral gene therapy: the promise of genes as pharmaceutical products. Hum Gene Ther. 1995;6:1129-44.

[221] Luo D, Saltzman WM. Synthetic DNA delivery systems. Nature Biotechnol. 2000;18:33-7.

[222] Battegay EJ, Rupp J, Iruela-Arispe L, Sage EH, Pech M. PDGF-BB modulates endothelial proliferation and angiogenesis in vitro via PDGF beta-receptors. J Cell Biol. 1994;125:917-28.

[223] Beyerle A, Irmler M, Beckers J, Kissel T, Stoeger T. Toxicity Pathway Focused Gene Expression Profiling of PEI-Based Polymers for Pulmonary Applications. Mol Pharm. 2010;7:727-37.

[224] Ball SG, Shuttleworth CA, Kielty CM. Vascular endothelial growth factor can signal through platelet-derived growth factor receptors. J Cell Biol. 2007;177:489-500.

[225] Chen F-M, Zhang M, Wu Z-F. Toward delivery of multiple growth factors in tissue engineering. Biomaterials. 2010;31:6279-308.

[226] Giannobile W. Periodontal tissue engineering by growth factors. Bone. 1996;19:S23-S37.

[227] Kaigler D, Cirelli JA, Giannobile WV. Growth factor delivery for oral and periodontal tissue engineering. Expert Opin Drug Deliv. 2006;3:647-62.

[228] Park S-Y, Kim K-H, Shin S-Y, Koo K-T, Lee Y-M, Seol Y-J. Dual delivery of rhPDGF-BB and bone marrow mesenchymal stromal cells expressing the BMP2 gene enhance bone formation in a critical-sized defect model. Tissue Eng Part A. 2013;19:2495-505.

[229] Connolly JF, Guse R, Tiedeman J, Dehne R. Autologous marrow injection for delayed unions of the tibia: a preliminary report. J Orthop Trauma. 1989;3:276-82.

[230] Lane JM, Tomin E, Bostrom MP. Biosynthetic bone grafting. Clin Orthop Relat Res. 1999;367:S107-S17.

[231] Petite H, Viateau V, Bensaid W, Meunier A, de Pollak C, Bourguignon M, et al. Tissue-engineered bone regeneration. Nature Biotechnol. 2000;18:959-63.

[232] Vacanti CA, Upton J. Tissue-engineered morphogenesis of cartilage and bone by means of cell transplantation using synthetic biodegradable polymer matrices. Clin Plast Surg. 1994;21:445-62.

[233] Jégoux F, Goyenvalle E, Cognet R, Malard O, Moreau F, Daculsi G, et al. Reconstruction of irradiated bone segmental defects with a biomaterial associating MBCP+®, microstructured collagen membrane and total bone marrow grafting: An experimental study in rabbits. J Biomed Mater Res A. 2009;91:1160-9.

[234] Lim H-C, Sohn J-Y, Park J-C, Um Y-J, Jung U-W, Kim C-S, et al. Osteoconductive effects of calcium phosphate glass cement grafts in rabbit calvarial defects. J Biomed Mater Res B Appl Biomater. 2010;95B:47-52.

[235] Yaszemski MJ, Payne RG, Hayes WC, Langer R, Mikos AG. Evolution of bone transplantation: molecular, cellular and tissue strategies to engineer human bone. Biomaterials. 1996;17:175-85.

[236] Aaboe M, Pinholt E, Hjorting-Hansen E. Healing of experimentally created defects: a review. Br J Oral Maxillofac Surg. 1995;33:312-8.

[237] Hermann J, Buser D. Guided bone regeneration for dental implants. Curr Opin Periodontol. 1995;3:168-77.

[238] Yang C, Unursaikhan O, Lee J-S, Jung U-W, Kim C-S, Choi S-H. Osteoconductivity and biodegradation of synthetic bone substitutes with different tricalcium phosphate contents in rabbits. J Biomed Mater Res B Appl Biomater. 2014;102:80-8.

[239] VandeVord PJ, Matthew HWT, DeSilva SP, Mayton L, Wu B, Wooley PH. Evaluation of the biocompatibility of a chitosan scaffold in mice. J Biomed Mater Res. 2002;59:585-90.

[240] Baldrick P. The safety of chitosan as a pharmaceutical excipient. Regul Toxicol Pharmacol. 2010;56:290-9.

[241] Azad AK, Sermsintham N, Chandrkrachang S, Stevens WF. Chitosan membrane as a wound-healing dressing: Characterization and clinical application. J Biomed Mater Res B Appl Biomater. 2004;69B:216-22.

[242] Kojima K, Okamoto Y, Miyatake K, Fujise H, Shigemasa Y, Minami S. Effects of chitin and chitosan on collagen synthesis in wound healing. J Vet Med Sci. 2004;66:1595-8.

[243] Chandy T, Sharma CP. Chitosan-as a biomaterial. Biomater Artif Cells Artif Organs. 1990;18:1-24.

[244] Muzzarelli R, Baldassarre V, Conti F, Ferrara P, Biagini G, Gazzanelli G, et al. Biological activity of chitosan: ultrastructural study. Biomaterials. 1988;9:247-52.

[245] Wang X, Ma J, Wang Y, He B. Bone repair in radii and tibias of rabbits with phosphorylated chitosan reinforced calcium phosphate cements. Biomaterials. 2002;23:4167-76.

[246] Rhazi M, Desbrieres J, Tolaimate A, Rinaudo M, Vottero P, Alagui A, et al. Influence of the nature of the metal ions on the complexation with chitosan.: Application to the treatment of liquid waste. Eur Polym J. 2002;38:1523-30.

[247] Kofuji K, Murata Y, Kawashima S. Sustained insulin release with biodegradation of chitosan gel beads prepared by copper ions. Int J Pharm. 2005;303:95-103.

[248] Schlick S. Binding sites of copper2+ in chitin and chitosan. An electron spin resonance study. Macromolecules. 1986;19:192-5.

[249] Hu GF. Copper stimulates proliferation of human endothelial cells under culture. J Cell Biochem. 1998;69:326-35.

[250] McAuslan B, Reilly W. Endothelial cell phagokinesis in response to specific metal ions. Exp Cell Res. 1980;130:147-57.

[251] Raju KS, Alessandri G, Ziche M, Gullino PM. Ceruloplasmin, copper ions, and angiogenesis. J Natl Cancer Inst. 1982;69:1183-8.

[252] Sen CK, Khanna S, Venojarvi M, Trikha P, Ellison EC, Hunt TK, et al. Copper-induced vascular endothelial growth factor expression and wound healing. Am J Physiol Heart Circ Physiol. 2002;282:H1821-7.

[253] Borkow G. Copper's Role in Wound Healing. 2004.

[254] Heldin CH. Structural and functional studies on platelet-derived growth factor. EMBO J. 1992;11:4251-9.

[255] Wake MC, Patrick Jr C, Mikos A. Pore morphology effects on the fibrovascular tissue growth in porous polymer substrates. Cell Transplantat. 1993;3:339-43.